

STATUS OF THESIS

Title of thesis

A Model of Naphtha Reforming in a Radial Flow Moving Bed Reactor

I NURUL SHAHIDA BINTI MOHAMED ZI

hereby allow my thesis to be placed at the Information Resource Center (IRC) of Universiti Teknologi PETRONAS (UTP) with the following conditions:

1. The thesis becomes the property of UTP.
2. The IRC of UTP may make copies of the thesis for academic purposes only.
3. This thesis is classified as

Confidential

Non-confidential

If this thesis is confidential, please state the reason:

The content of the thesis will remain confidential for _____ years.

Remarks on disclosure:

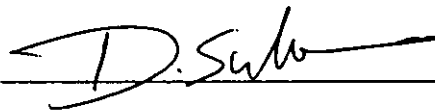


Signature of Author

Permanent Address: Lot 370, Kampung
Bukit Tanah, Selising, 16810 Pasir Puteh,
Kelantan.

Date: 09/09/2011

Endorsed by



Signature of Supervisor

Prof Dr. Duvvuri Subbarao
Universiti Teknologi PETRONAS

Date: 09/09/2011

UNIVERSITI TEKNOLOGI PETRONAS

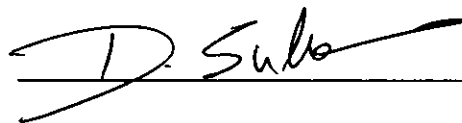
“A MODEL OF NAPHTHA REFORMING IN A RADIAL FLOW MOVING BED
REACTOR”

by

NURUL SHAHIDA BINTI MOHAMED ZI

The undersigned certify that they have read, and recommend to The Postgraduate Studies Programme for acceptance this thesis for the fulfillment of the requirements for the degree of Master of Science in Chemical Engineering.

Signature:



Main Supervisor:

Prof. Dr. Duvvuri Subbarao

Professor Dr D Subbarao
Chemical Engineering Department
Universiti Teknologi PETRONAS

Signature:



Head of Department: Assoc. Prof. Dr. Suhaimi Mahadzir

Date:

12/9/2011

Dr. Shuhaimi Mahadzir
Associate Professor & Head
Chemical Engineering Department
Universiti Teknologi PETRONAS

“A MODEL OF NAPHTHA REFORMING IN A RADIAL FLOW MOVING BED
REACTOR”

by

NURUL SHAHIDA BINTI MOHAMED ZI

A Thesis

Submitted to the Postgraduate Studies Programme

as a Requirement for the Degree of

MASTER OF SCIENCE

CHEMICAL ENGINEERING

UNIVERSITI TEKNOLOGI PETRONAS

BANDAR SERI ISKANDAR

PERAK

SEPTEMBER 2011

DECLARATION OF THESIS

Title of thesis

A Model of Naphtha Reforming in a Radial Flow Moving Bed Reactor

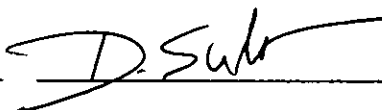
I NURUL SHAHIDA BINTI MOHAMED ZI

hereby declare that the thesis is based on my original work except for quotations and citations which have been duly acknowledged. I also declare that it has not been previously or concurrently submitted for any other degree at UTP or other institutions.



Signature of Author

Witnessed by



Signature of Supervisor

Permanent Address: Lot 370, Kampung
Bukit Tanah, Selising, 16810 Pasir Puteh,
Kelantan.

Prof. Dr. Duvvuri Subbarao
Universiti Teknologi PETRONAS

Date: 09 /09/ 2011

Date: 09/09/2011

Dedicated to my beloved family and friends

ACKNOWLEDGEMENT

I wish to express my appreciation to my thesis advisor Professor Dr. Duvvuri Subbarao for his invaluable support, encouragement, and patient guidance. Professor Subbarao has been more than mentor to me and working with him has been a great experience. I have had the opportunity to learn something from Prof. Subbarao every time I meet him. I will always be indebted to him.

This work could have not been possible without the academic and financial support received from Universiti Teknologi PETRONAS during my graduate studies.

Special thanks also go to the very valuable helps from the staffs in Chemical Engineering department and staffs in Postgraduate Office, Universiti Teknologi PETRONAS which gives a lot of helps and motivation for making my graduate years enjoyable and memorable.

I am sincerely thankful for the love and invaluable support received from my family and friends. This work is dedicated to them.

ABSTRACT

Catalytic reforming of naphtha is widely practiced in the petroleum industry to produce aromatics. Latest technology utilizes novel radial flow moving bed reactors for the reforming process as well as regeneration of the slowly decaying catalyst. Catalyst circulation between the reformer and regeneration units makes continuous operation of reformer-regenerator unit possible. In spite of their extensive use, very little is known about the performance of radial flow moving bed reformer unit.

The radial flow moving bed reformer consists of four reactor units (R_1 , R_2 , R_3 and R_4) stacked one on top of the other with catalyst flowing downward by gravity as a moving bed. In each reactor unit the catalyst flows downwards through an annulus with reactants flowing radially inwards through the moving bed of the catalyst. The reactants flow through the four units in series and are preheated before entering each unit. Temperature of the product stream exiting each unit is lower as the reactor is adiabatic and reactions are net endothermic.

A one dimensional compartment in series multiphase catalytic reactor model considering the catalyst deactivation is developed to explain the performance of a radial flow moving bed reformer. The model estimates on the trends of temperature and composition profiles are in reasonable agreement with the limited industrial information available. The model is used to simulate various scenarios to identify possible strategies to improve productivity of aromatics. Feeding the fresh feed in R_1 and R_3 and recovers the products at R_2 and R_4 is much better than feeding the fresh feed in R_1 and recovers the products in R_4 .

Simple models to account for pinning and rate of breakage of catalyst particles are proposed.

ABSTRAK

Reformasi nafta bermangkin dipraktikkan secara meluas dalam industri petroleum untuk menghasilkan aromatik. Teknologi terkini menggunakan reaktor lapisan bergerak aliran jejarian untuk proses reformasi dan regenerasi pemangkin. Peredaran pemangkin antara unit reformasi dan unit regenerasi memungkinkan proses reformasi berlaku berterusan. Walaupun penggunaan reaktor lapisan bergerak aliran jejarian sudah meluas, sangat sedikit kajian yang diterbitkan tentang prestasi lapisan bergerak aliran jejarian terhadap reformasi dan regenerasi nafta.

Reaktor lapisan bergerak aliran jejarian terdiri daripada empat unit reaktor (R_1 , R_2 , R_3 dan R_4) yang disusun di atas satu sama lain dengan mangkin mengalir ke bawah disebabkan tarikan graviti. Di dalam setiap reaktor, mangkin mengalir ke bawah melalui annulus dengan gas bahan tindakbalas mengalir secara selari ke dalam laluan mangkin yang bergerak. Bahan tindakbalas akan mengalir melalui keempat-empat reaktor secara bersiri dan dipanaskan terlebih dahulu kepada suhu tindakbalas sebelum masuk ke setiap reaktor. Suhu produk yang keluar dari setiap reaktor adalah lebih rendah kerana reaktor adalah adiabatik dan tindakbalas adalah endotermik.

Satu dimensi bersiri sel model dengan dua fasa reaktor bermangkin telah dibangunkan dengan mengambilkira ketidakaktifan mangkin untuk menerangkan tentang prestasi reaktor lapisan bergerak aliran jejarian. Model ini mendapati prestasi suhu dan komposisi adalah lebih menyerupai dengan yang diperolehi daripada industri. Model ini digunakan untuk simulasi bagi mengenalpasti strategi terbaik untuk meningkatkan pengeluaran aromatik dan didapati bahawa dengan kemasukan nafta pada R_1 dan R_3 dan produk dikeluarkan di R_2 dan R_4 adalah lebih baik.

Satu model telah diperkenalkan yang mengambilkira ‘pinning’ dan perpecahan mangkin.

In compliance with the terms of the Copyright Act 1987 and the IP Policy of the university, the copyright of this thesis has been reassigned by the author to the legal entity of the university,

Institute of Technology PETRONAS Sdn Bhd

Due acknowledgement shall always be made of the use of any material contained in, or derived from, this thesis.

© Nurul Shahida Binti Mohamed Zi, 2011

Institute of Technology PETRONAS Sdn Bhd

All right reserved.

TABLE OF CONTENTS

	PAGE
STATUS OF THESIS	i
APPROVAL PAGE	ii
TITLE PAGE	iii
DECLARATION	iv
DEDICATION	v
ACKNOWLEDGEMENT	vi
ABSTRACT	vii
COPYRIGHT PAGE	ix
LIST OF TABLES	xiv
LIST OF FIGURES	xv
LIST OF SYMBOLS	xviii
 Chapter	
1. INTRODUCTION	1
1.1 Naphtha Reforming.....	1
1.2 Naphtha Reforming Technology.....	2
1.3 Naphtha Reforming in Radial Flow Moving Bed Reactor.....	5
1.4 Problem Statement.....	6
1.5 Objectives.....	7
1.6 Scope of the study.....	7
2. REVIEW OF LITERATURE	9
2.1 Reforming Chemistry.....	9
2.1.1 Naphtha Reforming Catalyst.....	10
2.1.2 Kinetics of Reactions.....	10
2.1.2.1 Dehydrogenation of Paraffin to Naphthene..	10
2.1.2.2 Aromatization of Naphthene to Aromatic....	11
2.1.2.3 Hydro-cracking of Naphthene.....	11
2.1.2.4 Hydro-cracking of Paraffin.....	12
2.1.3 Catalyst Deactivation by Cooking Kinetics.....	12

2.2	Semi Regenerative Reforming (SRR) Technology.....	13
2.2.1	Reactor Models for SRR.....	14
2.3	Continuous Regenerative Reforming (CRR) Technology.....	14
2.3.1	Reactor Models for CRR.....	16
2.4	Radial Flow Moving Bed Reactor (RFMBR).....	17
2.5	Pinning.....	19
2.6	Particle Breakage.....	22
2.7	Conclusion.....	22
3.	MODEL OF THE REACTOR.....	23
3.1	The Radial Flow Moving Bed Reactor.....	23
3.2	Effective Reaction Rate Constant.....	26
3.3	Balance Equations over a Compartment.....	26
3.3.1	Mole Balance in <i>i-th</i> Compartment.....	27
3.3.2	Energy Balance in <i>i-th</i> Compartment.....	28
3.4	Kinetic Model.....	30
3.4.1	Dehydrogenation of Paraffin.....	31
3.4.2	Dehydrogenation of Naphthene.....	31
3.4.3	Naphthene Hydro-cracking.....	32
3.4.4	Paraffin Hydro-cracking.....	32
3.5	Catalyst Deactivation Model.....	32
3.6	Properties of Naphtha.....	34
3.6.1	Determination of Carbon Number, <i>n</i> for Hydrocarbon Feed.....	34
3.6.1.1	Paraffin.....	34
3.6.1.2	Naphthene.....	34
3.6.1.3	Aromatic.....	35
3.6.2	Density of Naphtha Feed.....	35
3.6.3	Velocity of Naphtha Feed.....	35
3.6.4	Reynolds Number of Naphtha Gas Flow.....	36
3.6.5	Liquid Hourly Space Velocity (LHSV).....	36
3.6.6	Weighted Average Inlet Temperature (WAIT).....	36
3.6.7	Catalyst Residence Time.....	36
3.7	Model Development.....	37

3.7.1	Simulation to identify the Correction Multiplier of Paraffin Dehydrogenation, η_{R1}	37
3.7.2	Simulation to identify the Correction Multiplier of Naphthene Dehydrogenation, η_{R2}	39
3.7.3	Simulation to identify the Correction Multiplier of Hydro-cracking, η_c	41
3.8	Problems in RFMBR.....	44
3.8.1	Pressure Drop.....	44
3.8.1.1	Pressure Drop in Axial Flow Beds.....	45
3.8.1.2	Pressure Drop in Radial Flow Packed Beds.....	45
3.8.2	Pinning in RFMBR.....	46
3.8.3	Particle Breakage in RFMBR.....	50
4.	MODEL VALIDATION	51
4.1	Model Evaluation.....	51
4.2	Temperature and Component Profiles.....	52
4.3	Discussions.....	56
5.	SIMULATION OF THE MODEL	57
5.1	Introduction.....	57
5.2	Feeding Pure Components.....	58
5.2.1	Naphthenes only in Fresh Feed.....	58
5.2.2	Paraffins only in Fresh Feed.....	59
5.3	Feeding Fresh Naphtha into R_1 and R_3 Reactors.	62
5.3.1	Hypothesis.....	62
5.3.2	Results.....	63
5.4	Feeding Fresh Naphtha into R_1 and R_4 Reactors	65
5.4.1	Hypothesis.....	65
5.4.2	Results.....	66
5.5	Feeding Fresh Feed in R_1 , R_3 and R_4 Reactors.....	68
5.5.1	Hypothesis.....	68
5.5.2	Results.....	69
5.6	Feeding Fresh Feed in R_1 , R_2 , R_3 and R_4 Reactors.....	71
5.6.1	Results.....	71
5.7	Summary and Conclusions.....	74

6.	CONCLUSIONS AND RECOMMENDATIONS	77
6.1	Conclusions.....	77
6.2	Recommendations.....	78
	REFERENCES	79
	APPENDICES	
Appendix A	Calculation the Properties of Naphtha	83
1.1	Density of Naphtha Feed.....	83
1.2	Velocity of Naphtha Feed.....	83
1.3	Reynolds Number of Naphtha Gas Flow.....	83
1.4	Liquid Hourly Space Velocity (LHSV).....	84
1.5	Weighted Average Inlet Temperature (WAIT).....	84
1.6	Catalyst Residence Time.....	85
Appendix B	Temperature and Composition Calculation at <i>i-th</i> Compartment In 1D Compartment in Series of RFMBR	87
2.1	Paraffin Dehydrogenation.....	88
2.2	Naphthenes Dehydrogenation.....	88
2.3	Naphthenes Hydro-cracking.....	89
2.4	Paraffins Hydro-cracking.....	89
2.5	Catalyst Activity.....	90
2.6	Mass of Catalyst.....	90
2.7	Changes of Components.....	91
2.8	Changes in Temperature.....	93
2.9	Results of Temperature and Flow Rate of Components.....	93
Appendix C	Compartment in Series Model for Naphtha Reforming in RFMBR reactors	95

LIST OF TABLES

Table 3.1	Reactor dimensions and moving bed properties.....	23
Table 3.2	The feed flow rate and inlet compositions.....	29
Table 3.3	Characteristic data of reforming catalyst.....	29
Table 3.4	The correction multiplier, η from Liang et al. and model results.....	30
Table 4.1	Summary of the feed and products for model and actual industrial data.....	55
Table 5.1	Summary of the input and output of reactors at diferrent scheme of fresh feed.....	61
Table 5.2	Summary of input and output of reactors at scheme of introducing fresh feed in R_1 and R_3 reactors.....	65
Table 5.3	Summary of input and output of reactors at scheme of introducing fresh feed in R_1 and R_4 reactors.....	68
Table 5.4	Summary of input and output of reactors at scheme of introducing fresh feed in R_1 , R_3 and R_4 reactors.....	71
Table 5.5	Summary of input and output of reactors at scheme of introducing fresh feed in R_1 , R_2 , R_3 and R_4 reactors.....	73
Table 5.6	Summary of the input and output of reactors at various schemes.....	74
Table 5.7	Screening for the best scheme.....	75

LIST OF FIGURES

Figure 1.1	Semi Regenerative Reforming (SRR) Technology.....	2
Figure 1.2	Fully Regenerative Reforming (FRR) Technology.....	3
Figure 1.3	Continuous Regenerative Reforming unit (CRR) with Radial Flow Moving Bed Reactor.....	4
Figure 1.4	A Diagram of Radial Flow Moving Bed Reactor (RFMBR)....	6
Figure 2.1	A flow Diagram for SRR Unit.....	14
Figure 2.2	A flow Diagram for CCR Unit.....	15
Figure 2.3	Schematic Diagram of RFMBR-CP-z Configuration.....	17
Figure 2.4	Four flow types of RFMBRs.....	18
Figure 2.5	Cavity Wall Profiles.....	19
Figure 2.6	Typical Flow Distribution over the Bed Length in a Radial Flow Reactor at the Same Flow rate for CP and CF configurations.	21
Figure 3.1(a)	Front view of radial flow moving bed reactor.....	24
Figure 3.1(b)	Top view of radial flow moving bed reactor.....	24
Figure 3.2	Compartment-in-series reactor model.....	25
Figure 3.3	An 'i-th' compartment reactor model.....	27
Figure 3.4	Effect of the correction multiplier of paraffin dehydrogenation, η_{R1} on the outlet temperature of the reactor..	38
Figure 3.5	Effect of the correction multiplier of paraffin dehydrogenation, η_{R1} on the aromatics production.....	38
Figure 3.6	Effect of the correction multiplier of paraffin dehydrogenation, η_{R1} on the hydrogen production.....	39
Figure 3.7	Effect of the correction multiplier of naphthene dehydrogenation, η_{R2} on the outlet temperature of the reactor..	40
Figure 3.8	Effect of the correction multiplier of naphthene dehydrogenation, η_{R2} on the aromatics production.....	40
Figure 3.9	Effect of the correction multiplier of naphthene dehydrogenation, η_{R2} on the hydrogen production.....	41
Figure 3.10	Effect of the correction multiplier of hydro cracking, η_c on the outlet temperature of the reactor.....	42

Figure 3.11	Effect of the correction multiplier of hydro cracking reaction, η_c on the aromatics production.....	42
Figure 3.12	Effect of the correction multiplier of hydro cracking reaction, η_c on the hydrogen production.....	43
Figure 3.13	An axial (a) and radial (b) gas flow.....	44
Figure 3.14	A RFMBR model before pinning occur.....	47
Figure 3.15	The pinning mechanism suggested by Ginestra and Jackson..	47
Figure 3.16	A mechanism of pinning at the downstream perforated wall...	48
Figure 4.1	Effect of catalyst weight fraction on the temperature along the radial flow moving bed reactor.....	53
Figure 4.2	Effect of catalyst weight distribution on the flow rate of naphtha components in the radial flow moving bed reactor.....	53
Figure 4.3	Profiles of catalyst activity versus residence time along the radial flow moving bed reactor.....	56
Figure 5.1	Effect of catalyst weight fraction on the temperature along the radial flow moving bed reactor when feeding naphthenes and hydrogen in fresh feed.....	58
Figure 5.2	Effect of catalyst weight fraction on the naphtha components in radial flow moving bed reactor when feeding naphthenes and hydrogen in fresh feed.....	59
Figure 5.3	Effect of catalyst weight fraction on the temperature along the radial flow moving bed reactor when feeding paraffins and hydrogen in fresh feed.....	60
Figure 5.4	Effect of catalyst weight fraction on the naphtha components in radial flow moving bed reactor when feeding paraffins and hydrogen in fresh feed.....	60
Figure 5.5	Effect of catalyst weight fraction on the temperature along the radial flow moving bed reactor when introducing fresh feed in R_1 and R_3 reactors.....	63
Figure 5.6	Effect of catalyst weight fraction on the naphtha components in radial flow moving bed reactor when introducing fresh feed in R_1 and R_3 reactors	64

Figure 5.7	Effect of catalyst weight fraction on the temperature along the radial flow moving bed reactor when introducing fresh feed in R_1 and R_4 reactors.....	66
Figure 5.8	Effect of catalyst weight fraction on the naphtha components in radial flow moving bed reactor when introducing fresh feed in R_1 and R_4 reactors	67
Figure 5.9	Effect of catalyst weight fraction on the temperature along the radial flow moving bed reactor when introducing fresh feed in R_1 , R_3 and R_4 reactors.....	69
Figure 5.10	Effect of catalyst weight fraction on the naphtha components in radial flow moving bed reactor when introducing fresh feed in R_1 , R_3 and R_4 reactors	70
Figure 5.11	Effect of catalyst weight fraction on the temperature along the radial flow moving bed reactor when introducing fresh feed in R_1 , R_2 , R_3 and R_4 reactors.....	72
Figure 5.12	Effect of catalyst weight fraction on the naphtha components in radial flow moving bed reactor when introducing fresh feed in R_1 , R_2 , R_3 and R_4 reactors	72

LIST OF SYMBOLS

α	Catalyst activity
A	Cross section of reactor (m^2)
C_t	Total molar concentration (kmol/m^3)
c_p	Specific heat ($\text{kJ}/\text{kmol.K}$)
d_p	Particle diameter (m)
d_b	Outer diameter of catalyst bed (m)
d_{cp}	Diameter of center pipe (m)
F_i	Flow rate of naphtha gas in i -th compartment (kmol/h)
F_t	Total molar flow rate (kmol/h)
F_{cat}	Flow rate of catalyst (kg/h)
f	Wall to bed friction factor
g	Acceleration due to gravity (m/s^2)
h_f	Heat transfer coefficient ($\text{W}/\text{m}^2.\text{K}$)
H/L	Height of reactor (m)
k_m	Mass transfer coefficient (m/s)
k_{f1}	Forward rate constant of paraffins dehydrogenation ($\text{kmol}/\text{kg.cat.h.MPa}$)
k_{f2}	Forward rate constant of naphthenes dehydrogenation ($\text{kmol}/\text{kg.cat.h.MPa}^2$)
k_{f3}	Forward rate constant of naphthenes hydro cracking ($\text{kmol}/\text{kg.cat.h.}$)

k_{f4}	Forward rate constant of paraffins hydro cracking (kmol/kg.cat.h.)
K_{e1}	Equilibrium constant of paraffin dehydrogenation (MPa ³)
K_{e2}	Equilibrium constant of naphthenes dehydrogenation (MPa ⁻¹)
k_R	Rittinger's constant
ρ_p	Density of catalyst bed (kg/m ³)
P_P	Partial pressure of paraffins (kPa)
P_N	Partial pressure of naphthenes (kPa)
P_A	Partial pressure of aromatics (kPa)
P_H	Partial pressure of hydrogen (kPa)
P_t	Total pressure (kPa)
Q_s	Mass flow rate (kg/h)
r_1	Reaction rates of paraffins dehydrogenation (kmol/kg.cat.h)
r_2	Reaction rates of naphthenes dehydrogenation (kmol/kg.cat.h)
r_3	Reaction rates of naphthenes hydro cracking (kmol/kg.cat.h)
r_4	Reaction rates of paraffins hydro cracking (kmol/kg.cat.h)
$-r_d'$	Deactivation rate (h ⁻¹)
R_i	radius for i -th compartment (m)
S_a	Specific surface area of catalyst pellet (m ² /kg)
T_H	Inlet temperature of gas into catalyst bed (K)
T_L	Output temperature of gas from catalyst bed (K)
T_i	Temperature in for each compartment (K)

t	Residence time (h)
u	Velocity of gas flow (m/s)
y	Mole fraction
ΔM_c	Catalyst weight (kg)
$-\Delta H_r$	Heat of reaction (kJ/kmol)
ΔR	Compartment size (m)

Greek letters

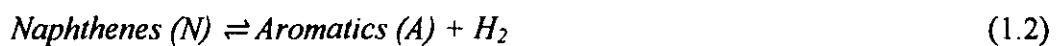
ε	Void fraction of bed
ε_f	fraction of fines
η_{R1}	Correction multiplier for paraffins dehydrogenation
η_{R2}	Correction multiplier for naphthenes dehydrogenation
η_c	Correction multiplier for hydro-cracking
ρ_p	Density of catalyst particle (kg/m ³)
ρ_c	Density of catalyst (kg/m ³)
ν_{ij}	Stoichiometric coefficient of reactant i in reaction j
μ	Viscosity of gas phase (kg/m.s)

CHAPTER 1

INTRODUCTION

1.1 Naphtha Reforming

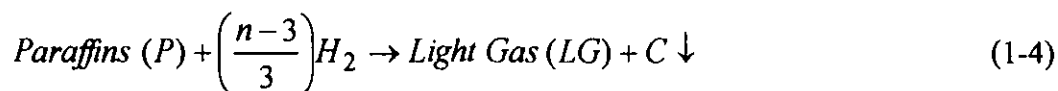
Naphtha is a complex mixture of C₅ to C₁₂ hydrocarbons in the boiling point range from 90 °C – 180 °C [1]. Catalytic reforming is extensively practiced in the petroleum-refining industry to rearrange the hydrocarbon molecules in the naphtha feedstock to produce higher octane number components such as isomers, naphthenes and aromatics. These high octane components are blended with naphtha to produce gasoline reformat with the necessary octane number. Aromatics are also needed for further processing to petrochemicals. Hydrogen is a by-product useful for other refining processes such as hydro-treating and hydro-cracking. The unit process reactions in reforming process include dehydrogenation and aromatization.



These reactions are reversible and endothermic in nature. Thermodynamically high temperature and low pressure favor these reactions. Some of the hydrogen is recycled to sustain reformer reactor pressure and to restrain coke formation.

Naphtha reforming needs a dual-function of catalyst with metal and acid catalyst functions. The metal (Pt or Pt-Re or Pt-Ir) is dispersed on alumina which has some acidity. Addition of chlorine to alumina enhances its acidity. The metal catalyst promotes dehydrogenation (extraction of hydrogen from hydrocarbons) and aromatization reactions while the acid catalyst promotes cracking reactions. Reforming reactions require a delicate balance between these metals and acid sites. Chlorinated alumina with Pt/Re is widely used as the catalyst.

Catalytic naphtha reforming processes are accompanied by side reactions such as hydro-cracking of naphtha which can consume hydrogen and produce lighter hydrocarbon molecules with carbonaceous deposits causing catalyst deactivation.



Where n is carbon number and $C \downarrow$ is coke deposition on the catalyst. These reactions are irreversible and exothermic in nature.

1.2 Naphtha Reforming Technology

Reforming is a net endothermic vapor phase reaction in presence of a slowly deactivating solid phase catalyst. Adiabatic packed bed reactors are used to carry out reforming process. There are three types of reforming process technologies - Semi Regenerative Reforming (SRR), Fully Regenerative Reforming (FRR) and Continuous Regenerative Reforming (CRR).

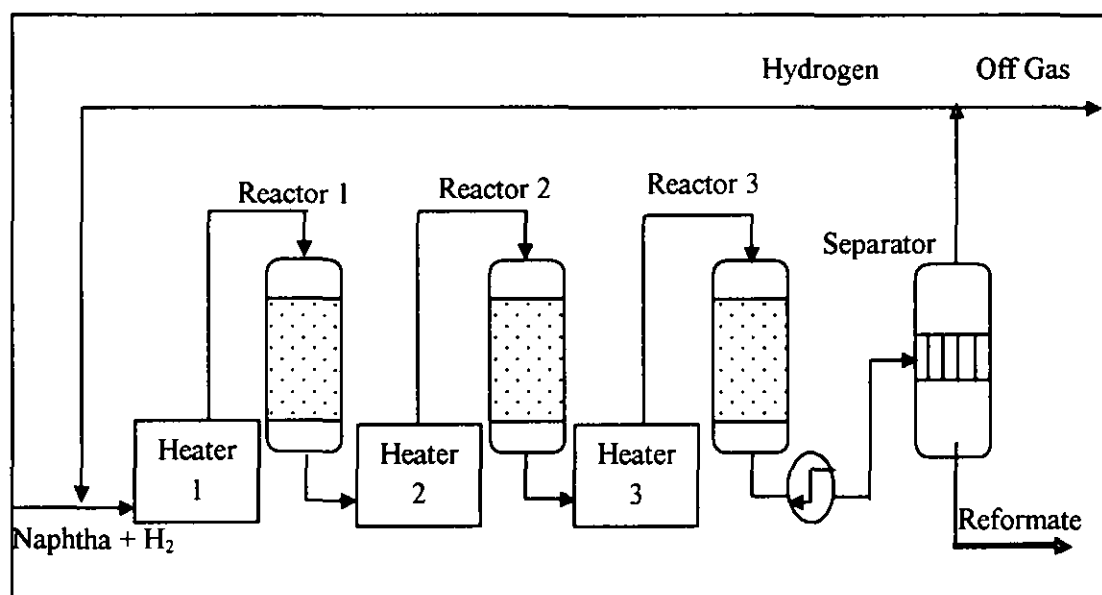


Fig. 1.1: Semi Regenerative Reforming (SRR) technology.

Fig. 1.1 shows the SRR technology. The SRR unit consists of three adiabatic fixed bed reactors in series with facility to pre-heat the feed to each unit. Early SRR units were operated at relatively high pressure (25 – 35 bars). The developments of improved catalysts that had lower tendency for coke formation enabled operation at lower pressure (15-20 bars), while maintaining same catalyst life (typically 1 year). The longer the required cycle length, the greater the amount of catalyst. The reformers are shut down periodically (typically six months) as catalyst activity declines because of coke deposition to regenerate the catalysts in situ by controlled coke burn off [2], [3]. The catalyst is also treated with chlorine in order to replenish acid sites of the catalyst.

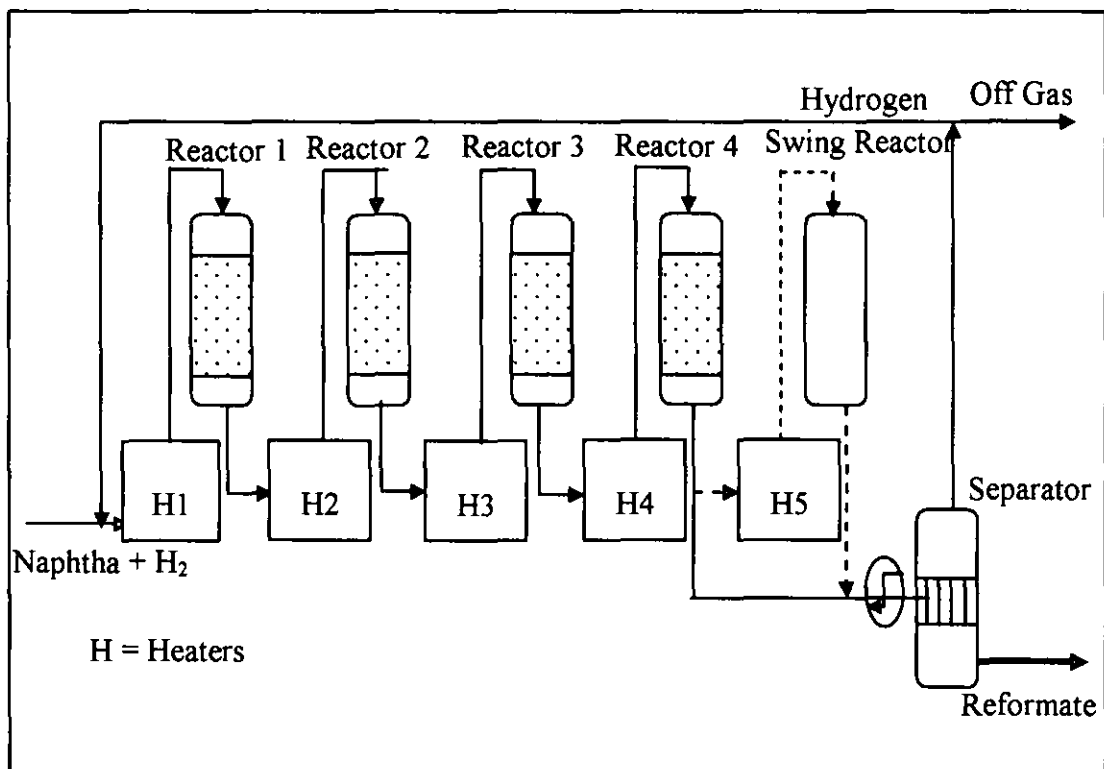


Fig. 1.2: Fully Regenerative Reforming (FRR) technology.

In Fully Regenerative Reforming (FRR) process technology shown in Fig. 1.2, an additional swing reactor is provided to allow one reactor to be taken off line at a time for regeneration while the rest of the reactors permit continuous production. Generally, the reactors are at the same size. FRR is able to operate without shutdown for two or three year [1] - [2].

Continuous Regenerative Reforming unit (CRR) developed by UOP and IFP is widely used in the industry and shown in Fig.1.3. It consists of a reformer and a regenerator. The reformer consists of four reactors, stacked one on top of the other and the catalyst particles move as a moving bed through the stack of four reactors from top to bottom while the reactant flows radially [1], [3]. Such reactors are known as radial flow moving bed reactors (RMFBR).

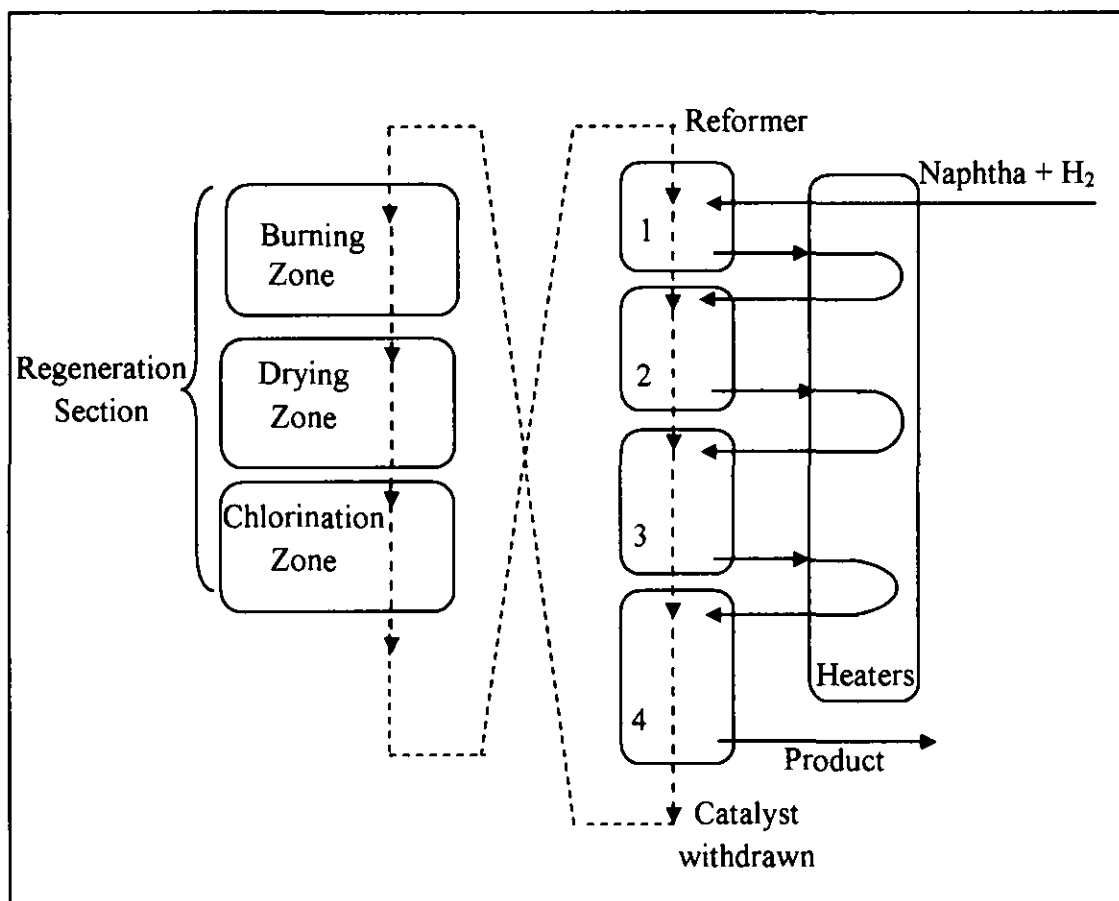


Fig. 1.3: Continuous Regenerative Reforming unit (CRR) with radial flow moving bed reactor.

Coked catalyst is continuously withdrawn from the bottom reactor and sent to the top of regeneration reactor; the catalyst moves downwards as a moving bed while they get regenerated by controlled coke burn off, get dried and chlorinated. Movement of catalyst particles generates fines due to attrition; the fines are removed and replenished with fresh catalyst while returning the fresh catalyst to the top of the first reforming reactor for continuous basis. Catalyst transports through the reactors and the regenerator is driven by gravitational force, whereas gas lift will transport the catalyst from the reactor/regenerator bottom to the top of the regenerator/reactor.

Catalyst circulation rate is controlled to maintain the reformat yield. The continuous reforming process is capable of operation at lower pressures and higher temperatures as the catalyst activity is maintained high by the continuous regeneration of the catalyst on catalyst circulation.

In CRR unit, naphtha gas is mixed with hydrogen and gets heated to the reaction temperature before it enters the first reactor. The effluent from the first reactor will reheat to reaction temperature before enters the second reactor and the effluent from second reactor get reheat before enters the third reactor. Effluent of third reactor gets reheat and enters the fourth reactor. Effluent from fourth reactor goes to separator to separate reformat, light gas and hydrogen.

1.3 Naphtha Reforming in Radial Flow Moving Bed Reactor

Generally the four reactors are quite tall and hence the pressure drop for such tall reactors can be excessively high. However, organizing the gas flow in the radial direction can decrease velocity as well as path length for flow and hence can reduce the pressure drop drastically. In radial flow reactors, the catalyst is held as an annular bed between two perforated coaxial cylinders; the reactant gas flow can be from outside to inside (or inside to outside) through the moving bed in the annular space in between the two coaxial perforated cylinders [4]. The packed bed of particles can move downwards to facilitate withdrawal of slowly decaying catalysts. Such beds are known as a radial flow moving bed reactor (RFMBR) as shown in Fig. 1.4.

A RFMBR is used in UOP/ IFP for reforming as well as catalyst regeneration by controlled coke burn off, drying and chlorination. The catalyst circulation rate is low as the catalyst decays in weeks. In contrast, catalyst circulation rates in FCC reactors are very high as the catalyst decays in seconds.

Thus, RFMBR is a unique energy efficient reactor used for naphtha reforming and dehydrogenation of propane. Though they are widely used in petroleum refineries, very little has been published about them in the open literature.

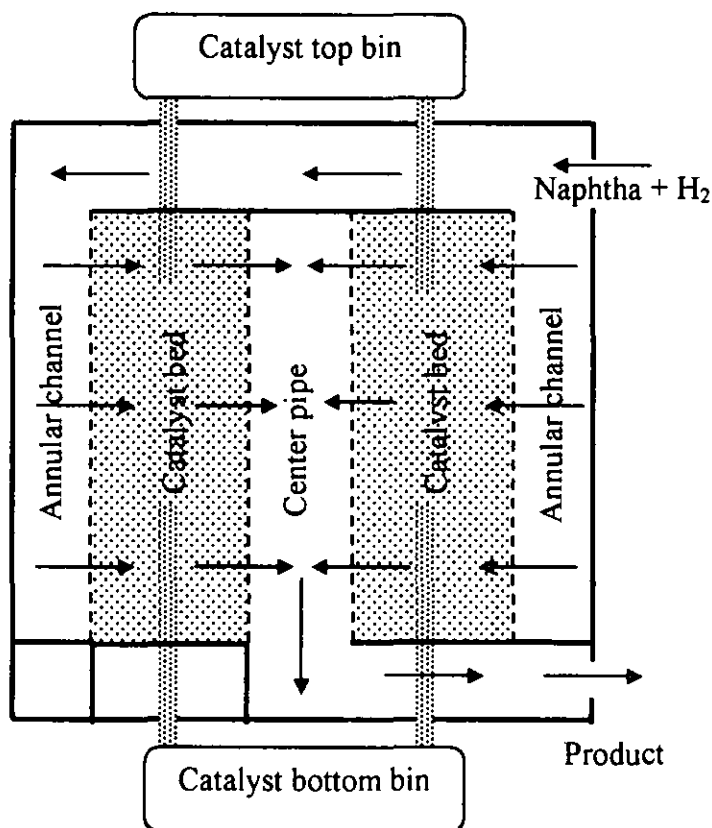


Fig. 1.4: A diagram of radial flow moving bed reactor (RFMBR).

1.4 Problem Statement

In a petroleum refinery, naphtha is reformed in a RFMBR (Radial Flow Moving Bed Reactor) to produce aromatics and hydrogen. A parallel (unwanted) hydro-cracking reaction may also convert naphtha to light gases with consumption of hydrogen. Very little is known in the open literature about the performance of naphtha reforming in a RFMBR to help in analyzing strategies to minimize hydro-cracking reactions. Performance of the RFMBR is dependent on the characteristics of catalyst, reaction rate constants, catalyst decay rate constants, gas velocity, particle velocity, pinning and particle attrition. Quantitative model to estimate conversions and yields incorporating the various factors affecting naphtha reforming in a RFMBR is needed to help in analyzing ways and means of reducing the parallel hydro-cracking reactions. Simple models to explain the phenomena of pinning and attrition are needed to reduce their impact on reactor performance. In this thesis, an attempt is

made to develop these models and suggest strategies to improve production of aromatics and hydrogen while reducing production of light gases.

1.5 Objectives

Followings are the main objectives of the project:

- To develop a heterogeneous gas-solid catalytic reactor model to represent the operation of naphtha reforming in radial flow moving bed reactor (RFMBR).
- To simulate and investigate the sensitivity of the model with various parameters.
- To develop simple models to explain the phenomena of pinning and attrition.
- To explore strategies to minimize production of light gases and improve the production of aromatics and hydrogen.

1.6 Scope of the Study

Naphtha reforming process is a matured technology and there is constant endeavor to improve the catalysts, reactors, regenerators and operating strategies to maximize aromatics and hydrogen production while reducing light gas production.

This work aims at developing a model to describe the performance of naphtha reforming in a radial flow moving bed reactor. The model will be used to simulate and investigate ways and means of improving the productivity of the reformer. This work also aims at developing simple models to explain the phenomena of pinning and attrition.

CHAPTER 2

LITERATURE REVIEW

2.1 Reforming Chemistry

Naphtha contains many C₅ to C₁₂ hydrocarbon components with an octane number of around 55. Straight chain paraffins have relatively low octane numbers whereas branched chain paraffins and aromatics have higher values. The reforming process will improve the octane number by conversion of paraffins and naphthenes to aromatics.

The network of reforming reactions in detail can be quite complex due to the large number of reactants, intermediates and products involved. To reduce the complexity, various chemical species are lumped together as pseudo components to describe the reaction kinetics. Smith [5] considered naphtha to consist of paraffins, naphthenes and aromatics; paraffins and naphthenes get converted to aromatics and hydrogen by dehydrogenation and aromatization as well as to lighter components by hydro-cracking. Mahdavian et al. [6], Hu et al. [7], Ancheyta-Juarez and Villafuerte-Macias [8], Li et al. [9], Behin and Kavianpour [10] and Stijepovic et al. [11] reviewed developments in reaction schemes with larger number of lumps.

Consideration of larger number of lumps increases the complexity of the reaction mechanism and increases the number of reaction kinetic constants needed to describe the process. Also, rate constants in the kinetic models depend on the feedstock and catalyst properties. To capture the performance of industrial reformers, information on the reactor configuration, gas and particle flows, heat and mass transfer need to be coupled with the reaction kinetics. Hence, using the minimum number of essential lumps to describe the kinetics is necessary to keep the model tractable. In the present work kinetics proposed by Smith [5] is used for the reactor modeling.

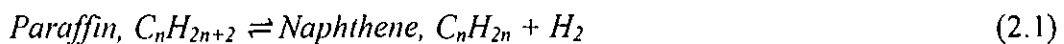
2.1.1 Naphtha Reforming Catalyst

Platinum supported on chlorinated alumina is the widely used industrial reforming catalyst. The metal sites are responsible for addition of hydrogen to the unsaturated species and reforming. Reforming reactions require a delicate balance between the metals and acid sites. Addition of rhenium to platinum reforming catalyst enhances the stability of platinum catalyst. Formulation based on Pt and Re, typically containing between 0.1 and 0.8 wt % of each metal, are among the most important industrial reforming catalysts. The advantage of the bimetallic catalyst is that they permit operation at lower pressures and higher temperatures.

2.1.2. Kinetics of Reactions

The reactions in naphtha reforming are (1) dehydrogenation of paraffin to naphthene (2) aromatization of naphthene to aromatic and (3) hydro-cracking of naphthene and paraffin. The kinetic equations and parameters reported by Smith [5] are as follows:

2.1.2.1. Dehydrogenation of Paraffin to Naphthene



$$r_1 = \left(\frac{k_{f1}}{K_{e1}} \right) (K_{e1} P_N P_H - P_P) \eta \alpha \quad (2.2)$$

$$k_{f1} = 9.87 \exp (35.98 - 58550/1.8T) \quad (2.3)$$

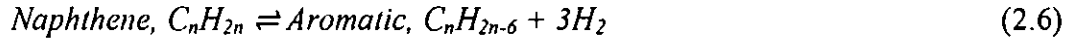
$$K_{e1} = 9.87 \exp (-7.12 + 8000/1.8T) \quad (2.4)$$

$$\Delta H_{r1} = -36953.33 \text{ kJ/kmol} \quad (2.5)$$

Where r_1 is reaction rates of paraffins dehydrogenation, (kmol/kg.cat.h), k_{f1} is forward rate constant, (kmol/ kg.cat.h.MPa), K_{e1} is equilibrium constant, (MPa³), η is correction multiplier, α is catalyst activity, ΔH_{r1} is heat of reaction, (kJ/kmol), P_N is

naphthene partial pressure, P_H is hydrogen partial pressure and P_P is paraffin partial pressure.

2.1.2.2. Aromatization of Naphthene to Aromatic



$$r_2 = \left(\frac{k_{f2}}{K_{e2}} \right) (K_{e2}P_N - P_A P_H^3) \eta a \quad (2.7)$$

$$k_{f2} = 9.87 \exp(23.21 - 36350/1.8T) \quad (2.8)$$

$$K_{e2} = 1.04 \cdot 10^{-3} \exp(46.15 - 50784/1.8T) \quad (2.9)$$

$$\Delta H_{r2} = 71038.06 \text{ kJ/kmol} \quad (2.10)$$

Where r_2 is reaction rates of aromatization reaction, (kmol/kg.cat.h), k_{f2} is forward rate constant, (kmol/ kg.cat.h.MPa²), K_{e2} is equilibrium constant, (MPa⁻¹) and P_A is aromatic partial pressure.

2.1.2.3. Hydro-cracking of Naphthene



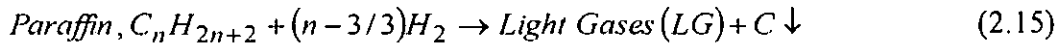
$$r_3 = k_{f3} (P_N / P) \eta a \quad (2.12)$$

$$k_{f3} = \exp(42.97 - 63800/1.8T) \quad (2.13)$$

$$\Delta H_{r3} = -51939.31 \text{ kJ/kmol} \quad (2.14)$$

Where r_3 is reaction rates of naphthene hydro-cracking, (kmol/kg.cat.h), k_{f3} is forward rate constant, (kmol/ kg.cat.h.) and P is total pressure in reactor.

2.1.2.4. Hydro-cracking of Paraffin



$$r_4 = k_{f4}(P_P/P)\eta a \quad (2.16)$$

$$k_{f4} = \exp(42.97 - 63800/1.8T) \quad (2.17)$$

$$\Delta Hr_4 = -56597.54 \text{ kJ/kmol} \quad (2.18)$$

Where r_4 is reaction rates of paraffins hydro-cracking, (kmol/kg.cat.h) and k_{f4} is forward rate constant, (kmol/ kg.cat.h.).

2.1.3. Catalyst Deactivation by Coking Kinetics

The activity of reforming catalyst decreases mainly due to carbon deposition on the catalyst surface as a result of undesired side reactions. Coke deposition is slow in packed bed reactors used in SRR process with a normal operating time of 18 to 20 months on stream. Reforming catalyst deactivation has been extensively studied, and while different approaches have been used it by coke formation there is no generally accepted model. Turpin's model proposes an exponential correlation between catalyst deactivation and coke deposition [13]. Tailleux and Davila [13] analyzed the reforming and deactivation process in terms of a 12 lumps kinetic model and two site deactivation model based on data obtained from four long-term micro-pilot plant tests. The deactivation kinetics for the metal and acid sites of the catalyst were proposed as

$$\frac{da_a}{dt} = -k_a a_a C_{ACP}^{0.5} \quad (2-19)$$

$$k_a = 5 \cdot 10^6 \exp\left(-\frac{32000}{RT}\right) \quad (2-20)$$

$$\frac{da_m}{dt} = -k_m a_m \frac{C_{ACP}^{0.5}}{1 + bP_{H_2}} \quad (2-21)$$

$$k_m = 1.2 \cdot 10^4 \exp\left(-\frac{25000}{RT}\right) \quad (2-22)$$

Where α_a , catalyst activity for acid sites, α_m , catalyst activity for metal sites, k_a , deactivation rate constant for acid sites, k_m , deactivation rate constant for metal sites, C_{ACP} is concentration of alkylcyclopentane and P_{H_2} is hydrogen partial pressure.

Rahimpour [14] proposed catalyst deactivation kinetics as

$$\frac{da}{dt} = -k_d a^7 \quad (2-23)$$

$$k_d = 5.926 \cdot 10^{-5} \exp\left(-\frac{164200}{R}\left(\frac{1}{T} - \frac{1}{770}\right)\right) a^7 \quad (2-24)$$

2.2. Semi Regenerative Reforming (SRR) Technology

A flow diagram for semi regenerative reforming technology is shown in Fig. 2.1. It consists of three reactors R_1 , R_2 and R_3 in series. The naphtha feed is mixed with recycled hydrogen and heated in the fired heater F1 to the reaction temperature before entering the first reactor R_1 . As the reactions are endothermic in nature and reactors are operated in adiabatic mode, gas stream exiting reactor R_1 and R_2 need to be reheated to the reaction temperature in fired heaters F2 and F3 respectively. Due to the high inlet temperature and fresh feed, reaction rate in the first reactor is high and consequently temperature decreases rapidly; the temperature cannot be allowed to drop below a critical value to maintain reasonable reaction rates; hence, the first reactor is always smaller than the other reactors and the last reactor is the biggest. The product stream from the last reactor is cooled to separate hydrogen from liquid hydrocarbon reformat [1] - [2], [15].

The activity of the catalyst decays over a period of time (6 to 12 months) and the unit needs to be shut down for catalyst regeneration. The catalyst can be regenerated in situ 5-10 times before its activity falls below the economic minimum. The time required for regeneration is 3 to 6 days and depends upon the amount of carbon deposited on catalyst to be burned off.

quantities of slightly deactivated catalyst is continuously withdrawn from the bottom of the reforming reactor tower, transported to the top of the regeneration tower for catalyst regeneration as the catalyst moves down the regenerator, the regenerated catalyst is withdrawn from regeneration reactor tower and returned to the top of the reforming reactor tower. The reforming reactor tower consists of four reactor units stacked one above the other to facilitate flow of the catalyst by gravity. Catalyst transport through the reactors and regenerators is by gravity flow, while lift from bottom to the top of reactors is by pneumatic transport. [1], [3].

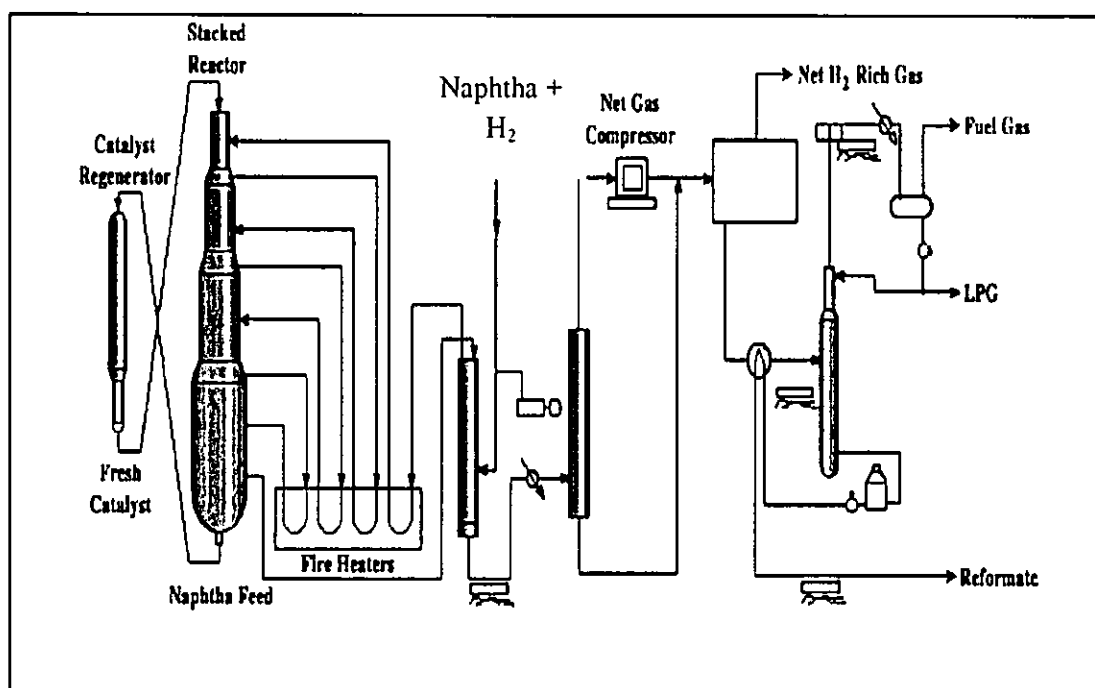


Fig. 2.2: A flow Diagram for CRR Unit [1].

The continuous reforming process is capable of operation at low pressures and high severity due to the continuous regeneration of the catalyst. Operating pressures are in the 44-60 psi (300-400 kPa) range, and design reformate octane number is in the range of 95-108. There are some advantages of CRR such as production of higher aromatics even working with low feed quality, lower required recycles ratio and lower pressure with higher hydrogen yield [1]-[3].

Though these units are widely used, very little has been published about their performance in the open literature. Problems associated with product selectivity, catalyst pinning and breakage are a few of the issues that need to be addressed.

Information available in the literature on reforming reactor in CRR technology is presented in the following section.

2.3.1. Reactor Models for CRR

Lee et al. [22] formulated steady state and dynamic flow sheets for naphtha reforming unit with a catalyst circulation and regeneration system with an aim to workout economic benefits. They modeled the reforming unit to consist of 7 CSTRs; the catalyst particles flow through the 7 CSTRs in series while gaseous reactants flow in parallel through the 7 CSTRs. Naphtha considered contains of paraffins, naphthenes and aromatics only and the reaction kinetics proposed by Smith was adopted; and tuned the kinetic parameters such as activation energies and heat of reactions with the actual data using SPEEDUP (Estimation section). Deactivation of catalyst as it flows through 7 CSTRs was considered by measured the time delay effect caused by deposition of coke on the catalyst. Deactivation in each CSTR was estimated considering it consists of 7 fragments. (Essentially this means catalyst flow is assumed to be in plug flow through the 7 CSTRs each with 7 Fragments.). Gaseous reactants were assumed to flow through the 7 CSTRs in parallel; that is gas flow in each CSTR is well mixed. The regenerator was also modeled in a similar way. With the steady state flow sheets, the results are more precise with a relative error 1.2%.

Hu et al. [7] considered reaction matrix of naphtha feed containing four paraffins (P_6, P_7, P_8, P_9), four naphthenes (N_6, N_7, N_8, N_9) and four aromatics (A_6, A_7, A_8, A_9); on reaction they get reformed to the 12 naphtha cuts and five light gases (C_1, C_2, C_3, C_4, C_5); considering such a scheme, they developed a model for commercial catalytic reforming process to designing new process, monitor and optimize the process performance for improving aromatic yield. They assumed plug flow for reactants as well as catalyst. Catalyst deactivation due to coking was accounted in terms an average deactivation function as well as the adsorption of chemical lumps on the catalyst surface. The parameters were estimated by minimization of the sum of the squares of the deviations between plant and calculated values of key variables such as composition of components and outlet temperatures of reformers. The

validated model was used to simulate and optimize; they observed that the yield of aromatics could be increased from 65.22% to 67.45%.

These two models are macroscopic in nature and provide very little information on the various factors that go into the model. As a first step in this direction, structure and operational details of radial flow moving bed reactor are presented in the following section.

2.4. Radial Flow Moving Bed Reactor

Radial flow moving bed reactor (RFMBR) consists of three coaxial pipes - reactor shell (annular channel), outer pipe with perforated wall and inner pipe with perforated wall (center pipe) as shown in Fig. 2.3.

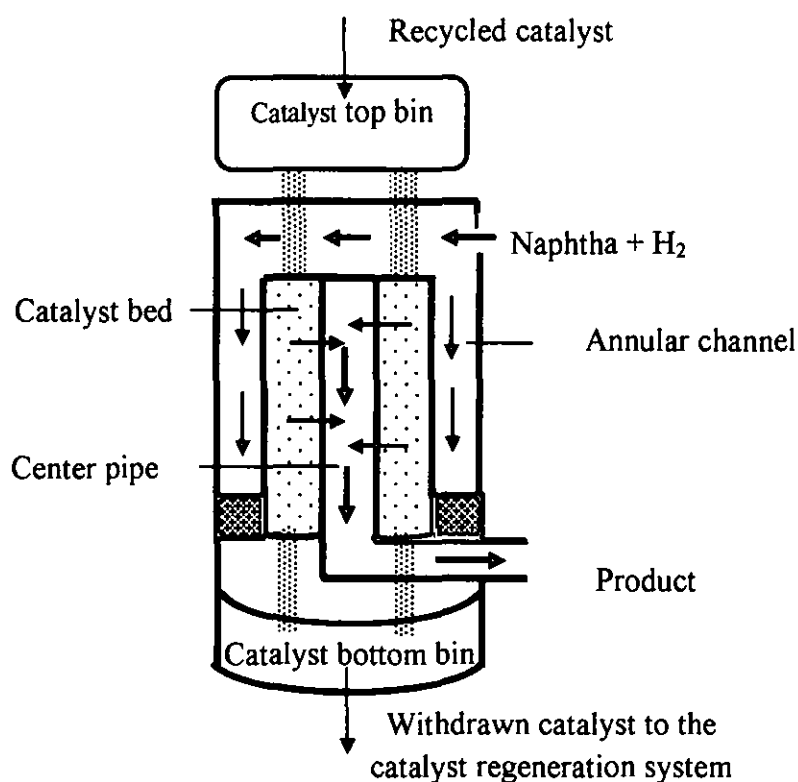


Fig. 2.3: Schematic diagram of a RFMBR- CP-z Flow Configuration.

Gas is introduced into the reactor shell and it flows radially inward through the outer and inner perforated walls of and exit through the inner pipe in concurrent flow with respect to input flow in the outer channel. The catalyst particles flow

downwards under gravity in the vertical annular region formed between the outer and inner pipes in a moving bed form and the reactant mixture (gas phase) flows radially across the catalyst bed. This structure is generally referred to as CP-z (centripetal flow) configuration.

Variants of RFMBR flow structures are shown in Fig.2.4. Gas flow can be from outer channel to inner channel (CP structure) or inner channel to outer channel (CF structure). Also the gas flow direction in the inner and outer channels can be concurrent (Z-structure) or countercurrent (π -structure). Together, there are four possibilities CP-Z, CP- π , CF-Z and CF- π . These variant RFMBR flow structures are shown in Fig.2.4.

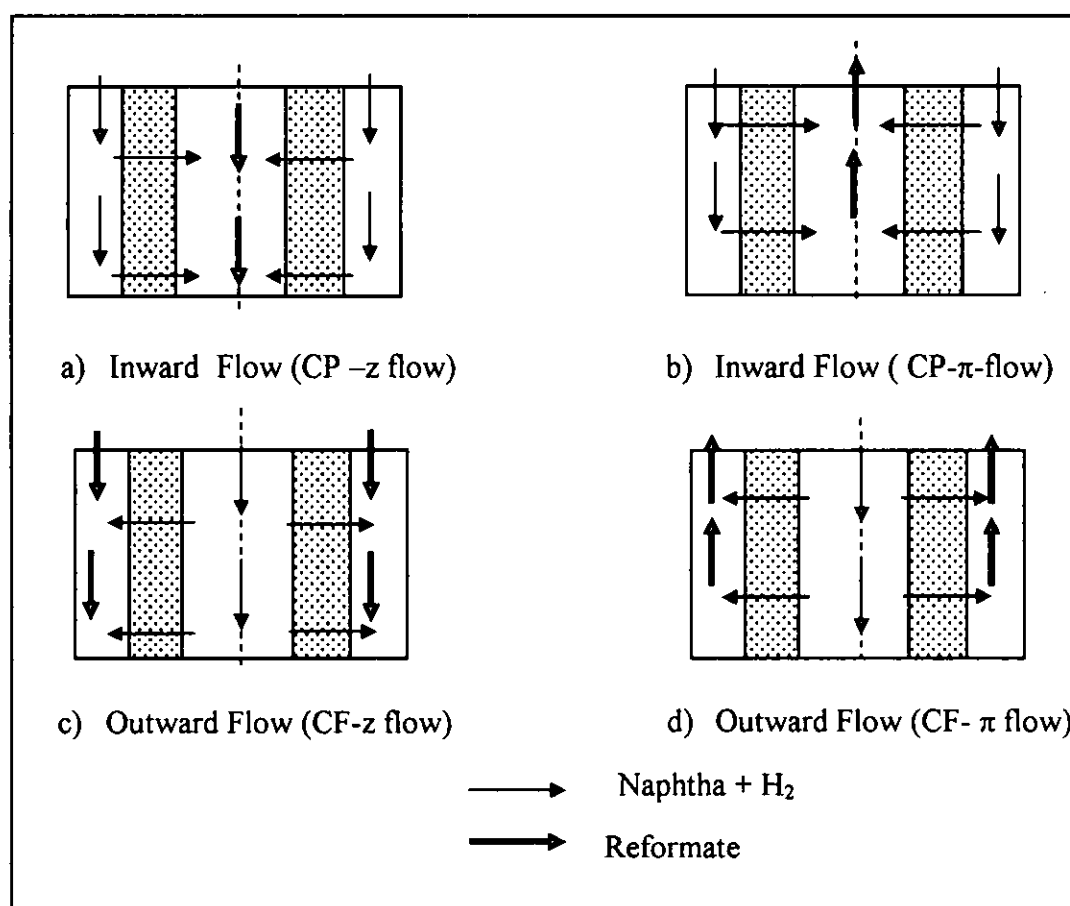


Fig. 2.4: Four flow types of RFMBRs [24].

It has been reported that gas flow can hinder the particle flow by the phenomena known as “pinning”.

2.5. Pinning

Bridgwater [23] observed that the drag force exerted by the flowing gas forces the catalyst bed against the downstream porous wall, thus increasing the frictional stress which opposes sliding of the material over this wall. If the gas flow is large enough, the resulting frictional force is sufficient to support the weight of the bed and downward motion ceases, at least in some region adjacent to the downstream wall. The bed is then said to be “pinned” by the gas flow, and the catalyst held immobile in this way becomes completely deactivated by coking, preventing continued operation of the reactor.

Ginestra and Jackson [24] observed that gas entry at the upstream wall pushes the particles away from perforated wall and reduces friction between moving solids and the upstream wall. This can compact the particles increasing resistance to gas flow through the bed of particles. This can lead to bed cavity accumulating near the upstream wall and grow with increasing pressure as shown in Fig. 2.5.

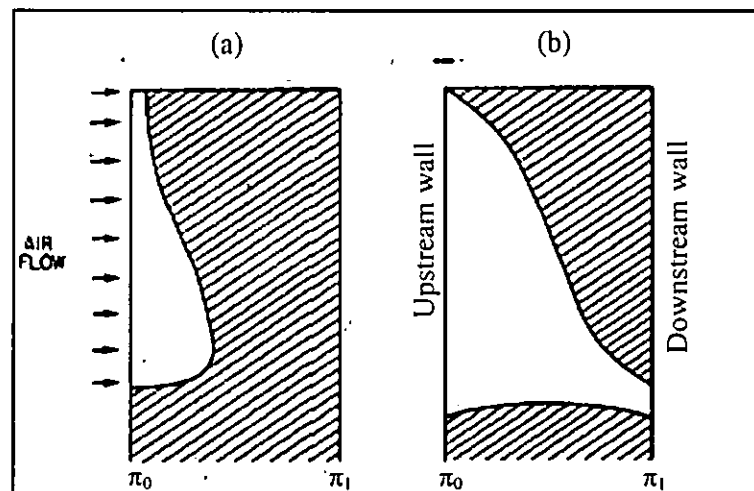


Fig. 2.5: Cavity wall profiles: (a) for $\pi_0 < \pi < \pi_1$ and (b) for complete pinning with $\pi = \pi_1$. [26]

The cavity is initiated at a critical π_0 ($=f\Delta P/D\rho g$) and can grow to reach the downstream wall at a value of π_1 blocking the flow of solid particles. This can increase the residence time of the catalyst particles in the reactor leading to catalyst deactivation and possible agglomeration of catalyst particles. Ginestra and Jackson

[24] concluded that for sufficiently slender deep beds (small values of D/L ratio), pinning and blockage of particle flow can be abrupt as π_0 equals π_1 .

Doyle et al. [25] extended the model of Ginestra and Jackson [24] for pinning in annular bed in an RFMBR by developed a model with assumption that catalyst bed behaves as a Coulomb material, with forces of dry friction where it slides over solid surfaces. The predicted gas pressure drops required for pinning are larger than those observed, but never by as much as a factor of two.

Chen et al. [26] observed that when the gas flow pressure drop increased to a critical value causing pinning, some particles close to the downstream face of the gas flow would stick together on the face and stop moving downwards. They observed that the pinning thickness increased linearly with the increase of pressure drop. Under the same gas velocity, the pinning thickness in the bed with wider cross-flow section of the gas flow is larger than that in the bed with narrower cross-flow section.

The dimensionless pinning thicknesses are almost equal for moving beds with different widths. As this paper is not accessible, details of their experimental work and proposed model cannot be fully appreciated. Thus, pinning still needs to be quantitatively accounted to describe particle residence time distribution.

Kareeri et al. [27] studied effects of radial flow maldistribution and flow direction of gas flow due to non-uniformity on radial flow reactor performance. Fig. 2.6 showed typical flow distributions in a radial reactor. To have a uniform flow distribution, the gas mass flow should be equally divided to produce an even carbon concentration over the catalyst bed height. If the mass flow is not equally divided, some parts of the bed will be under utilized and non uniform carbon concentration over the catalyst bed height.

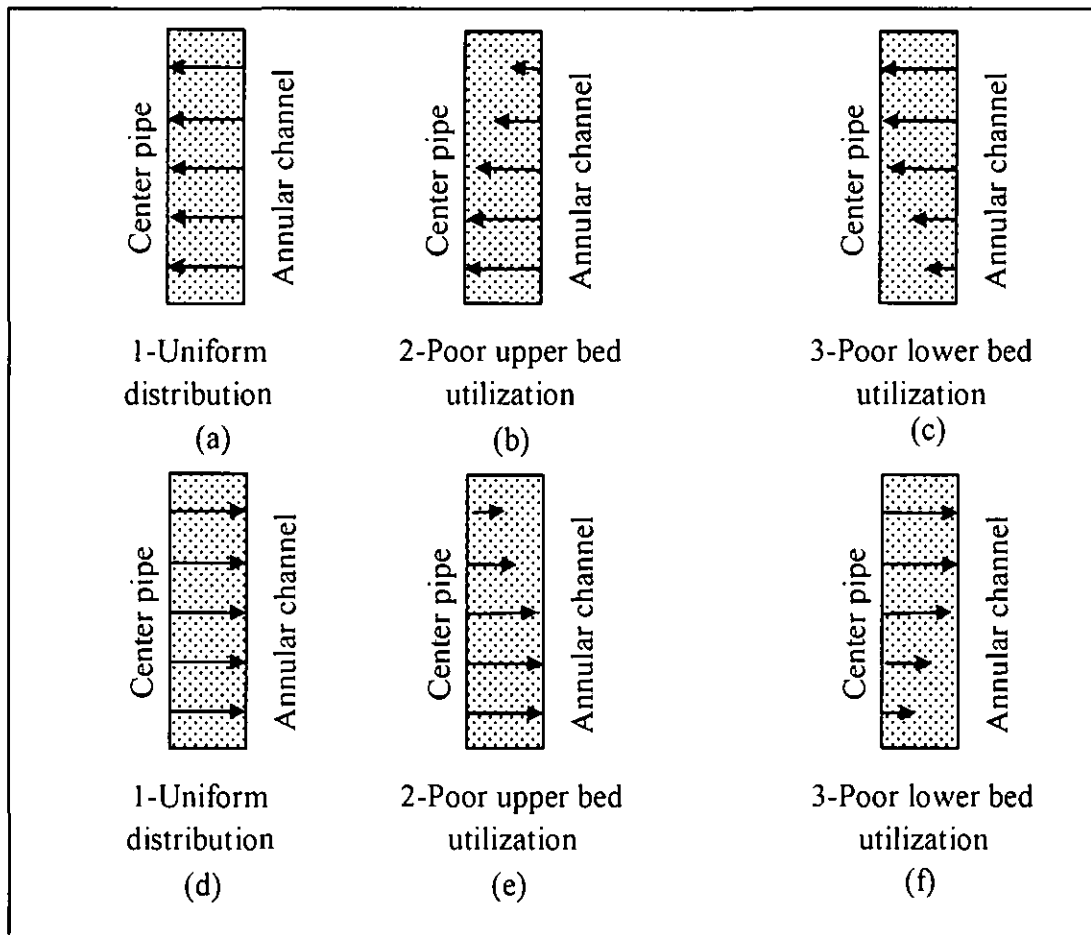


Fig. 2.6: Typical flow distribution over the bed length in a radial flow reactor at the same feed flow rate for CP configurations (a-c) and for CF configurations (d-f).

The arrow length represents the mass flow rate magnitude [27].

When a non uniform flow occurs, probability increased to have pinning against the center pipe or initiating cavity between annular channel and catalyst bed at the upper or bottom of the bed as showed in fig. 2.6(b) and fig. 2.6(c) for CP configurations. While in CF configurations in fig. 2.6(e) and fig. 2.6(f), the pinning will against the annular channel and the cavity between the center pipe and catalyst bed. A non uniform flow distribution affects the reaction conversion and selectivity and the temperature profile. The pinned catalyst maybe flow to regeneration section and may contain coke higher than limitation design for regeneration section. Hence, the equipment in regeneration section could damage.

Kareeri et al. [27] also analyzed the velocity profile of the gas flow in the annular channel and center pipe. The radial velocities in CF configurations are much closer

to each other than in CP configurations because of the unique radial pressure drop in each configurations. High radial velocity produces high radial pressure drop which increase the possibility of pinning to take place.

2.6. Particle Breakage

In a RFMBR unit operation, when the catalyst is moving, the dust is generated inside the reactor which can clog the movement of reactants and catalyst and contribute to pinning. This is due to the breakage of the catalyst during movement downward through the reactor. Kareeri [28] analyzed that having a small cavity is not a major problem but having a breakage of catalyst becomes a major problem in operation of RFMBR as it will affect the reactor performance.

2.7 Conclusion

In recent times, continuous catalytic reforming is carried out in radial flow moving bed reactors. Very little is known about their performance in terms of conversion as a function of operating variables. Excessive hydro-cracking is reducing productivity of aromatics and hydrogen. Particle breakage and catalyst decay add to operational difficulty. There is great need to develop reactor models which can explain their performance and help in developing strategy for enhancing their productivity. An attempt in this direction is presented in this thesis.

CHAPTER 3

MODEL FOR THE REACTOR

3.1. The Radial Flow Moving Bed Reactor

A schematic diagram of radial flow moving bed reactor, RFMBR, (front view) is shown in Fig. 3.1(a). The reactor consists of three concentric cylindrical pipes. The inner two cylindrical pipes are made of perforated walls and between them the catalyst flows downwards as a moving bed under the influence of gravity at a very low velocity of around 0.05 mm/s. The gas enters into the outer pipe and flows through the outer pipe, moving bed and inner pipe before flowing out through the inner pipe.

Top view of the reactor is shown in Fig. 3.1 (b). Gas at a temperature of T_H (793 K) flows radially inward through the moving catalyst bed. As the reforming reactions are net endothermic, gas and bed temperature decreases with position along the gas flow path. Cylindrical symmetry is assumed and a sector, as shown in Fig. 3.1(b) (highlighted in blue line), is considered for developing the reactor model. Table 3.1 shows the reactor dimensions and moving bed properties.

Table 3.1: Reactor dimensions and moving bed properties.

	L_b , m	L_p , m	D_{cp} , m	D_b , m	ΔR , m $= (D_b - D_{cp})/2$	ΔW , wt %
Reactor 1	8.7	7.9	0.4	1.2	0.4	14
Reactor 2	7.1	6.1	0.4	1.4	0.5	16
Reactor 3	8.3	7.1	0.4	1.6	0.6	25
Reactor 4	11.7	10.3	0.4	1.8	0.7	45

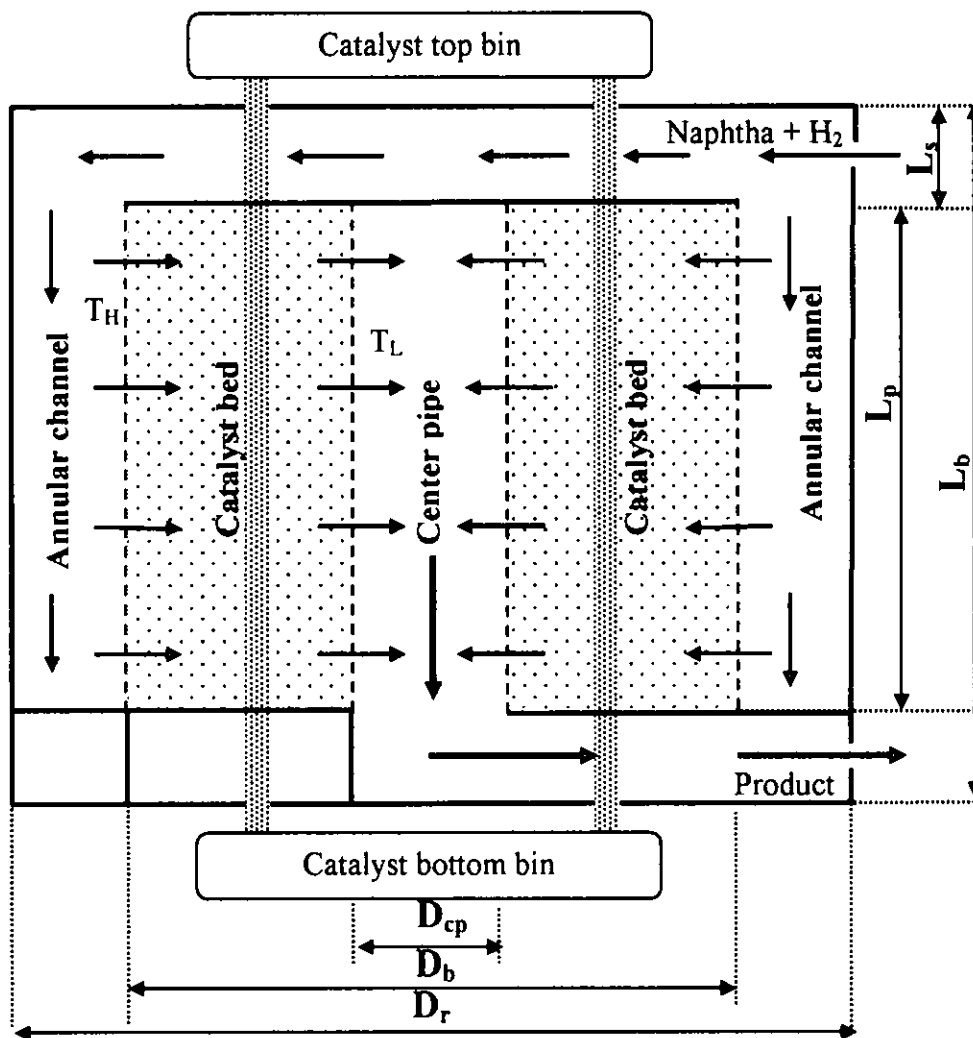


Fig. 3.1(a): Front view of radial flow moving bed reactor.

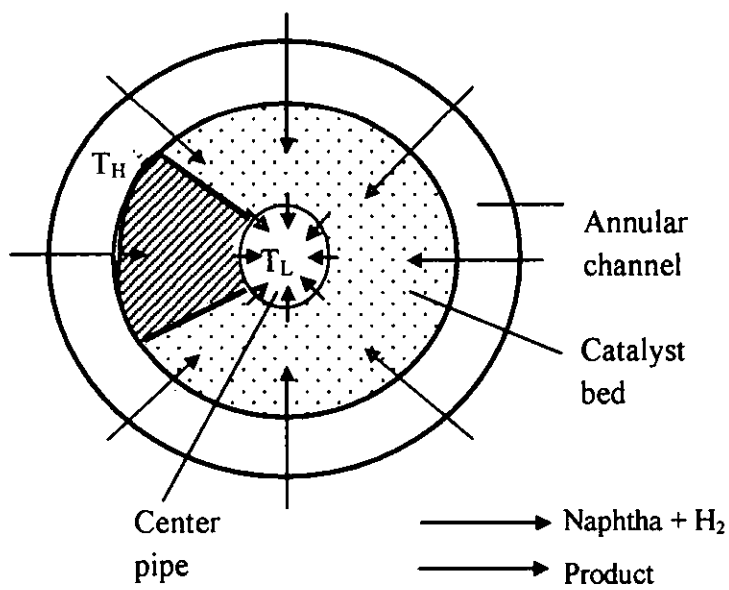


Fig. 3.1(b): Top view of radial flow moving bed reactor

A sector from annular catalyst bed is assumed to consist of n -compartments in series (each of ΔR length) in the direction of gas flow as shown in Fig. 3.2.

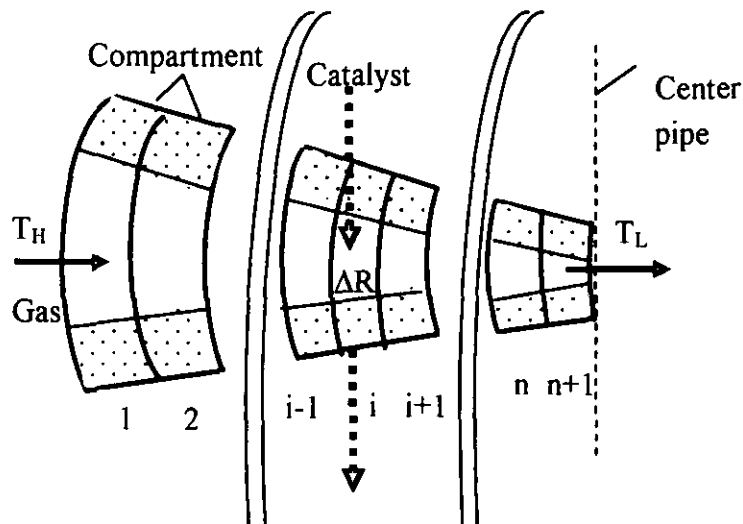


Fig. 3.2: Compartment-in-series reactor model.

The following assumptions are proposed during model this reactor:

- i. Catalyst particles move downwards in plug flow.
- ii. Reactant gas flow is uniform along the length of the reactor.
- iii. Reactant gas flows radially through ' n ' annular compartment in series.
- iv. Each compartment consists of two phases, gas phase and solid-catalyst phase.
- v. Gas in each phase in each compartment is considered to be well mixed.
- vi. Reactions take place in solid-catalyst phase.
- vii. Mass transfer aids in the transport of reactants and products to/from the catalyst surface;
- viii. Heat transfer from gas phase to solid catalyst phase supplies heat of reaction.

3.2. Effective Reaction Rate Constant

The reactant reaches the external surface of the catalyst particle by mass transfer; diffuse through the catalyst pores and reach the catalyst surface so that the reactions could take place. After that, the products diffuse from the catalyst surface and reach the bulk flow by mass transfer. The effects of the mass transfer resistance ($1/k_m$), effectiveness factor due to pore diffusion ξ , catalyst activity of a decaying catalyst, α and intrinsic rate constant k_r can be put together to obtain an effective rate constant, k_{reff} based on weight of particles as

$$\frac{1}{k_{\text{reff}} \rho_p} = \frac{1}{k_m} + \frac{1}{\xi \alpha k_r \rho_p} \quad (3.1)$$

The effect of external mass transfer resistance can be ignored when the Reynold's number is more than four [18]. For endothermic reactions with possible decay in catalyst activity, reaction rate constants are small and this reduces Thiele Modulus and hence reduces the possibility of pore diffusion control. Also, in reforming process, gas velocity and particle size are chosen to eliminate mass transfer and pore diffusion effects. Hence,

$$\frac{1}{k_{\text{reff}} \rho_p} = \frac{1}{\alpha k_r \rho_p} \quad (3.2)$$

3.3. Balance Equations over a Compartment

Processes taking place in the "i-th compartment" are shown in Fig. 3.3.

Equations for steady-state mole and energy balance, over a compartment can be expressed as:

$$\text{Input rate} - \text{Output rate} - \text{Consumption rate} = \text{Accumulation rate} = 0 \quad (3.3)$$

Thus,

$$\text{Input rate} - \text{Output rate} = \text{Consumption rate} \quad (3.4)$$

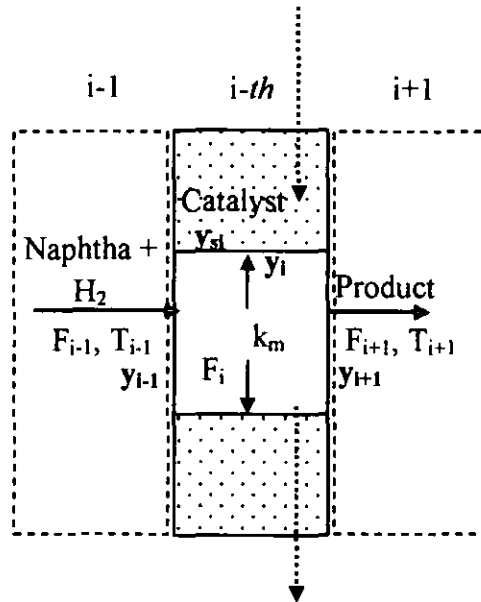


Fig. 3.3: An 'i-th' compartment reactor model.

3.3.1. Mole Balance in *i-th* compartment

Mole balance equation of each species is written as following:

a. Gas Phase:

$$\frac{F_t}{\Delta Mc} y_{i-1} - \frac{F_t}{\Delta Mc} y_i = k_m S_a C_t (y_i - y_{si}) \quad (3.5)$$

Mole in - Mole out = Mole transfer to solid phase

$$\frac{F_t}{\Delta Mc} (y_{i-1} - y_i) = \frac{F_t}{\Delta Mc} \Delta y_i = k_m S_a C_t (y_i - y_{si}) \quad (3.6)$$

b. Solid Phase:

$$k_m S_a C_t (y_i - y_{si}) = \sum v_{ij} r_j \quad (3.7)$$

Mole transfer to solid = Mole convert by reactions

From equation (3.6) and (3.7),

$$\frac{F_t}{\Delta Mc} \Delta y_i = \sum v_{ij} r_j \quad (3.8)$$

$$\Delta Mc = \rho (2 \pi R_i \Delta R H) \quad (3.9)$$

$$F_t \frac{\Delta y_i}{\Delta R} = \frac{\Delta F_i}{\Delta R} = (2 \pi R_i H \rho) \sum v_{ij} r_j \quad (3.10)$$

$$F_i = F_{i-1} + \Delta F_i = F_{i-1} + [(2 \pi R_i H \rho) \sum v_{ij} r_j] (\Delta R) \quad (3.11)$$

The calculations of flow rate for each component in naphtha and products in *i*-th compartment are shown in appendix B.

3.3.2. Energy Balance in *i*-th compartment

Energy balance equation of each species is written as following:

c. Gas Phase:

$$\frac{F_t}{\Delta Mc} c_p T_{i-1} - \frac{F_t}{\Delta Mc} c_p T_i = h_f \Delta R S_a C_t (T_i - T_{si}) \quad (3.12)$$

Heat in - Heat out = Heat transfer to solid phase

$$\frac{F_t}{\Delta Mc} c_p (T_{i-1} - T_i) = \frac{F_t}{\Delta Mc} c_p \Delta T_i = h_f \Delta R S_a C_t (T_i - T_{si}) \quad (3.13)$$

d. Solid Phase:

$$h_f \Delta R S_a C_t (T_i - T_{si}) = \sum v_{ij} (-\Delta H_r)_j r_j \quad (3.14)$$

Heat transfer to solid = Heat consumption by reactions

From equation (3.13) and (3.14),

$$\frac{F_t}{\Delta Mc} c_p \Delta T_i = \sum v_{ij} (-\Delta H_r)_j r_j \quad (3.15)$$

$$\frac{F_t}{\rho (2 \pi R_i \Delta R H)} c_p \Delta T_i = \sum v_{ij} (-\Delta H_r)_j r_j \quad (3.16)$$

$$\frac{\Delta T_i}{\Delta R} = (2 \pi R_i H \rho) \sum v_{ij} (-\Delta H_r)_j r_j \quad (3.17)$$

$$T_i = T_{i-1} + \Delta T_i = T_{i-1} + [(2 \pi R_i H \rho) \sum v_{ij} (-\Delta H_r)_j r_j] (\Delta R) \quad (3.18)$$

The calculations of catalyst bed temperature for *i*-th compartment are shown in appendix B.

The operating conditions of temperature, pressure, H₂/HC ratio and properties of naphtha feed are given in Table 3.2. Meanwhile, Table 3.3 shows the characteristic data of the reforming catalyst.

Table 3.2: The feed flow rate and inlet compositions.

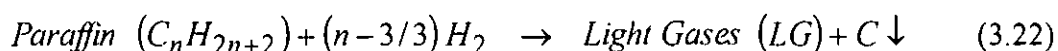
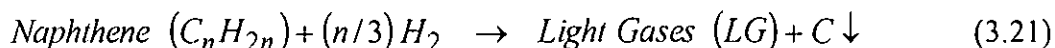
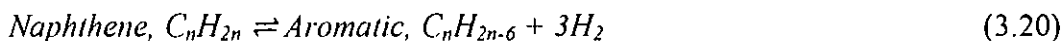
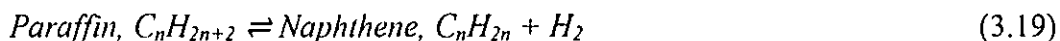
Parameter	Numerical value	Molecular weight g/mol	Unit
Inlet Gas Temperature (R ₁ , R ₂ , R ₃ , R ₄)	793	-	K
Inlet Gas Pressure (R ₁ , R ₂ , R ₃ , R ₄)	794, 765, 725, 698	-	kPa
H ₂ /HC mole ratio	3.0	-	-
Naphtha feedstock	113655	-	kg/h
Paraffin	50.26 mole%	115.9	-
Naphthene	39.75 mole%	113.9	-
Aromatic	9.99 mole%	107.9	-

Table 3.3: Characteristic data of reforming catalyst.

Kind of catalyst	R-264 (UOP)
Platinum wt%	0.25
Catalyst density, ρ _p	670 kg/m ³
Diameter, d _p	1.6 mm
Shape	sphere
Catalyst circulation rate	433.22 kg/h

3.4. Kinetic Model

There are four reactions occur in catalytic naphtha reforming. The chemical reactions are as follows:



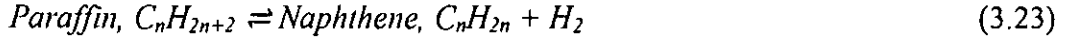
Most of the researchers (Rahimpour [14], Arani et al. [19], Liang et al. [20], Mostafazadeh and Rahimpour [21] and Lee et al. [22]) have utilized the kinetic parameters from Smith [5]. This kinetics obtained for the catalysts available at that time may not be relevant to present day catalysts. However, assuming that the activation energies do not change significantly, the same kinetics is adopted with a correction multiplier; η . Liang et al. [20] explained that for different periods of catalyst activity, the carbon accumulation extent is not same. Thus, the values for η are different. For new catalyst, $\eta = 1$ and in other conditions, $0 < \eta < 1$.

Numerical value of the correction multiplier is fitted to match the model predictions to the actual current day industrial data by using trial and error method. The methodology of arriving at the choice is presented in section 3.7 and the results are shown in Table 3.4.

Table 3.4. The correction multiplier, η from Liang et al. and model results.

Reaction	Correction Multiplier, η (Liang et al.[20])	Correction Multiplier, η (model)
Paraffins dehydrogenation, η_{R1}	0.432	0.9
Aromatization of naphthenes, η_{R2}	0.432	0.8
Hydro-cracking, η_C	0.432	0.5

3.4.1. Dehydrogenation of Paraffin



$$r_1 = (k_{f1} / K_{e1})(K_{e1}P_N P_H - P_P) \eta a \quad (3.24)$$

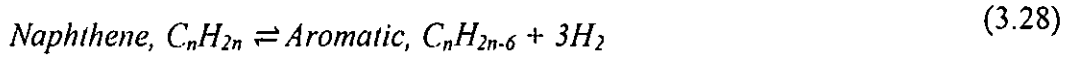
$$k_{f1} = 9.87 \exp(35.98 - 58550/1.8T) \quad (3.25)$$

$$K_{e1} = 9.87 \exp(-7.12 + 8000/1.8T) \quad (3.26)$$

$$(-\Delta H_{r1}) = -36953.33 \text{ kJ/kmol} \quad (3.27)$$

Where r_1 is reaction rates of paraffins dehydrogenation, (kmol/kg.cat.h), k_{f1} is forward rate constant, (kmol/ kg.cat.h.MPa), K_{e1} is equilibrium constant, (MPa³), η is correction multiplier, a is catalyst activity, ΔH_{r1} is heat of reaction, (kJ/kmol), P_N is naphthene partial pressure, P_H is hydrogen partial pressure and P_P is paraffin partial pressure.

3.4.2. Aromatization of Naphthene



$$r_2 = (k_{f2} / K_{e2})(K_{e2} P_N - P_A P_H^3) \eta a \quad (3.29)$$

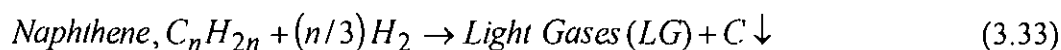
$$k_{f2} = 9.87 \exp(23.21 - 36350/1.8T) \quad (3.30)$$

$$K_{e2} = 1.04 \cdot 10^{-3} \exp(46.15 - 46045/1.8T) \quad (3.31)$$

$$(-\Delta H_{r2}) = 71038.06 \text{ kJ/kmol} \quad (3.32)$$

Where r_2 is reaction rates of aromatization reaction, (kmol/kg.cat.h), k_{f2} is forward rate constant, (kmol/ kg.cat.h.MPa²), K_{e2} is equilibrium constant, (MPa⁻¹) and P_A is aromatic partial pressure.

3.4.3. Naphthene Hydro-Cracking



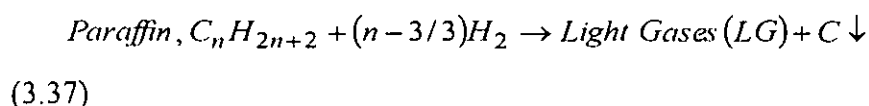
$$r_3 = \left(k_{f3} / P_t \right) P_N \eta a \quad (3.34)$$

$$k_{f3} = \exp \left(42.97 - 63800 / 1.8T \right) \quad (3.35)$$

$$(-\Delta H r_3) = -51939.31 \text{ kJ/kmol} \quad (3.36)$$

Where r_3 is reaction rates of naphthene hydro-cracking, (kmol/kg.cat.h), k_{f3} is forward rate constant, (kmol/ kg.cat.h.) and P is total pressure in reactor.

3.4.4. Paraffin Hydro-Cracking



$$r_4 = \left(k_{f4} / P_t \right) P_p \eta a \quad (3.38)$$

$$k_{f4} = \exp \left(42.97 - 63800 / 1.8T \right) \quad (3.39)$$

$$(-\Delta H r_4) = -56597 \text{ kJ/kmol} \quad (3.40)$$

Where r_4 is reaction rates of paraffins hydro-cracking, (kmol/kg.cat.h) and k_{f4} is forward rate constant, (kmol/ kg.cat.h.).

3.5. Catalyst Deactivation Model

Cracking reactions generate carbon deposits on the catalyst surface leading to catalyst deactivation. The activity of a catalyst particle is defined as:

$$a = \frac{\text{Reaction rate on catalyst particle}}{\text{Reaction rate on a fresh catalyst particle}} = \frac{-r'_d}{-r_{d0}} \quad (3.41)$$

The activity of catalyst is 1 for a fresh catalyst and declines with reaction time as coke forms and deposits on the catalyst surface. Reaction rate declines with coke deposition and this in turn reduces coke formation and reduction in the activity of the catalyst. In cracking and reforming reactions, reactants as well as the products can crack to deposit coke. Thus, the kinetics of reduction in catalyst activity is dependent on the reduction in catalyst surface (directly affecting the catalyst activity, α) and can be expressed as:

$$-\frac{da}{dt} = k_d a^d \quad (3.42)$$

Assuming first order catalyst decay kinetics with Arrhenius type temperature dependence:

$$-r_d' = -\frac{da}{dt} = k_{d0} \cdot \exp\left(-\frac{E_d}{RT}\right) a^d \quad (3.43)$$

Tailleur and Davila [13] reported experimental observation on the declining catalyst activity as a function of time up to 2400 hrs at temperatures of 740, 760 and 780 K based on a semi regenerative reforming (SRR) pilot plant. In a continuous regenerative reforming (CRR) unit, the catalyst residence time in radial flow moving bed reactor is less than 100 hrs and the catalyst decay within this period is very small and the decay can be assumed to be linear. Hence, the "d" is close to zero.

$$-r_d' = -\frac{da}{dt} = k_{d0} \cdot \exp\left(-\frac{E_d}{RT}\right) \quad (3.44)$$

And the catalyst activity, α can be obtained as:

$$a = 1 - \left\{ k_{d0} t \exp\left(-\frac{E_d}{RT}\right) \right\} \quad (3.45)$$

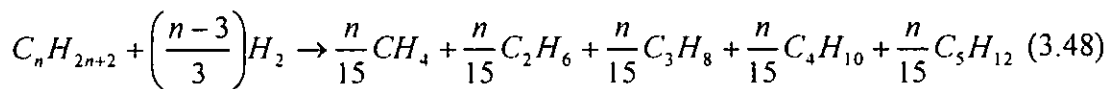
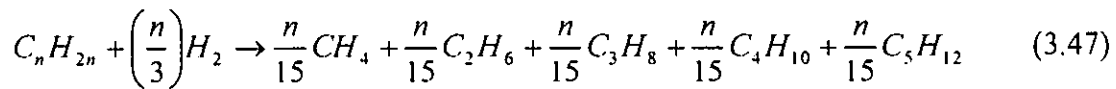
Comparing this equation with observations by Tailleir and Davila [13] on declining activity up to 100 hours, the constants in the equation are estimated and obtained as

$$a = 1 - \left\{ 35 \exp \left(-\frac{83073}{RT} \right) \right\}^t \quad (3.46)$$

3.6. Properties of Naphtha

3.6.1. Determination of Carbon Number n for the Hydrocarbon Feed

From Smith [5], hydro-cracking will produce the same amount of moles of C_1 to C_5 cuts (light gases). Thus, for equation (3.33) and (3.37) can be represented by the following formula:



Where n = carbon number

For a certain reforming feed stock, the value of n can be obtained through the average molecular weight, M_f (kg/ kmol) of the feed stock.

3.6.1.1. Paraffin

Formula molecule: $C_n H_{2n+2}$

$$\text{Molecular weight: } 12n + 2n + 2 = 14n + 2 \quad (3.49)$$

3.6.1.2. Naphthene

Formula molecule: $C_n H_{2n}$

$$\text{Molecular weight: } 12n + 2n = 14n \quad (3.50)$$

3.6.1.3. Aromatic

Formula molecule: C_nH_{2n-6}

$$\text{Molecular weight: } 12n + 2n - 6 = 14n - 6 \quad (3.51)$$

Thus, average molecular weight is:

$$M_f = \chi_p (14n + 2) + \chi_N (14n) + \chi_A (14n - 6) \quad (3.52)$$

$$M_f = 14n \chi_p + 2 \chi_p + 14n \chi_N + 14n \chi_A - 6 \chi_A \quad (3.53)$$

$$M_f - 2 \chi_p + 6 \chi_A = 14n (\chi_p + \chi_N + \chi_A) \quad (3.54)$$

$$\text{Where } (\chi_p + \chi_N + \chi_A) = 1 \quad (3.55)$$

From equation (3.55) into (3.54),

$$14n = M_f - 2 \chi_p + 6 \chi_A \quad (3.56)$$

3.6.2. Density of Naphtha Feed

Density of naphtha in liquid form at 25 °C = 750 kg/m³

Density of naphtha in gas form at 520 °C =

$$\rho_{520^\circ C} = \frac{M_f (\text{kg/kmol}) \times 273 (\text{K}) \times P (\text{atm}) \times 1000 (\text{L})}{22400 (\text{L/kmol}) \times 793 (\text{K}) \times 1 (\text{atm}) \times 1 (\text{m}^3)} \quad (3.57)$$

3.6.3. Velocity of Naphtha Feed

$$\text{Velocity of naphtha gas entering the reactor, } u = \frac{F}{\rho A} \quad (3.58)$$

3.6.4. Reynolds Number of Naphtha Gas Flow

$$\text{Reynolds number of naphtha gas flow in the reactor, } N_{Re} = \frac{d_p u \rho}{\mu} \quad (3.59)$$

With $\mu = 2.87 \cdot 10^{-5}$ kg/ m.s

3.6.5. Liquid Hourly Space Velocity (LHSV)

$$\text{LHSV} = \frac{\text{cubic feet of charge per hour}}{\text{cubic feet of catalyst(all reactors)}} \quad (3.60)$$

3.6.6. Weighted Average Inlet Temperature (WAIT)

$$\begin{aligned} \text{WAIT} = & (\text{Catalyst fraction in } R_1 * T_{in, R1}) + (\text{Catalyst fraction in } R_2 * T_{in, R2}) \\ & + (\text{Catalyst fraction in } R_3 * T_{in, R3}) + (\text{Catalyst fraction in } R_4 * T_{in, R4}) \quad (3.61) \end{aligned}$$

3.6.7. Catalyst Residence Time

Circulation rate of catalyst: 433.22 kg/h

Total length of catalyst flow from top of first reactor to the bottom of fourth reactor,

$$L_t = 8.1 + 6.32 + 7.4 + 8.65 = 30.47 \quad (3.62)$$

Area of catalyst flow in each reactor,

$$A_c = \frac{\pi}{4} (d_b^2 - d_{cp}^2) \quad (3.63)$$

Time for catalyst to flow from top to the bottom of reactor,

$$t_{Ri} = \frac{L_{Ri} \cdot \rho_{cat} \cdot A_c}{F_{cat}} \quad (3.64)$$

Total residence time of catalyst to flow from top to the bottom in CCR unit is:

$$t_T = t_{R1} + t_{R2} + t_{R3} + t_{R4} \quad (3.65)$$

3.7. Model Development

Correction multiplier, η is developing in the reaction rates of the reactions in naphtha reforming with kinetics obtained from Smith [5]. There are three major reactions occur in naphtha reforming. The first reaction is dehydrogenation of paraffin to naphthene and after that the naphthene will be converting to aromatic. However, at the same time, hydro-cracking also takes place to produce light gas. There are three different value of correction multiplier: η_{R1} is stands for paraffin dehydrogenation correction multiplier, η_{R2} is stated for naphthene aromatization correction multiplier, and η_C is considered as hydro-cracking reaction correction multiplier.

3.7.1 Simulation to identify the Correction Multiplier of Paraffin Dehydrogenation, η_{R1}

At first, the correction multiplier of paraffin dehydrogenation, η_{R1} was simulated at different value in the range of 0.2 and 1.4 while η_{R2} and η_C were fixed as 1. The results are shown in Fig. 3.4, 3.5 and 3.6.

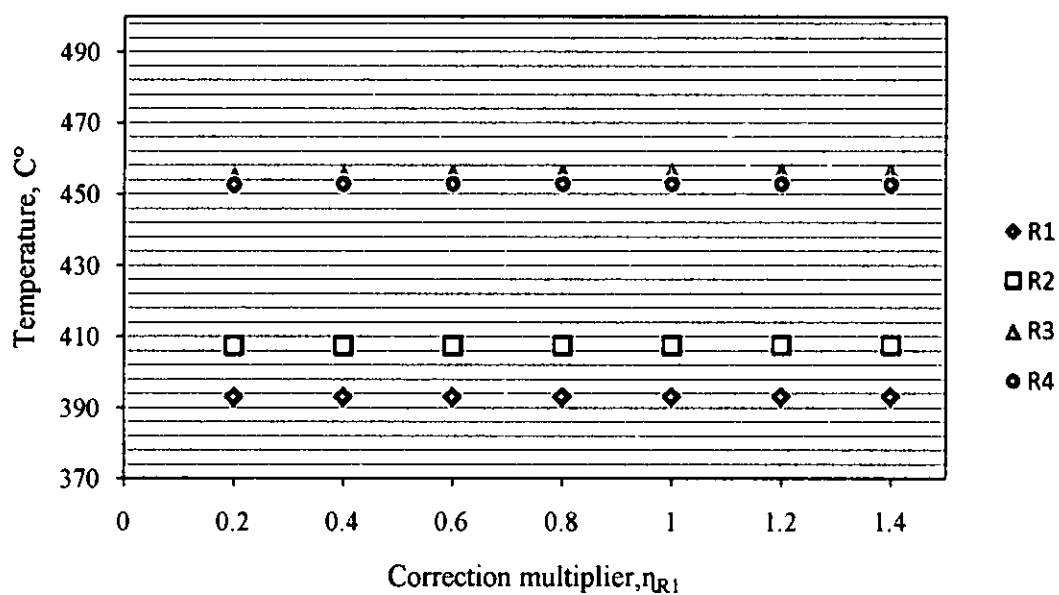


Fig. 3.4: Effect of the correction multiplier of paraffin dehydrogenation, η_{R1} on the outlet temperature of the reactor.

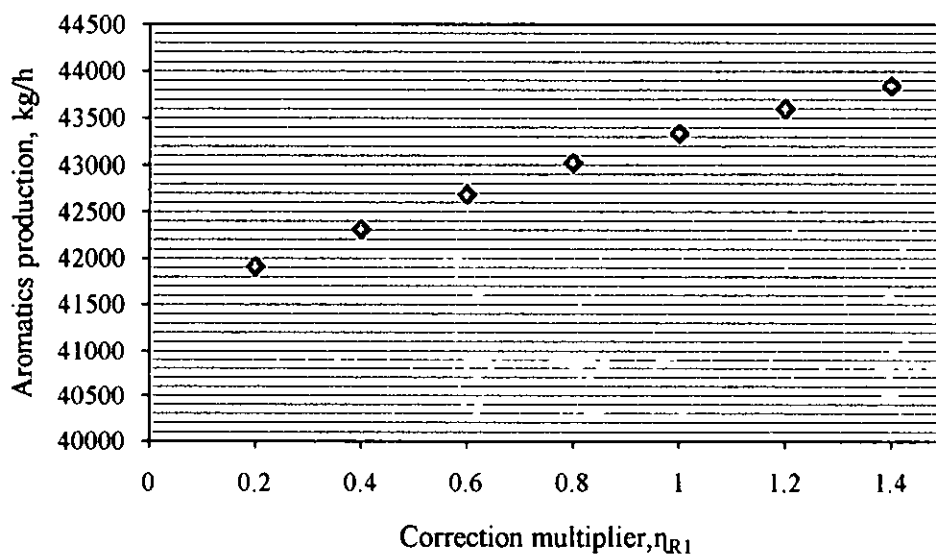


Fig. 3.5: Effect of the correction multiplier of paraffin dehydrogenation, η_{R1} on the aromatics production.

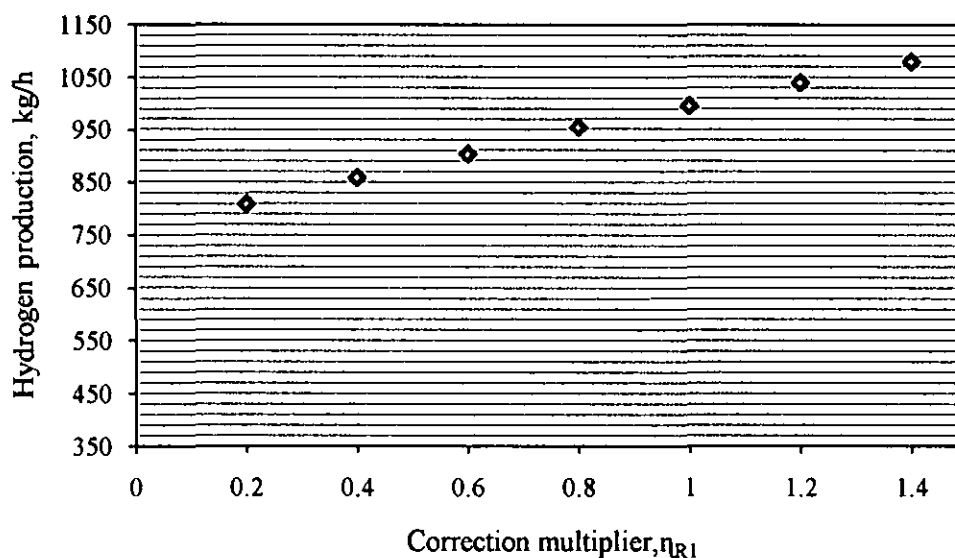


Fig. 3.6: Effect of the correction multiplier of paraffin dehydrogenation, η_{R1} on the hydrogen production.

Fig. 3.4 shows the outlet temperature in radial flow moving bed reactor when correction multiplier of paraffin dehydrogenation, η_{R1} is simulated. The temperature profile is almost same although introduced higher value of η_{R1} . It means that paraffin dehydrogenation is quite difficult to occur in the reactor because favoured at high temperature. The predominant reaction is naphthenes aromatization as the aromatics and hydrogen production increase.

3.7.2 Simulation to identify the Correction Multiplier of Naphthenes Aromatization, η_{R2}

After that, the simulation was take place on correction multiplier for naphthene aromatization, η_{R2} in the range of 0.6 and 1.8. The other catalyst correction multiplier, η_{R1} and η_C were fixed as 1. The results are shown in Fig. 3.7, 3.8 and 3.9.

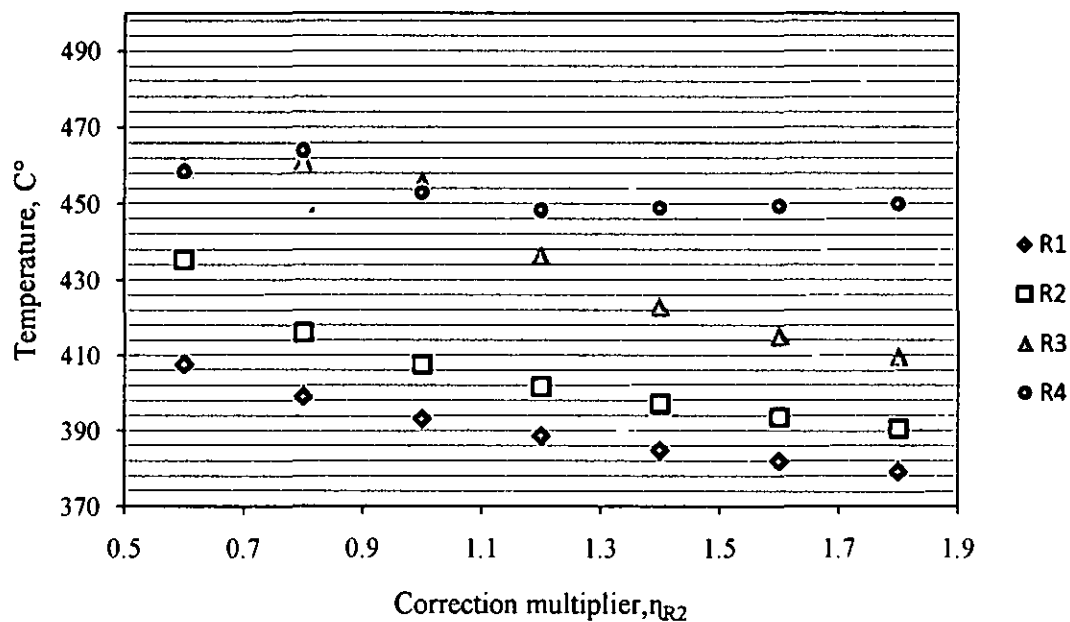


Fig. 3.7: Effect of the correction multiplier of naphthene aromatization, η_{R2} on the outlet temperature of the reactor.

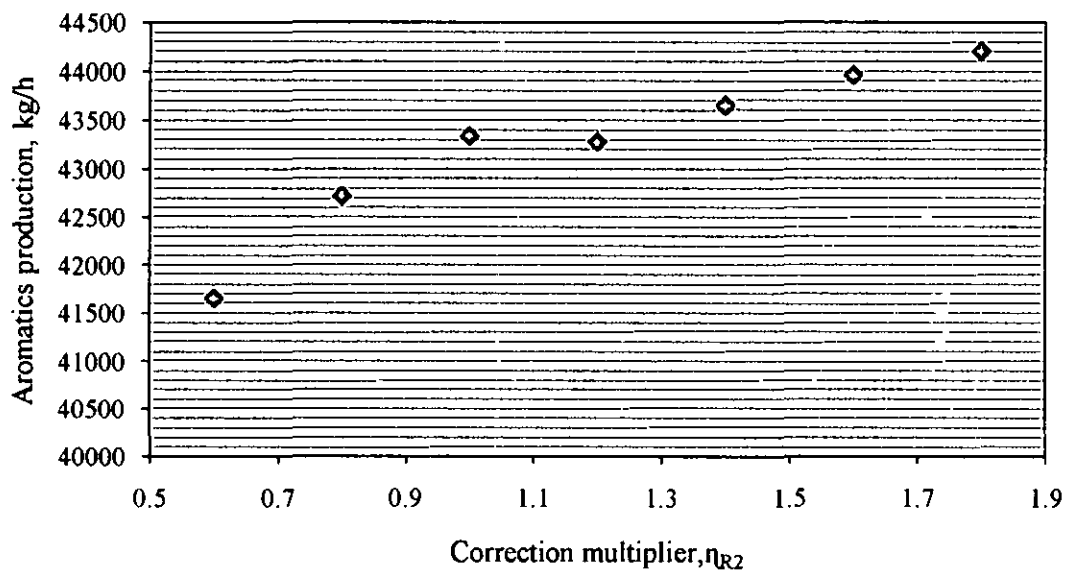


Fig. 3.8: Effect of the correction multiplier of naphthene aromatization, η_{R2} on the aromatics production.

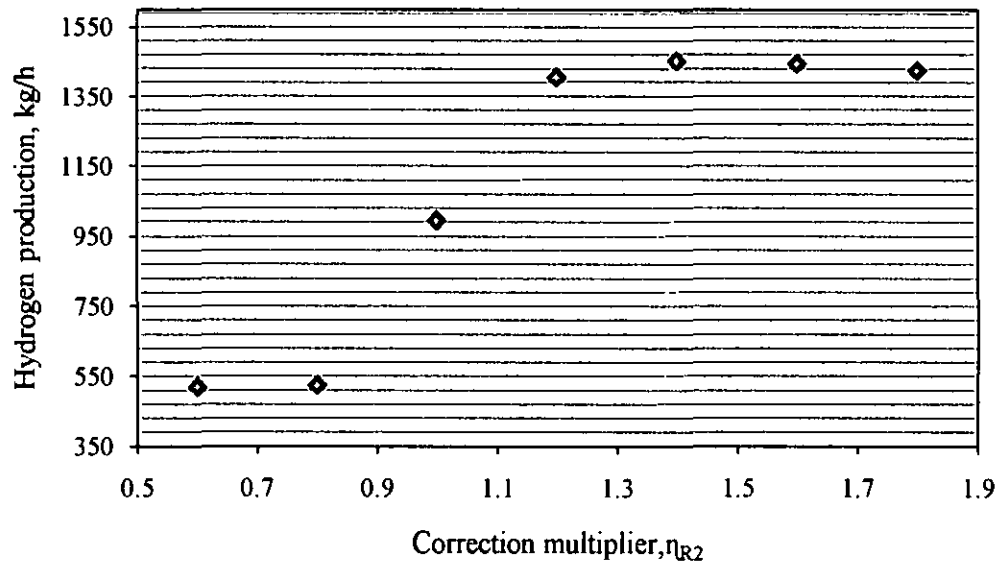


Fig. 3.9: Effect of the correction multiplier of naphthene aromatization, η_{R2} on the hydrogen production.

Most of the temperature in every reactor will decrease as the endothermic reaction by naphthenes aromatization. As the η_{R2} increases, higher reaction rates of naphthenes aromatization. Thus, the temperature drop in every reactor increases. Mostly, the naphthenes get converted to aromatics, thus aromatics production increases. At the same time, the production of hydrogen also increases.

3.7.3 Simulation to identify the Correction Multiplier of Hydro-cracking, η_c

Lastly, the correction multiplier for hydro-cracking reaction, η_c was simulated in the range of 0.6 and 1.8. The other correction multiplier, η_{R1} and η_{R2} were fixed as 1. The results are shown in Fig. 3.10, 3.11 and 3.12.

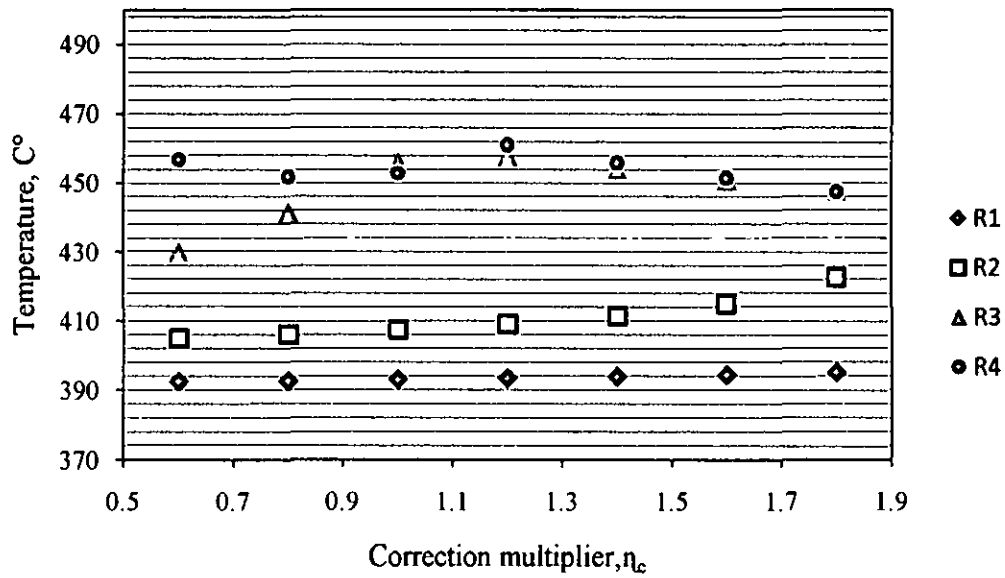


Fig. 3.10: Effect of the correction multiplier of hydro-cracking, η_c on the outlet temperature of the reactor.

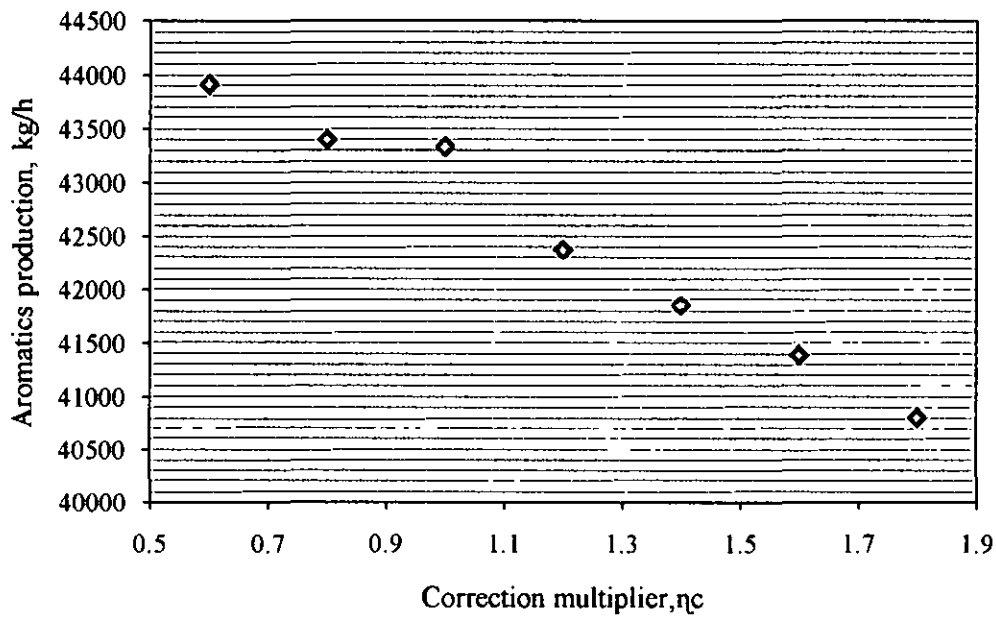


Fig. 3.11: Effect of the correction multiplier of hydro-cracking reaction, η_c on the aromatics production.

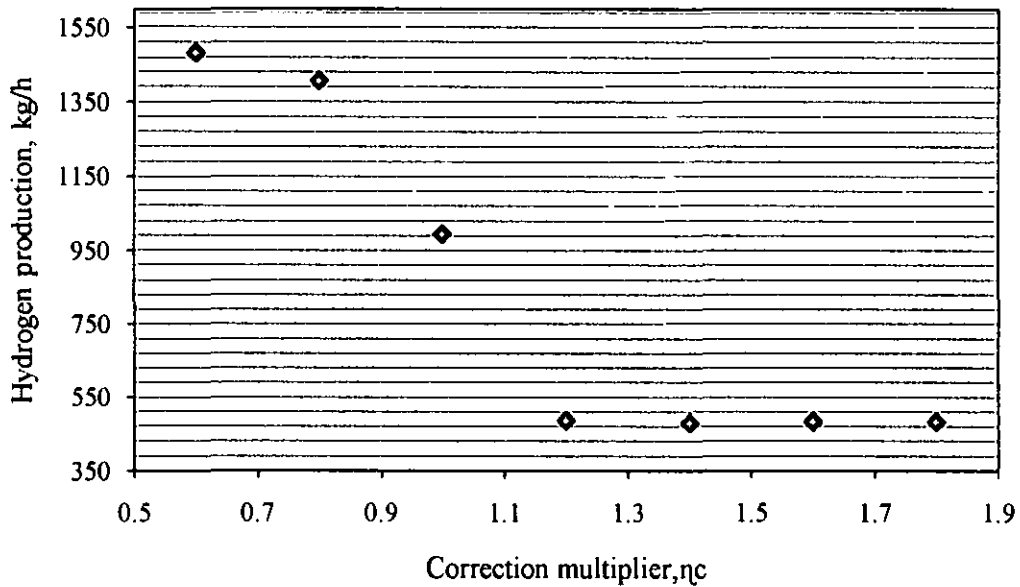


Figure 3.12: Effect of the correction multiplier of hydro-cracking reaction, η_c on the hydrogen production.

Hydro-cracking is an exothermic reaction. Therefore, the temperature will increase as the correction multiplier of hydro-cracking reaction, η_c increases. As the η_c increases, the reaction rates of paraffins and naphthenes hydro-cracking is higher than reaction rates of naphthenes dehydrogenation. Thus, more of light gas is produced and the aromatics decreases. As the production of aromatics decreases, the production of hydrogen also decreases.

However, to get the best of correction multiplier for each reactions so that the profile of temperature and reformate is match with the industrial data, trial and error method was applied. The correction multiplier of η_{R1} , η_{R2} and η_c was simulated simultaneously to get the best result. After a few trial and error section, the best results for temperature drop, aromatics and hydrogen production occurs when the value for correction multiplier as follow: $\eta_{R1}=0.9$, $\eta_{R2}=0.8$ and $\eta_c=0.5$.

3.8 Problems in RFMBR

3.8.1 Pressure Drop

Compared to packed beds of length L , radius R_a and volume of V with normal gas (axial) flow, radial gas flow in the same volume of bed offers lower pressure drop. Fig. 3.13 shows an axial and radial gas flow in a reactor.

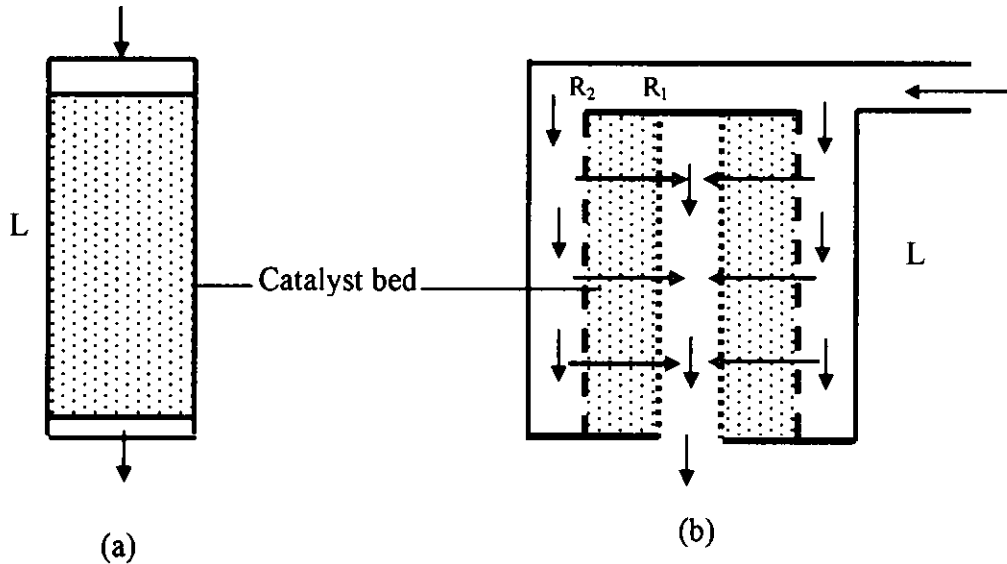


Fig. 3.13: An axial (a) and radial (b) gas flow.

Ergun's equation [29] is generally presented as:

$$\frac{\Delta P}{L} \cdot \frac{d_p}{\rho u_0^2} \cdot \frac{\varepsilon^3}{(1-\varepsilon)} = \frac{150(1-\varepsilon)\mu}{d_p u_0 \rho} + 1.75 \quad (3.66)$$

For laminar flow,

$$\Delta P = 150 \frac{(1-\varepsilon)^2}{\varepsilon^3} \frac{\mu u_0}{d_p^2} L \quad (3.67)$$

And for turbulent flow,

$$\frac{\Delta P}{L} \cdot \frac{d_p}{\rho u_0^2} \cdot \frac{\varepsilon^3}{(1-\varepsilon)} = 1.75 \quad (3.68)$$

3.8.1.1 Pressure Drop in Axial Flow Beds

In axial flow packed bed reactor of length L and radius R_a , the path length of flow is L and gas velocity is

$$u_{oa} = \frac{F}{\pi R_a^2} \quad (3.69)$$

For axial flow packed bed reactor in laminar flow,

$$\Delta P_{(ax)} = 150 \frac{(1-\varepsilon)^2}{\varepsilon^3} \frac{\mu F}{d_p^2} \frac{L}{\pi R_a^2} \quad (3.70)$$

For axial packed bed reactor in turbulent flow,

$$\Delta P_{(ax)} = 1.75 \frac{(1-\varepsilon)}{\varepsilon^3} \frac{\rho F^2}{d_p} \frac{L}{(\pi R_a^2)^2} \quad (3.71)$$

3.8.1.2 Pressure drop in Radial flow packed beds

In radial flow packed bed reactors of length L , the packed bed is confined between outer radius of R_2 and inner radius of R_1 . To compare axial flow packed beds with radial flow packed beds, the bed volumes and gas flow rates need to be same.

$$\text{Volume of packed bed} = \pi R_a^2 L = \pi(R_2^2 - R_1^2)L \quad (3.72)$$

$$R_a^2 = R_2^2 - R_1^2$$

In radial flow packed bed reactor, gas flows from outer radius R_2 to inner radius R_1 (the path length is $(R_2 - R_1)$) and velocity based on average radius is

$$u_{orad} = \frac{F}{\pi(R_2 + R_1)L} \quad (3.73)$$

Using Ergun's equation for radial flow reactors for laminar flow,

$$\Delta P_{(rad)} = 150 \frac{(1-\varepsilon)^2}{\varepsilon^3} \frac{\mu F}{d_p^2} \frac{(R_2 - R_1)}{(\pi(R_2 + R_1)L)} \quad (3.74)$$

For turbulent flow,

$$\Delta P_{(rad)} = 1.75 \frac{(1-\varepsilon)}{\varepsilon^3} \frac{\rho F^2}{d_p} \frac{(R_2 - R_1)}{(\pi(R_2 + R_1)L)^2} \quad (3.75)$$

So, pressure reduction for laminar flow in both reactors is:

$$\frac{\Delta P_{(rad)}}{\Delta P_{(ax)}} = \left(\frac{(R_2 - R_1)}{L} \right)^2 \quad (3.76)$$

So, pressure reduction in turbulent flow for both reactors is,

$$\frac{\Delta P_{(rad)}}{\Delta P_{(ax)}} = \left(\frac{(R_2 - R_1)}{L} \right)^3 \quad (3.77)$$

The $(R_2 - R_1/L)$ term is very small (<1) and hence radial flow reactors offer great reduction in pressure losses. Pressure drop reduction is higher in turbulent flow than in laminar flow. The reduction in pressure drop reduces the energy consumed in the process operation.

3.8.2 Pinning in RFMBR

Although the radial flow gives the low pressure drop, it can create the problem of “pinning” which can hinder the flow of solids in the downward direction. Fig. 3.14 shows a radial flow moving bed reactor before pinning occurs. The reactant gas flows radially inward while the particles solid bed moves downward by gravity.

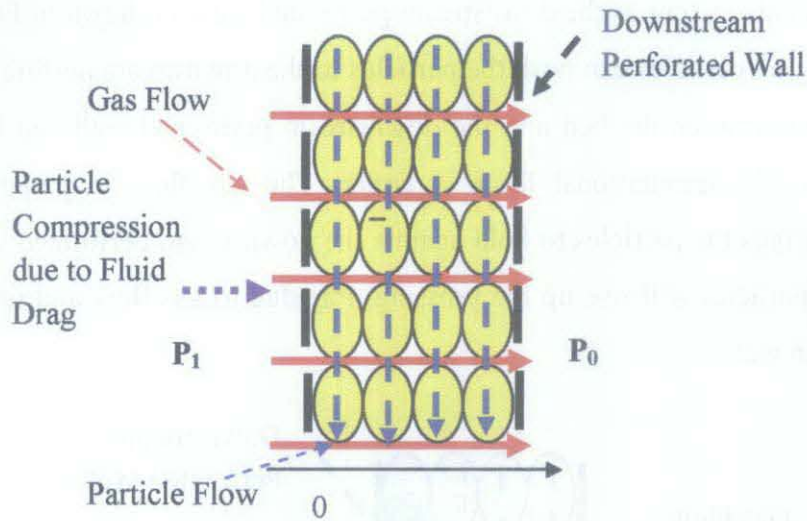


Fig. 3.14: A RFMBR model before pinning occurs.

Gas flow over a particle exerts force on the particle in the direction of flow. With radial flow in the moving bed, the particles experience drag force in the radial direction while they are trying to move downwards by gravitational force. If the drag force on particles increases, the normal stress between the particles and the upstream wall will be decreased. The bed particles start to lose contact with the upstream wall when the normal stress is reduced zero. A thin cavity could occur between the catalyst bed and the upstream wall. The size of cavity closest to the upstream wall will increase until it expands to the size of catalyst bed. When the size of cavity ultimately spans the full width of the catalyst bed, the bed may not move down at all. The bed is said to be completely pinned. This mechanism was suggested by Ginestra and Jackson [24] as shown Fig. 3.15.

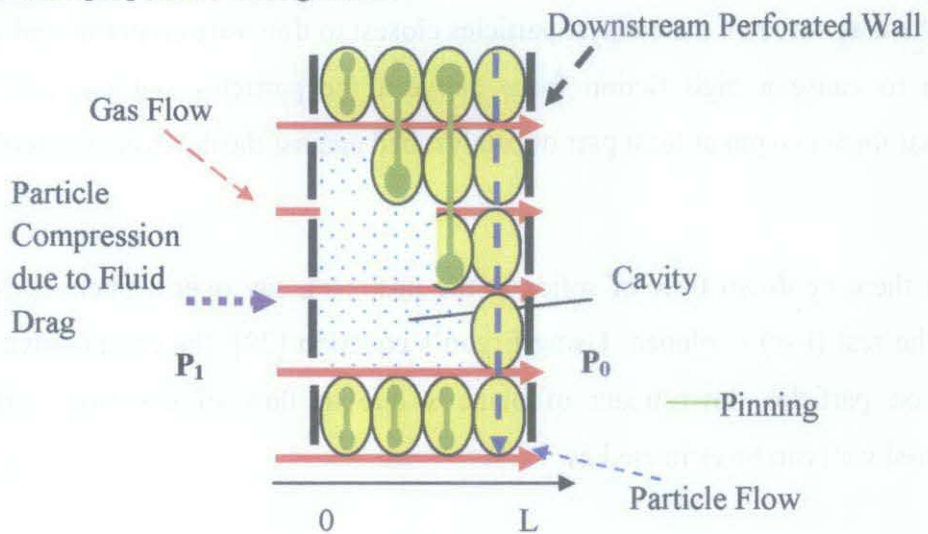


Fig. 3.15: The pinning mechanism suggested by Ginestra and Jackson [24].

Pinning can also occur at the downstream perforated wall as shown in Fig. 3.16. The radial drag on particles can push the particles to the downstream perforated wall and the friction between the bed and the downstream perforated wall can hold the particles unless the gravitational force is larger. The gas flow in perpendicular direction will drag the particles to hold against the downstream perforated wall and the weight of particles will rise up the pressing drag due to gas flow and friction at the downstream wall.

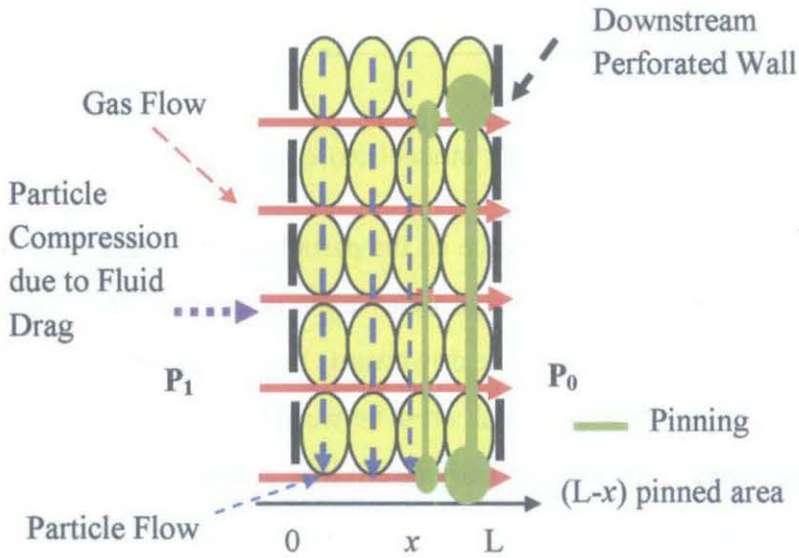


Fig. 3.16: A mechanism of pinning at the downstream perforated wall.

The highest pressing drag on the particles and friction occur near the downstream perforated wall and least at the upstream perforated wall. Partially pinned occur when the drag force on the catalyst particles closest to downstream perforated wall is enough to cause a high friction force between the particles and the wall. This frictional force can pin at least part of catalyst bed against the downstream perforated wall.

Let there be down flow of solids at the upstream, say over a thickness of “ x ” while the rest $(L-x)$ is pinned. Using Ergun’s equation [29], the compressive stress acting on particles downstream of plane x due to flow of gas from upstream perforated wall can be estimated as:

$$P_1 - P_x = x \left(\frac{150(1-\varepsilon)^2}{\varepsilon^3} \frac{\mu u_0}{d_p^2} + \frac{1.75(1-\varepsilon)}{\varepsilon^3} \frac{\rho u_0^2}{d_p} \right) \quad (3.78)$$

This stress acts on the particles downstream to pin particles between the plane x and downstream perforated wall by developing frictional resistance to counter the movement due to the weight of particles per unit area.

$$(P_1 - P_x) f = (L - x)(\rho_p - \rho_g)(1 - \varepsilon) g \quad (3.79)$$

These two equations can be combined to obtain

$$\frac{(L - x)}{x} = \frac{L \left(\frac{150(1-\varepsilon)^2}{\varepsilon^3} \frac{\mu u_0}{d_p^2} + \frac{1.75(1-\varepsilon)}{\varepsilon^3} \frac{\rho u_0^2}{d_p} \right) f}{L(\rho_p - \rho_g)(1 - \varepsilon) g} \quad (3.80)$$

$$\frac{(L - x)}{x} = \frac{(P_1 - P_0) f}{L(\rho_p - \rho_g)(1 - \varepsilon) g} \quad (3.81)$$

Pinned film thickness,

$$(L - x) = \frac{(P_1 - P_0) f}{(\rho_p - \rho_g)(1 - \varepsilon) g} \left\{ 1 - \frac{(P_1 - P_0) f}{L(\rho_p - \rho_g)(1 - \varepsilon) g} + \dots \right\} \quad (3.82)$$

From this equation, it can be seen that pinning film thickness increases with gas velocity; and the bed can get pinned for small particles, low particle densities and at high gas velocities. Hence, pinning can be reduced by using larger and high density particles and minimizing the wall friction at the downstream perforated wall.

Deactivation is the result of deposition of carbon like higher molecular weight waxy hydrocarbons on the catalyst surface. This can lead to formation of catalyst particle lumps which can start moving due to their larger size. Thus occurrence of catalyst lumps is an indication of pinning and catalyst deactivation.

3.8.3 Particle Breakage in RFMBR

Particle breakage can be a serious problem in CRR operation and usually occur in the reformer, regenerator and lift lines. The presence of fines particle will clog the gas flow lines and cause pinning phenomena. Energy dissipated due to particle motion in the moving bed results in the generation of fine particles and new particle surface area. These phenomena can be quantified through Rittenger's law [30] as:

$$\begin{array}{l} \text{Energy dissipated by} \\ \text{the solid flow} \end{array} = \begin{array}{l} \text{Increase in energy of fresh} \\ \text{surface area created} \end{array} \quad (3.83)$$

$$Q_s \cdot g \cdot H = k_R \left[\frac{6}{d_{p,final}} - \frac{6}{d_{p,initial}} \right] \quad (3.84)$$

Assuming fraction of the catalyst particles is ground to fines by attrition, ϕ_f

$$\frac{6}{d_{p,final}} = \frac{6(1-\phi_f)}{d_{p,initial}} + \frac{6\phi_f}{d_{p,fines}} \quad (3.85)$$

Resulting in

$$Q_s \cdot g \cdot H = k_R \phi_f \left[\frac{6}{d_{p,fines}} - \frac{6}{d_{p,initial}} \right] \quad (3.86)$$

Thus, fraction of fines produced is proportional to the mass flow rate of solids and bed height.

$$\frac{\phi_f}{d_{p,fines}} \propto Q_s \cdot g \cdot H \quad (3.87)$$

Thus, particle breakage can be reduced by decreasing the catalyst circulation rate. This increases the residence time of catalyst particles in the reactor leading to higher decay in catalyst activity. However, as the decay in catalyst activity in RFMBR reactor is very insignificant, reducing the catalyst circulation rate by a factor of two also will not adversely affect the reactor performance.

CHAPTER 4

MODEL VALIDATION

4.1. Model Evaluation

The model equations developed in chapter 3 for radial flow moving bed reformer reactor in a continuous regenerative reforming (CRR) unit are simulated to compare with the limited industrial data available. Input information needed for the model evaluation are given in Tables 3.2 and 3.3 and represented here for convenience.

Table 3.2: The feed flow rate and inlet compositions.

Parameter	Numerical value	Molecular weight g/mol	Unit
Inlet Gas Temperature (R ₁ , R ₂ , R ₃ , R ₄)	793	-	K
Inlet Gas Pressure (R ₁ , R ₂ , R ₃ , R ₄)	794, 765, 725, 698	-	kPa
H ₂ /HC mole ratio	3.0	-	-
Naphtha feedstock	113655	-	kg/h
Paraffin	50.26 mole%	115.9	-
Naphthene	39.75 mole%	113.9	-
Aromatic	9.99 mole%	107.9	-

Table 3.3: Characteristic data of reforming catalyst.

Kind of catalyst	R-264 (UOP)
Platinum wt%	0.25
Catalyst density, ρ_p	670 kg/m ³
Diameter, d_p	1.6 mm
Shape	sphere
Catalyst circulation rate	433.22g/h

Choice of the compartment size, ΔR is a critical decision. It cannot be smaller than the catalyst particle size. The model equations are simulated with ΔR from 1.6 mm to 5 mm. The results with $\Delta R = 1.6$ mm represent the observations on the temperature and conversion profiles reasonably well. Naphtha contains paraffins, naphthenes and aromatics. The dehydrogenation reaction convert paraffins to naphthenes and naphthenes to aromatics. Hydro-cracking reactions convert paraffins and naphthenes to light gases with deposition of coke on the catalyst surface. The coke deposition on catalyst surface reduces the catalyst activity. The results on temperature and component flow profiles in the reactors as a function of the catalyst fraction (ratio of catalyst weight to the weight of the catalyst in all the four reactors) are presented in the next section. Model estimates on output material flow rates in comparison with the limited industrial information are summarized in Table 4.1.

4.2 Temperature and Component Profiles

Temperature profiles and component profiles in the four reactors are shown in Fig. 4.1 and 4.2 respectively. The four reactors operate adiabatically with the same inlet temperature, 520 °C. The solid lines represent the model estimates and the industrial data are shown as symbols.

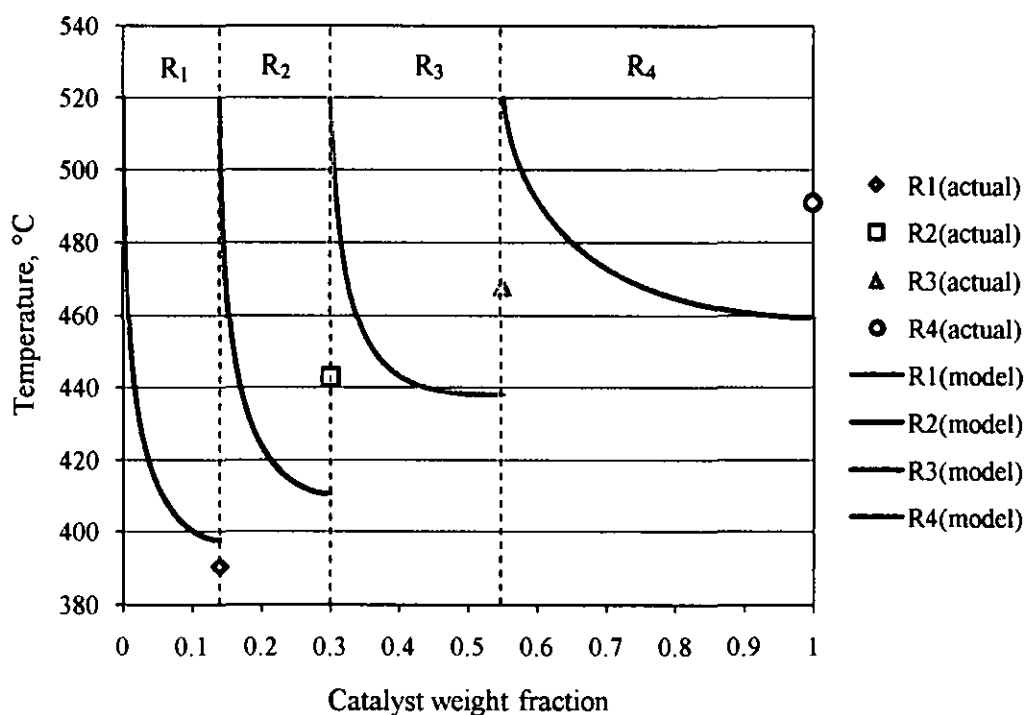


Fig. 4.1: Effect of catalyst weight fraction on the temperature along the radial flow moving bed reactor.

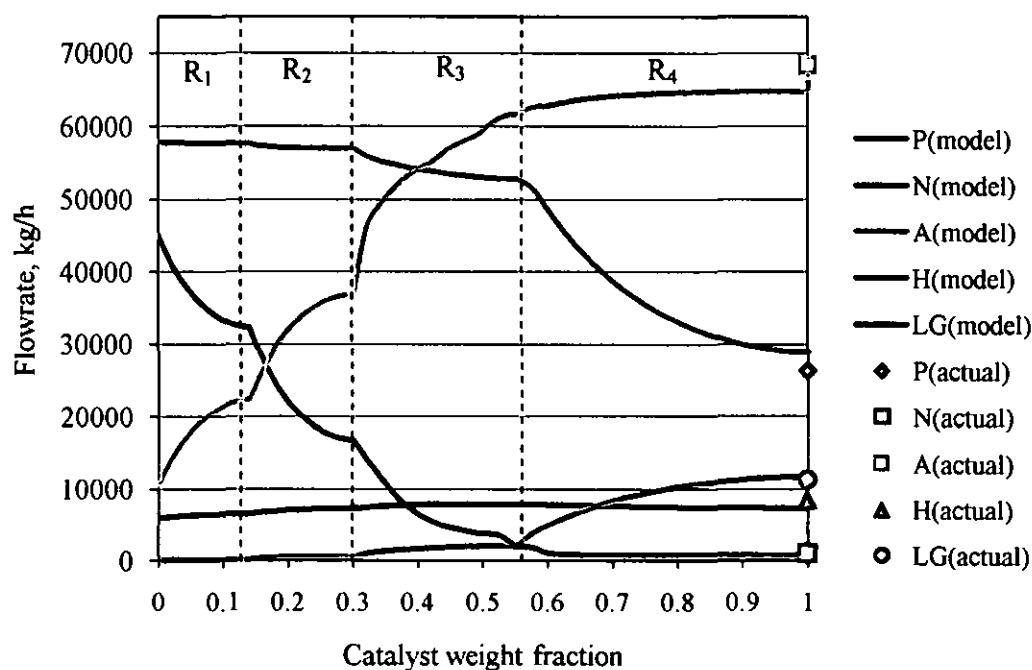


Fig. 4.2: Effect of catalyst weight fraction on the flow rate of naphtha components in radial flow moving bed reactor.

The first reactor contains 14% of the catalyst and the temperature drops from 520 °C to 397 °C (393°C observed in the industry) due to the very rapid endothermic conversion of naphthenes to aromatics with formation of hydrogen. The resultant temperature decrease in the first reactor slows down all the reactions. Conversion of paraffins and formation of light gases is very limited. The products of first reactor need to be withdrawn and reheated to 520 °C before entering the second reactor for further conversion.

The second reactor contains 16% of the catalyst and the temperature drops from 520°C to 410°C (443°C reported in the industry) due to the endothermic aromatization of naphthenes with formation of hydrogen. Though the quantity of catalyst is more compared to first reactor, conversion of naphthenes is lower due to the depleted availability of naphthenes. The resultant temperature decrease in the second reactor is sufficient to slow down conversion of paraffins and formation of light gases. The products from second reactor are then reheated up to 520 °C before feeding into the third reactor for further reaction.

The third reactor contains 25% of the catalyst and the temperature drops from 520°C to 440°C (468°C reported in the industry). The temperature drop is much lesser than in the first two reactors due to the depletion of naphthenes and conversion of naphthenes to aromatics with formation of hydrogen is almost complete. The resultant increase in the average temperature in the reactor and availability of catalyst favours initiation of exothermic hydro-cracking of paraffins/naphthenes with formation of light gases with consumption of hydrogen. The products from the third reactor are then reheated up to 520 °C before feeding into the fourth reactor for further reaction.

The fourth reactor contains 45 % of the catalyst and the temperature drops from 520°C to 467°C (493°C reported in the industry). In the virtual absence of naphthenes and endothermic aromatization reactions, temperature in the fourth reactor is high enough to facilitate exothermic hydro-cracking of paraffins to produce large quantities of light gases with consumption of hydrogen.

Fig. 4.2 shows the component profiles in the radial flow moving bed reactor. Endothermic aromatization of naphthenes to aromatics is dominant in the first, second and third reactor (up to 55% of catalyst), while in fourth reactor amounting to 45% of catalyst exothermic conversion of paraffins to light gases is more predominant. Temperature decreases to a higher extent in the first two reactors due to the endothermic aromatization in nature. Lesser aromatization in the fourth reactor increases the bed temperature causing increased exothermic hydro-cracking to produce unwanted light gases with consumption of valuable hydrogen. The net flow rates of each component as per the model and actual industrial information are tabulated in Table 4.1. The deficiency in material balance could be due to coke formation and the model estimates compare well with actual industrial information.

Table 4.1: Summary of the feed and products for model and actual industrial data.

	Component	F _{in} , (kg/h)	F _{out} , (kg/h)	ΔF (kg/h)	% coke formation
Model	Paraffin	57,920	28,965	-28,955	$= (F_{in} - F_{out}) / F_{in} * 100\%$ $= \{(119,622 - 115,470) / 119,622\} * 100\%$ $= 3.47\%$
	Naphthene	45,018	718	-44,300	
	Aromatic	10,718	66,531	55,813	
	Hydrogen	5,966	7,445	1,479	
	Light Gases	0	11,811	11,811	
	Total	119,622	115,470	-	
Actual	Paraffin	57,920	26,364	-31,556	$= (F_{in} - F_{out}) / F_{in} * 100\%$ $= \{(119,622 - 115,773) / 119,622\} * 100\%$ $= 3.22\%$
	Naphthene	45,018	1,084	-43,934	
	Aromatic	10,718	68,355	57,637	
	Hydrogen	5,966	8,597	2,631	
	Light Gases	0	11,373	11,373	
	Total	119,622	115,773	-	

4.3 Discussions

The catalyst takes about 100 hours to flow through the CRR before going out for regeneration compared to 3 to 6 months of operation before regeneration in SRR units. Catalyst activity in SRR units can decline up to 0.8. The residence time of catalyst in the radial flow moving bed reactor is less than 100 hours (around 4 days). Based on the proposed linear deactivation model, catalyst activity as it flows through the four reactors in about 97 hours is shown in Fig. 4.3.

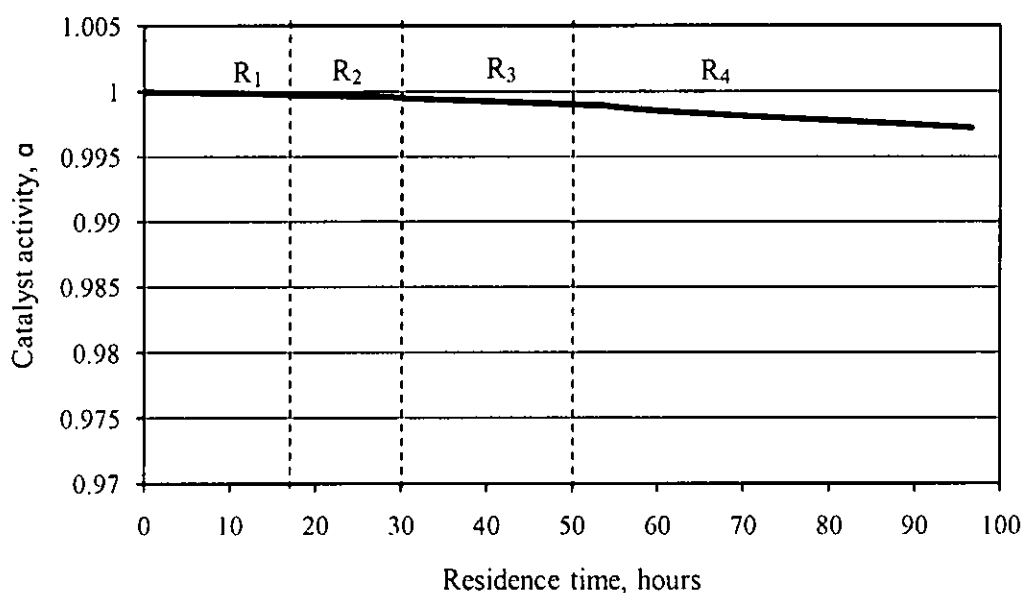


Fig. 4.3: Profiles of catalyst activity versus residence time along the radial flow moving bed reactor.

The catalyst activity is greater than 0.998 and hence for all the practical purposes, the catalyst activity in CRR units is close to 1. Coke formation up to about 3.22% is reported in the industry. This could be due to non ideal flow of catalyst particles such as pinning. This suggests that reducing circulation rate of catalysts will not adversely affect the conversions while it can reduce particle attrition. About 2% catalyst particle attrition is observed in the industry.

CHAPTER 5

SIMULATION OF THE MODEL

5.1. Introduction

The main duty of a reformer is aromatization of naphthenes to produce aromatics and hydrogen. Ways and means to improve the production of aromatics and minimization of the conversion to light gases can be explored using the model developed in Chapter 3 and 4. Flow rate cannot be increased as it can alter the level of pinning. Aromatics in the feed dilute the main reactant naphthenes and do not contribute to the aromatics production. Paraffins in the feed appear not to contribute to the aromatics production. Section 5.2 explores the possibility of feeding the reformer with naphthenes alone and hydrogen or paraffins alone and hydrogen. Section 5.3 considers the scheme with possibility of introducing fresh naphtha and hydrogen into reactors R_1 and R_3 with product withdrawn from R_2 and R_4 . Section 5.4 considers the scheme with introducing fresh naphtha and hydrogen into reactor R_1 and R_4 with product withdrawn from R_3 and R_4 . Section 5.5 considers the scheme with possibility of introducing fresh naphtha and hydrogen into reactors R_1 , R_3 and R_4 with product withdrawn from R_2 , R_3 and R_4 . Section 5.6 explores the scheme with possibility of introducing fresh naphtha and hydrogen to reactors R_1 , R_2 , R_3 , and R_4 with product withdrawn from R_1 , R_2 , R_3 and R_4 . The results are discussed in terms of improvement in aromatics and hydrogen production with reduction in light gases production compared to the base case of naphtha feed to R_1 and product withdrawn from R_4 .

5.2. Feeding Pure Component

The pure components need to be obtained from naphtha feed as naphtha contains 39.75% naphthenes, 50.26% paraffins and 9.99% aromatics. To feed naphthenes alone, 2.52 times naphtha need to be processed; similarly to feed paraffins alone, 1.96 times naphtha need to be processed.

5.2.1 Naphthenes only in Fresh Feed

Temperature profile in each reactor when the fresh feed contains naphthenes only with hydrogen is presented in Fig. 5.1. The component profiles through the reactors are presented in Fig. 5.2. In every reactor, the main reaction is aromatization of naphthenes which is endothermic reversible in nature. Therefore, the temperature will drop in each reactor. In last two reactors, the temperature drop is slightly higher compared to first two reactors as the last two reactors contain 70% of catalyst.

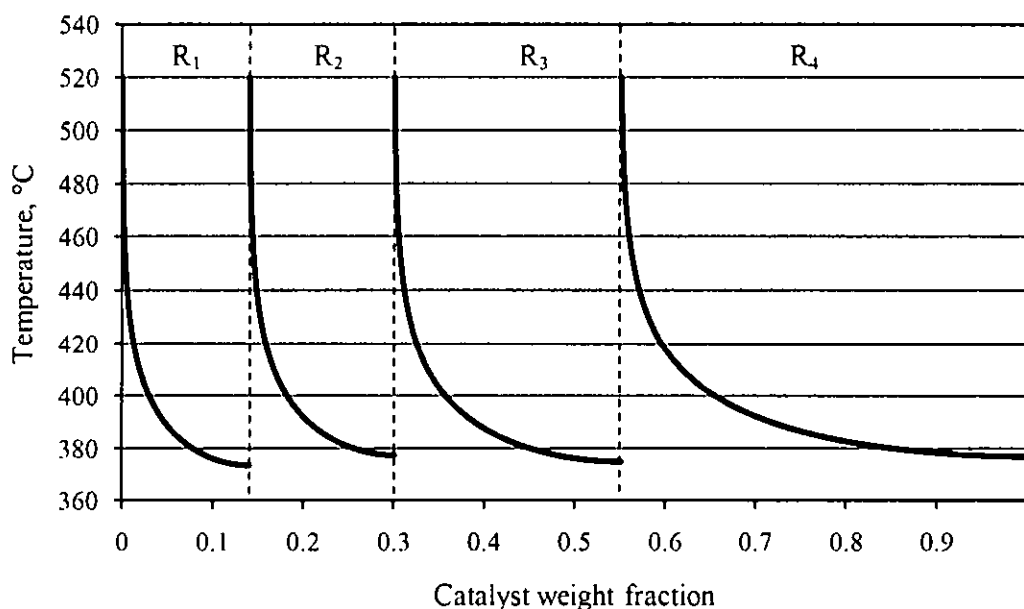


Fig. 5.1: Effect of catalyst weight fraction on the temperature along the radial flow moving bed reactor when feeding naphthenes and hydrogen in fresh feed.

Fig. 5.2 shows the component profiles when feeding naphthenes alone with hydrogen as fresh feed. Production of aromatics and hydrogen increase as

naphthenes get dehydrogenated to aromatics. Also, the hydro-cracking of naphthenes produce around 0.21% light gas. Table 5.1 compares the results of the two schemes (with pure naphthene feed and pure paraffin feed) with the base case naphtha feed.

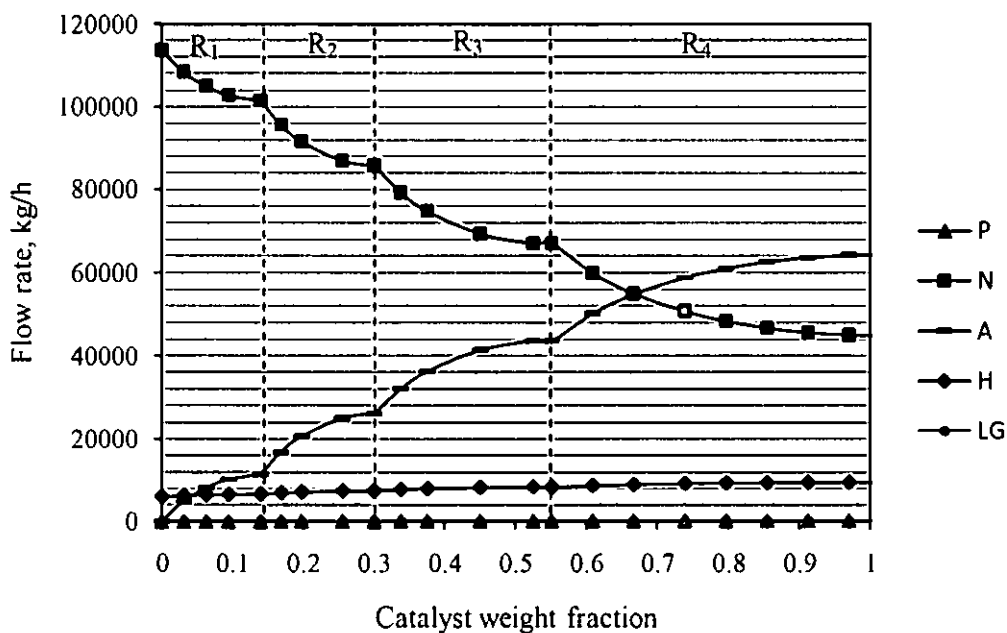


Fig. 5.2: Effect of catalyst weight fraction on the naphtha components in radial flow moving bed reactor when feeding naphthenes and hydrogen in fresh feed.

5.2.2 Paraffins only in Fresh Feed

Temperature profile in each reactor with feed containing paraffin alone is shown in Fig. 5.3. The component profiles through the reactors are presented in Fig. 5.4. The flow rate of paraffins decreases due to the dehydrogenation and hydro-cracking to form naphthenes and light gases. The naphthenes so formed get further dehydrogenated endothermically to aromatics. Reactions of dehydrogenation are endothermic while hydro-cracking of paraffins are exothermic in nature. Thus, the production of naphthenes passes through a maximum while aromatics and light gases keep increasing in each reactor. Naphthenes formed in the first two reactors contribute to aromatics production in the last two reactors. Temperature drop in the last two reactors is slightly more compared to first two reactors.

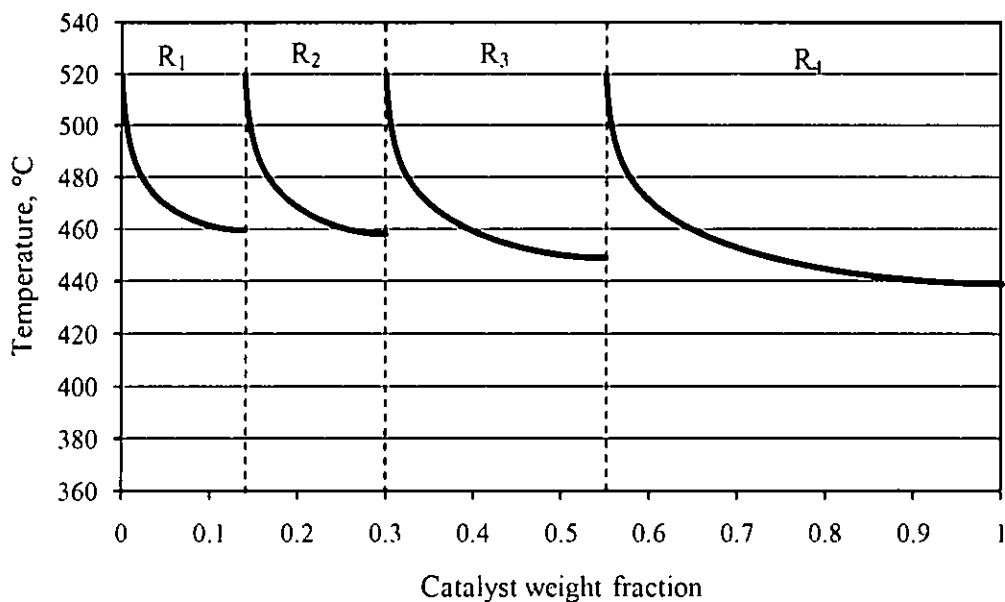


Fig. 5.3: Effect of catalyst weight fraction on the temperature along the radial flow moving bed reactor when feeding paraffins and hydrogen in fresh feed.

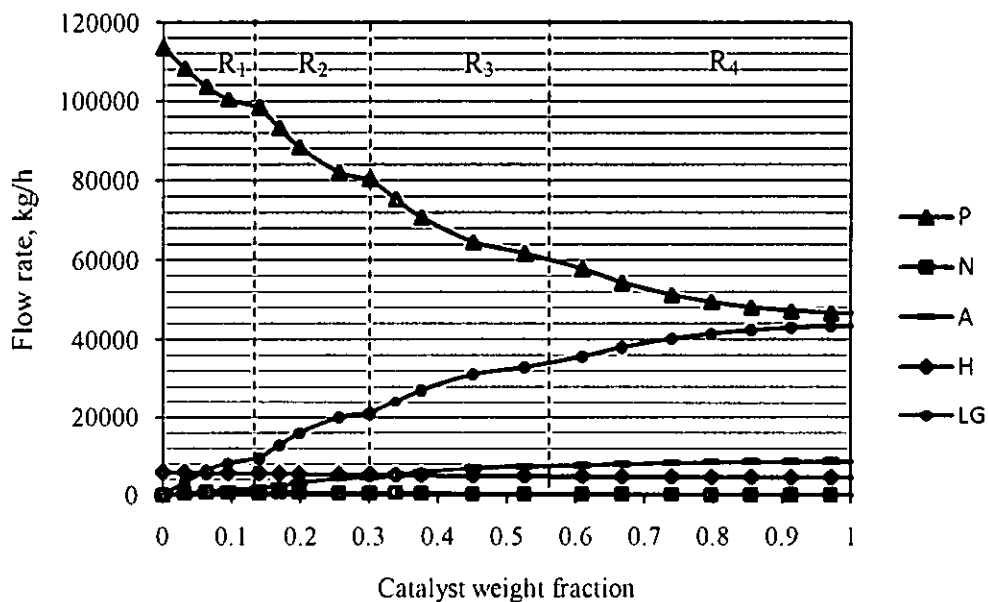


Fig. 5.4: Effect of catalyst weight fraction on naphtha components in radial flow moving bed reactor when feeding paraffins and hydrogen only in fresh feed.

Table 5.1 compares the results of the two schemes (with pure naphthene feed and pure paraffin feed) with the base case naphtha feed.

Table 5.1: Summary of the input and output of reactors at different scheme of fresh feed.

Scheme	Component	F _{in} , (kg/h)	F _{out} , (kg/h)	ΔF (kg/h)	% Coke =(F _{in} - F _{out}) / F _{in} * 100%
Naphthenes only in fresh feed (obtained from 286,942 kg/h of naphtha)	Paraffin	-	243	243	0.36%
	Naphthene	113,655	44,932	-68,723	
	Aromatic	-	64,259	64,259	
	Hydrogen	5,987	9,522	3,535	
	Light gas	-	252	252	
	Total	119,642	119,208	-	
Paraffins only in fresh feed (obtained from 223,024 kg/h of naphtha)	Paraffin	113,655	46,831	- 66,824	13.26%
	Naphthene	-	133	133	
	Aromatic	-	8,775	8,775	
	Hydrogen	5,884	4,560	-1,324	
	Light gas	-	43,395	43,395	
	Total	119,539	103,694	-	
Base (113,656 kg/h of naphtha)	Paraffin	57,920	28,965	-28,955	3.47% (compares reasonably well with industrial information of 3.22%)
	Naphthene	45,018	718	-44,300	
	Aromatic	10,718	66,531	55,813	
	Hydrogen	5,966	7,445	1,479	
	Light gas	0	11,811	11,811	
	Total	119,622	115,470	-	

Aromatics are essentially produced by conversion of naphthenes. From Table 5.1 it can be seen that feeding naphthenes alone can increase production of aromatics to 64,259 kg/h compared to the base case of 55,813 kg/h while reducing light gases to 252 kg/h compared to the base case of 11,811 kg/h and reducing coke formation to 0.36% compared to 3.47%. This also increases hydrogen production to 3,535 kg/h compared to 1,479 kg/h in the base case.

It can be seen from Table 5.1 that feeding paraffin alone can increase light gases, carbon deposition and consumption of hydrogen while reducing production of aromatics drastically. Feeding paraffins alone can be very disadvantageous and is not recommended.

5.3 Introducing Fresh Naptha into R₁ and R₃ Reactors

5.3.1 Hypothesis:

In the base system as explained in section 4.2, most of the naphthenes are converted to aromatics in the reactors R₁, R₂ and R₃. As the aromatization of naphthenes is an endothermic process, reduction in temperature is high in R₁ and R₂ and much less in R₃ and R₄. Higher temperatures in R₃ and R₄ favor exothermic hydro-cracking reactions to produce light gas and consume hydrogen. To minimize the production of light gases and consumption of hydrogen in R₃ and R₄ reactors, it is necessary to reduce the reactor temperature. Addition of fresh feed/naphthenes to promote endothermic dehydrogenation reactions is one possibility to reduce the reactor temperature and reduce hydro-cracking reactions. However, the reactant flow rates in each reactor can not be increased to avoid pinning of catalyst particles.

To avoid hydrocracking reactions in R₃ and R₄ reactors in the present base system, one possible scheme is to withdraw the exit stream from R₂ as product and fresh feed may be processed through R₃ and R₄ reactors. Fresh naptha feed to R₃ favors aromatization of naphthenes which can help lower the reactor temperature to minimize hydro-cracking reactions. The exit stream from R₃ can be introduced to R₄. Aromatization of naphthenes increases because of the availability of 25% of the catalyst in R₃ and 45% of the catalyst in R₄. Together, by this scheme, there can be two product streams; one exiting from R₂ and the other exiting from R₄; with improved production of aromatics and lowering of production of light gases.

5.3.2. Results

Temperature profile in each reactor with introducing naphtha and hydrogen as feed to R_1 and R_3 reactors with product streams from R_2 and R_4 reactors is presented in Fig. 5.5. The performance of the first two reactors, R_1 and R_2 is exactly same as the one presented in section 4.2 for the base case operation. With feeding fresh feed at the temperature 520 °C to the reactor R_3 , the temperature decreased to 383 °C due to endothermic dehydrogenation reactions. The product from third reactor then reheated up to 520 °C before it enters the fourth reactor. The temperature drops to 394 °C in the fourth reactor. Compared to the base operation (as presented in section 4.2), the temperatures in R_3 and R_4 decreased because of the endothermic reaction. Fig. 5.6 presents the component profiles (paraffins, naphthenes, aromatics, hydrogen and light gases).

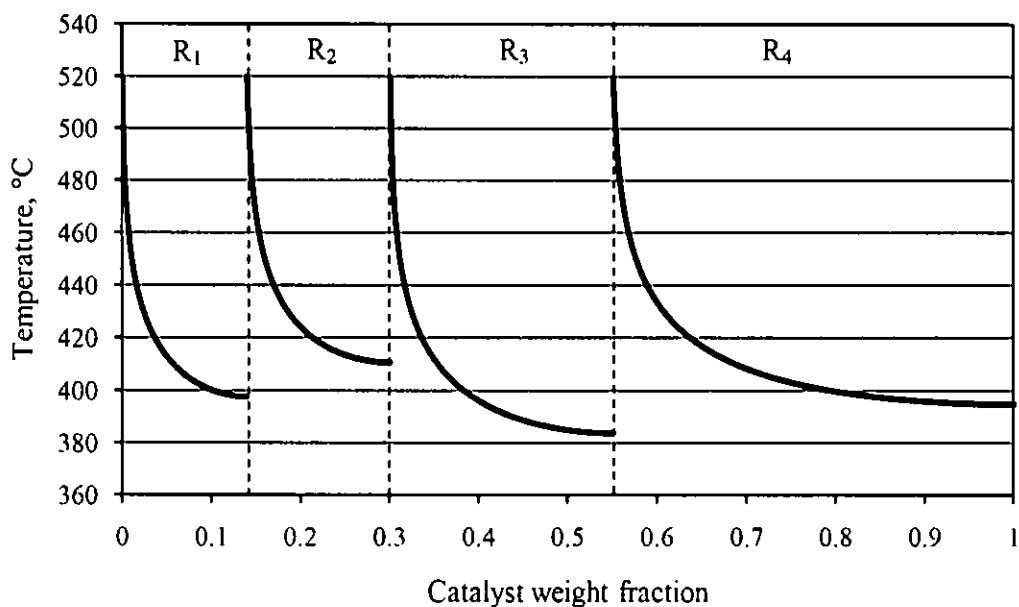


Fig. 5.5: Effect of catalyst weight fraction on the temperature along the radial flow moving bed reactor when introducing fresh feed in R_1 and R_3 reactors.

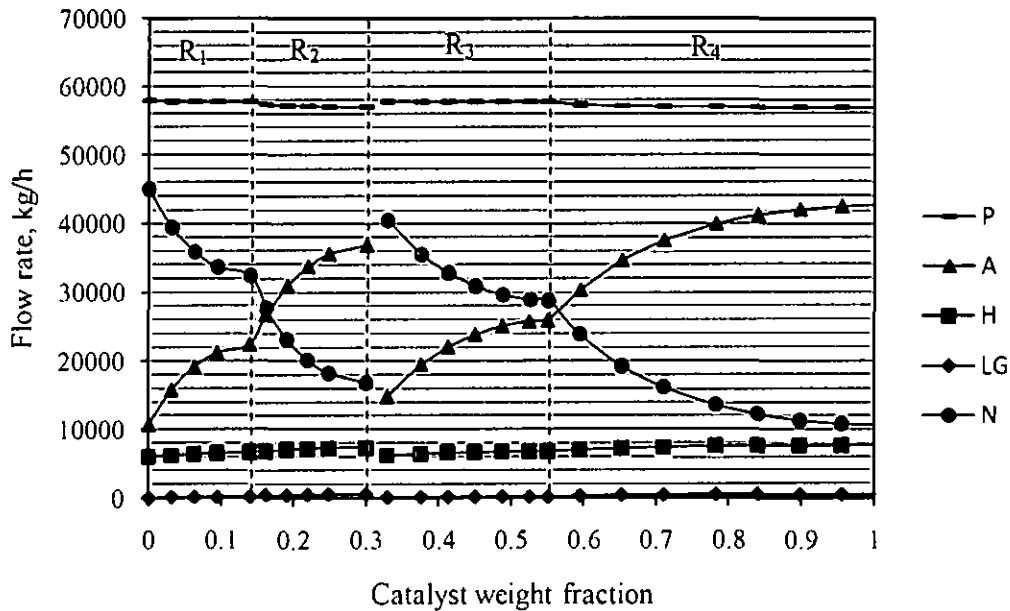


Fig. 5.6: Effect of catalyst weight fraction on the naphtha components in radial flow moving bed reactor when introducing fresh feed in R_1 and R_3 reactors.

In reactors R_1 and R_2 , flowrate of naphthenes decreases and flow of aromatics increases from 10,717 up to 36,931 kg/h which can be taken out as product at the exit of R_2 . With fresh feed to the reactor R_3 , flowrate of naphthenes decreases and flow of aromatics increases from 10,717 up to 42,732 kg/h at the exit of R_4 . Thus net aromatic production is 58,229 kg/h compared to 55,813 kg/h in the base case with fresh feed to R_1 only. At the same time, the light gases decreased from 11,811 kg/h in the base case to 1,121 kg/h. It is interesting to note that paraffins conversion is just 1,897 kg/h compared to 28,955 kg/h in base case. Meanwhile, the hydrogen produced is 3,117 kg/h compare to 1,479 kg h in the base case. These results are summarized in Table 5.2.

Table 5.2: Summary of the input and output of reactors at scheme of introducing fresh feed in R₁ and R₃ reactors.

	F _{in} (kg/h)		Total in (kg/h)	F _{out} (kg/h)		Total out (kg/h)	ΔF (kg/h)	% coke
	R ₁	R ₃		R ₂	R ₄			
P	57,918	57,918	115,836	57,019	56,920	113,939	-1897	0.81 %
N	45,016	45,016	90,032	16,810	10,719	27,529	-62,503	
A	10,717	10,717	21,434	36,931	42,732	79,663	58,229	
H	5,966	5,966	11,932	7,364	7,685	15,049	3,117	
LG	0	0	0	548	573	1,121	1,121	
Grand Total			239,234	Grand Total		237,301	-	

By this modification, production of aromatics can increase by a factor of around 1.043. Also production of light gases is reduced by a factor of 10 times and production of hydrogen increased by a factor of 2.

This option of adding fresh feed in R₁ and R₃ and withdrawn of products from R₂ and R₄ is encouraging. Other similar options are explored to improve the reactor system for increased production of aromatics and reduction in the production of light gases.

5.4 Introducing Fresh Naphtha into R₁ and R₄ Reactors

5.4.1 Hypothesis

Reactors R₁, R₂ and R₃ contain 55% of catalyst while R₄ contains 45% of catalyst. In the base case, as most of the naphthenes get converted in the R₁, R₂ and R₃ reactors, hydro cracking reactions predominate in R₄ reactor due to higher temperature.

Hence, it is worthwhile to withdraw the products from R₃ and introduce fresh feed to R₄ and withdrawn product stream from R₄.

5.4.2 Results

Temperature profile in each reactor R₁,R₂,R₃ and R₄ with introduction of fresh feed to R₁ and R₄ reactors and withdrawn of product streams from R₃ and R₄ reactors is presented in Fig. 5.7. The performance of the first three reactors R₁, R₂ and R₃ is exactly same as the one presented in section 4.2 for the base operation. Introducing the fresh feed to R₄ decrease the reactor temperature until 373 °C. Compared to the base operation (as presented in section 4.2), the temperature in R₄ decreased more because of the higher content of catalyst. Fig. 5.8 presents the flow rate of various components (paraffins, naphthenes, aromatics,hydrogen and light gases).

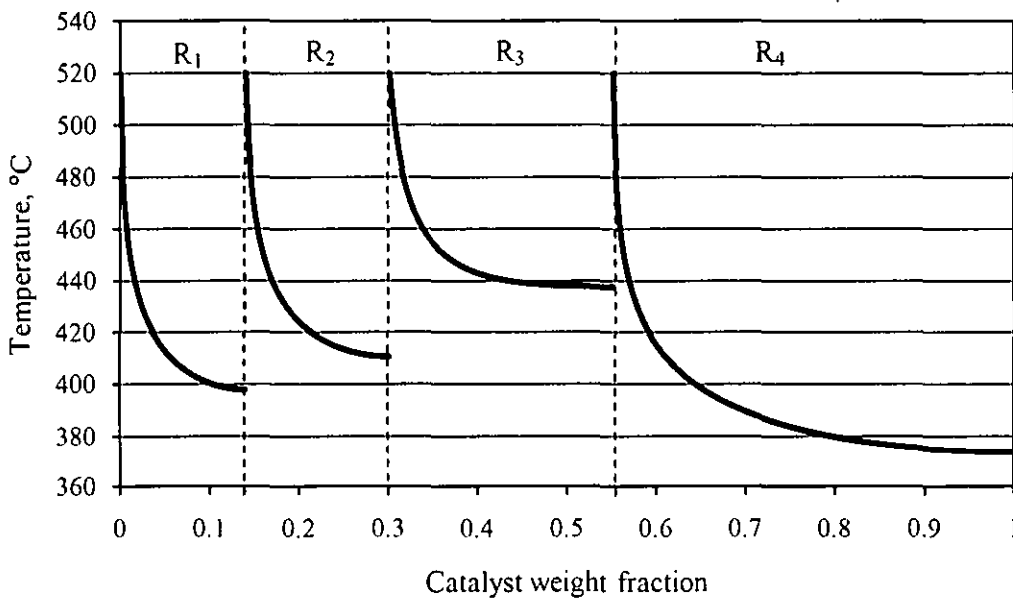


Fig. 5.7: Effect of catalyst weight fraction on the temperature along the radial flow moving bed reactor when introducing fresh feed in R₁ and R₄ reactors.

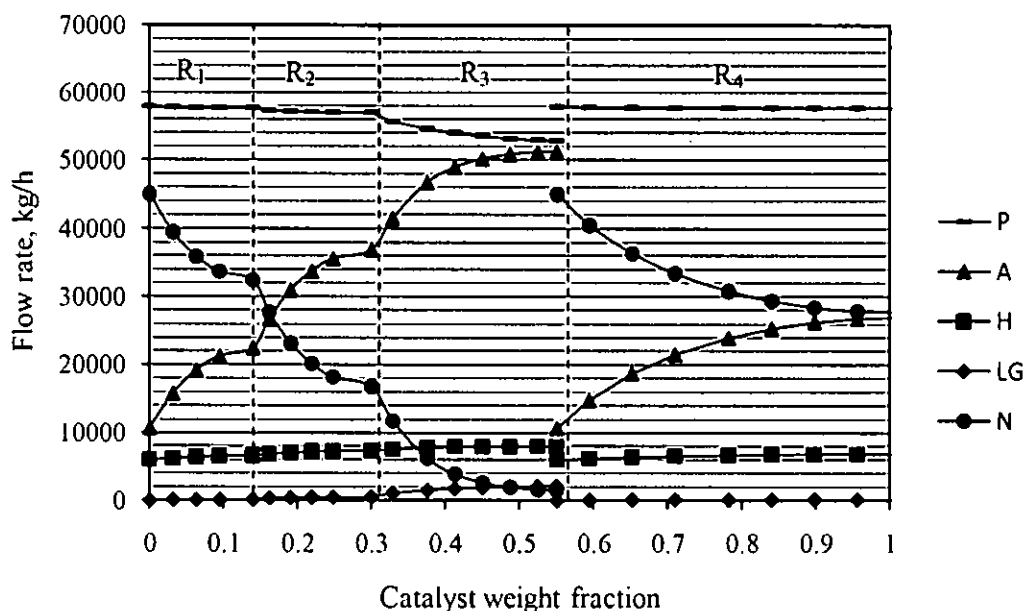


Fig. 5.8: Effect of catalyst weight fraction on the naphtha components in radial flow moving bed reactor when introducing fresh feed in R_1 and R_4 reactors.

In reactors R_1 , R_2 and R_3 , flowrate of naphthenes decreases and flow of aromatics increases from 10,717 up to 51,244 kg/h which can be taken out as product at the exit of R_3 . With fresh feed to the reactor R_4 , flowrate of naphthenes decreases and flow of aromatics increases from 10,717 up to 26,929 kg/h at the exit of R_4 . Thus net aromatic production is 56,739 kg/h compared to 55,813 kg/h in the base case with feed to R_1 only. At the same time, the light gases decreased from 11,811 kg/h in the base case to 2,317 kg/h. It is interesting to note that paraffins conversion is just 5,281 kg/h compared to 28,954 kg/h in base case. Flow rate of hydrogen increases to 2,930 kg/h compare to 1,479 kg h in the base case. These results are summarized in Table 5.3.

Table 5.3: Summary of the input and output of reactors at scheme of introducing fresh feed in R₁ and R₄ reactor.

	F _{in} (kg/h)		Total (kg/h)	F _{out} (kg/h)		Total (kg/h)	ΔF (kg/h)	% coke
	R ₁	R ₄		R ₃	R ₄			
P	57,918	57,918	115,836	52,866	57,689	110,555	-5,281	
N	45,016	45,016	90,032	1,608	27,721	29,329	-60,703	
A	10,717	10,717	21,434	51,244	26,929	78,173	56,739	
H	5,966	5,966	11,932	8,012	6,850	14,862	2,930	
LG	0	0	0	2,160	157	2,317	2,317	
Grand Total			239,234	Grand Total		235,231	-	

By this modification, increase in production of aromatics is very low compared to the base case though this scheme reduced production of light gases by a factor of 5 and improved hydrogen production by a factor of 2.

5.5 Introducing Fresh Feed in R₁, R₃ and R₄ Reactors

To explore further, possibility of introducing three fresh feeds is considered in this section.

5.5.1 Hypothesis

Conversion of naphthenes in R₁ and R₂ is about 63% using about 30% of the catalyst as presented in section 4.2. With fresh feed to R₃, conversion of naphthenes in R₃ and R₄ is 74% using 70% of the catalyst. R₃ has 25% of the catalyst and would account for most of the conversion leaving very little naphthene for conversion in the R₄ which has 45% of the total catalyst. This suggests the possibility of further improvements with feeds to reactors R₁, R₃ and R₄.

5.5.2. Results

Temperature profile in each reactor with feed to R_1 , R_3 and R_4 reactors and product streams from R_2 , R_3 and R_4 reactors is presented in Fig. 5.9. The performance of the first two reactors R_1 and R_2 is exactly same as the one presented in section 5.3 and 5.4 for the two feed operation. With the feed at the temperature 520 °C to the reactor R_3 , the temperature decreased to 383 °C. With another fresh feed to reactor R_4 , the temperature drops until 373 °C. Compared to the two feed operation (as presented in section 5.3 and 5.4), the temperature in R_4 decreased more because of the higher quantity of catalyst and naphthenes.

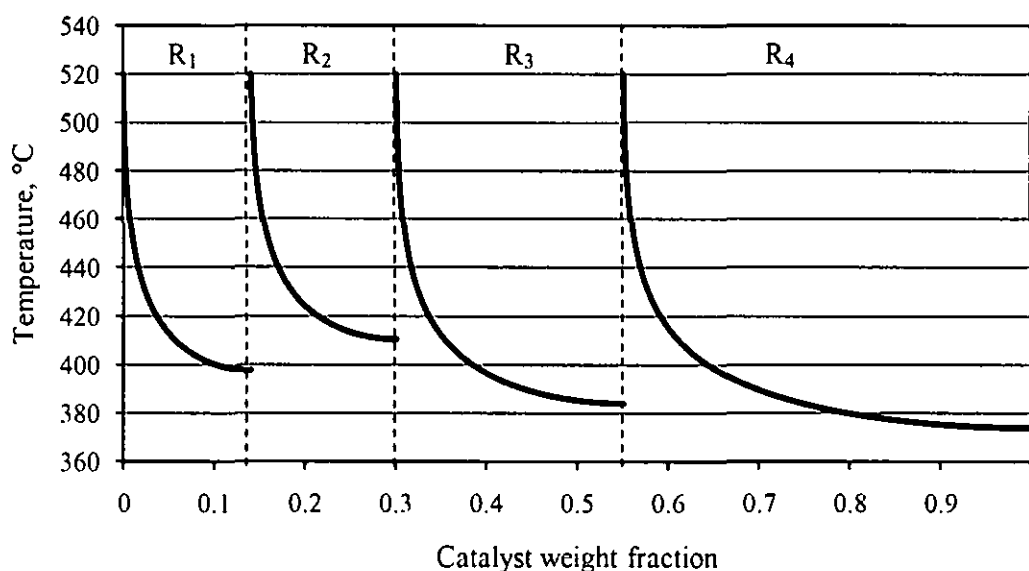


Fig. 5.9: Effect of catalyst weight fraction on the temperature along the radial flow moving bed reactor when feeding feed in R_1 , R_3 and R_4 reactors.

Fig. 5.10 presents the flow of various components (paraffins, naphthenes, aromatics, hydrogen and light gases). The aromatics are produced mainly by dehydrogenation of naphthenes. Therefore, the flowrate of naphthenes decrease while flow rate of aromatics increases while flow rate of paraffins decreases slightly. Due to low reactor temperature because of endothermic dehydrogenation, production of light gases is very limited.

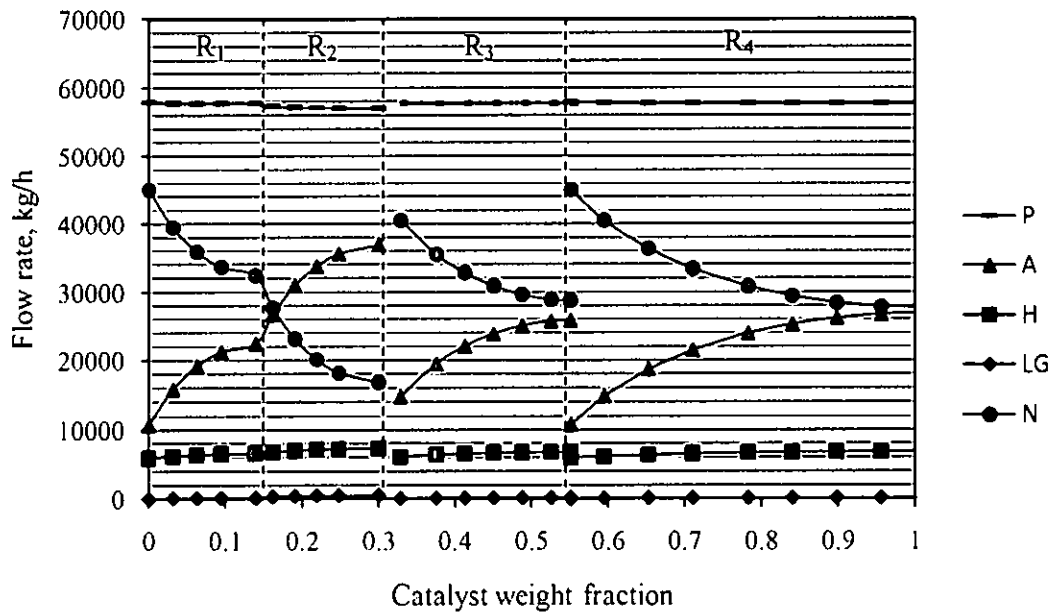


Fig. 5.10: Effect of catalyst weight fraction on naphtha components in radial flow moving bed reactor when feeding feed in R₁, R₃ and R₄ reactors.

Aromatics increased from 10,717 kg/h up to 36,931 , 25,916 and 26,928 kg/h in reactors R₂, R₃, and R₄ respectively. Together, net aromatics production increased to 57,624 kg/h compared to 55,813 kg/h in the base case with feed to R₁ only. Light gas flow decreased to 887 kg/h compared to 11,811 kg/h in the base case. Flow rate of hydrogen increases from 5,966 kg/h up to 7,364 , 6,790 and 6,850 kg/h in reactors R₂, R₃, and R₄ respectively. Thus, net hydrogen production is 3,106 kg/h compare to 1,479 kg h in the base case. These results are summarized in Table 5.4.

Table 5.4: Summary of the input and output of reactors at scheme of feeding feed in R₁, R₃ and R₄ reactors.

	F _{in} (kg/h)	Total (kg/h)	F _{out} (kg/h)			Total (kg/h)	ΔF (kg/h)	% coke
	R ₁ , R ₃ , R ₄		R ₂	R ₃	R ₄			
P	57,918 x 3	173,754	57,019	57,664	57,689	172,372	-382	0.43 %
N	45,016 x 3	135,048	16,810	28,748	27,722	73,280	-61,768	
A	10,717 x 3	32,151	36,931	25,916	26,928	89,775	57,624	
H	5,966 x 3	17,898	7,364	6,790	6,850	21,004	3,106	
LG	0	0	548	183	157	888	888	
Grand Total		358,851	Grand Total			357,319	-	

By this modification, improvement over two feed case is marginal.

5.6 Feeding Fresh Feed in R₁, R₂, R₃ and R₄ Reactors

For completeness sake, fresh feed to each of the reactors is explored in this section.

5.6.1 Results

Temperature profile in radial flow moving bed reactor R₁, R₂, R₃ and R₄ with feed to R₁, R₂, R₃ and R₄ reactors with product streams from R₁, R₂, R₃ and R₄ reactors is presented in Fig. 5.11. The performance of the reactor R₁, R₃ and R₄ is exactly same as the one presented in section 5.5 for the three feed operation. With fresh feed at the temperature 520 °C to the reactor R₂, the temperature decreased to 395 °C. Fig. 5.12 presents the flow of various components (paraffins, naphthenes, aromatics, hydrogen and light gases).

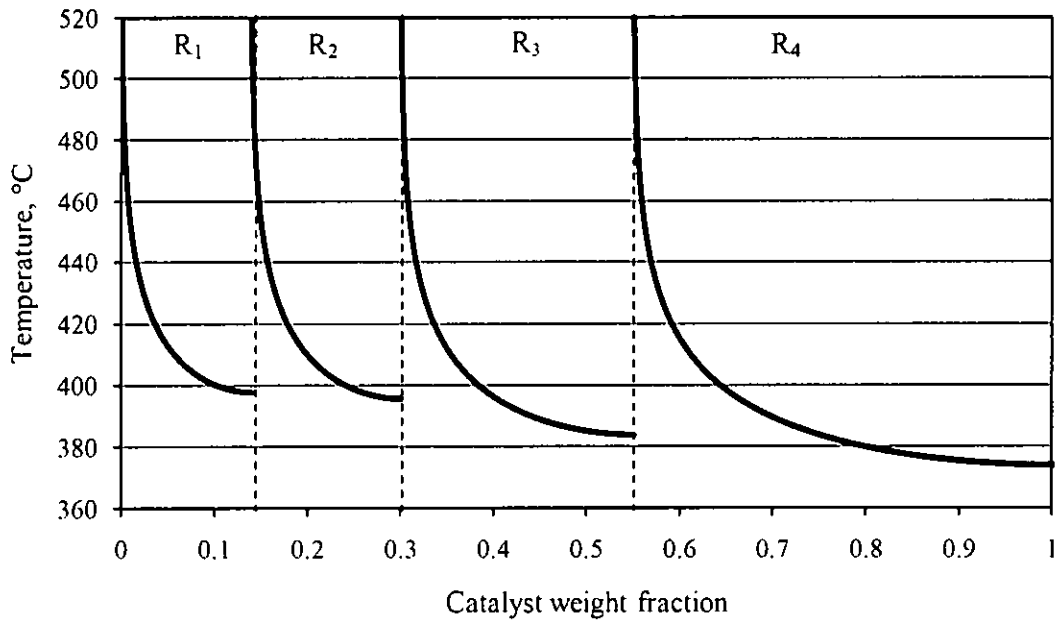


Fig. 5.11: Effect of catalyst weight fraction on the temperature along the radial flow moving bed reactor when feeding feed in R_1, R_2, R_3 and R_4 reactors.

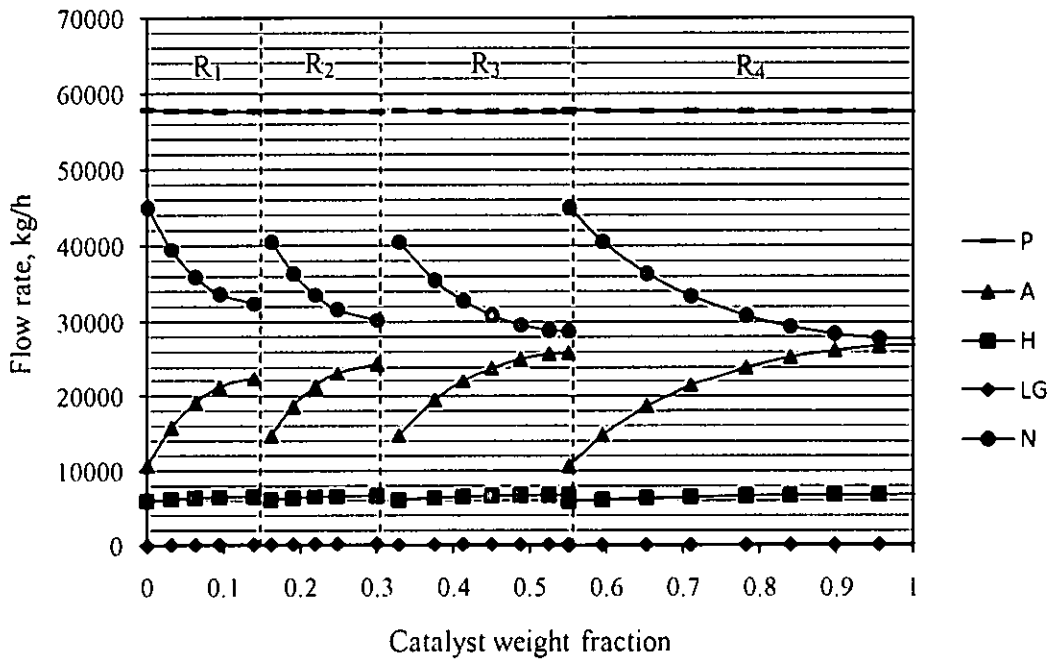


Fig.5.12: Effect of catalyst weight fraction on naphtha components in radial flow moving bed reactor when feeding feed in R_1, R_2, R_3 and R_4 reactors.

Aromatics increases from 10,717 kg/h up to 22,458 , 24,487, 25,916 and 26,928 kg/h in reactors R₁, R₂, R₃, and R₄ respectively. Together, net aromatics production increased to 56,921 kg/h compared to 55,813 kg/h in the base case with feed to R₁ only. Light gas flow decreased to 708 kg/h compared to 11,811 kg/h in the base case.; however there is less reduction in light gases compared to three or two feed options. Flow rate of hydrogen increases from 5,966 kg/h up to 6,600 , 6,709, 6,790 and 6,850 kg/h in reactors R₁, R₂, R₃, and R₄ respectively. Thus, net hydrogen production is 3,085 kg/h compare to 1,479 kg h in the base case. These results are summarized in Table 5.5.

Table 5.5: Summary of the input and output of reactors at scheme of feeding feed in R₁, R₂, R₃ and R₄ reactors.

	F _{in} (kg/h)	Total (kg/h)	F _{out} (kg/h)				Total (kg/h)	ΔF (kg/h)	% coke
	R ₁ , R ₂ , R ₃ , R ₄		R ₁	R ₂	R ₃	R ₄			
P	57,918 x 4	231,672	57,694	57,642	57,664	57,689	230,689	-983	
N	45,016 x 4	180,064	32,408	30,231	28,748	27,722	119,109	-60,955	
A	10,717 x 4	42,868	22,458	24,487	25,916	26,928	99,789	56,921	
H	5,966 x 4	23,864	6,600	6,709	6,790	6,850	26,949	3,085	
LG	0	0	167	201	183	157	708	708	
Grand Total		478,468	Grand Total				477,244	-	

By this modification, increase in production of aromatics is very low compared to the base case though this scheme reduced production of light gases by a factor of 16 and improved hydrogen production by a factor of 2.

5.7 Summary and Conclusions

The summary of various feed schemes and product distributions for all the simulations are presented in Table 5.6.

Table 5.6: Summary of the input and output of reactors at various schemes.

Feed Scheme	Total Feed (kg/h)	Paraffin Product (kg/h)	Naphthene Product (kg/h)	Aromatic Product (kg/h)	Hydrogen Product (kg/h)	Light Gas Product (kg/h)	% coke
Naphthene only	119,642	243	44,932	64,259	3,535	252	0.36
Paraffin only	119,539	46,831	133	8,775	-1,324	43,395	13.26
R ₁ (Base)	119,622	28,965	718	55,813	1,479	11,811	3.47
R ₁ & R ₃	239,234	113,939	27,529	58,229	3,117	1,121	0.81
R ₁ & R ₄	239,234	110,555	29,329	56,739	2,930	2,317	1.67
R ₁ , R ₃ & R ₄	358,851	172,372	73,280	57,624	3,106	888	0.43
R ₁ , R ₂ , R ₃ & R ₄	478,468	230,689	119,109	56,921	3,085	708	0.26

The best scheme is the one which gives more aromatics, more hydrogen, less light gases with less recycle requirements. Table 5.7 shows the factors that need to be considered in choosing the best scheme to increase the production of aromatics, hydrogen and reduce light gases.

Table 5.7: Screening for the best feed scheme.

Feed Scheme	Aromatic per naphtha feed	Hydrogen per naphtha feed	Light gases per naphtha feed	Aromatic Production (kg/h)
Naphthene only	= (64,259 / 286,942) = 0.223	= (3,535 / 286,942) = 0.0123	= (252 / 286,942) = 0.0008	64,259
Paraffin only	= (8,775 / 223,024) = 0.0393	= (-1,324 / 223,024) = -0.0059	= (43,395 / 223,024) = 0.1946	8,775
R ₁ (Base)	= (55,813 / 119,622) = 0.4666	= (1,479 / 119,622) = 0.01236	= (11,811 / 119,622) = 0.0987	55,813
R ₁ & R ₃	= (58,229 / 239,234) = 0.2433	= (3,117 / 239,234) = 0.01303	= (1,121 / 239,234) = 0.00468	58,229
R ₁ & R ₄	= (56,739 / 239,234) = 0.2372	= (2,930 / 239,234) = 0.01225	= (2,317 / 239,234) = 0.00969	56,739
R ₁ , R ₃ & R ₄	= (57,624 / 358,851) = 0.1606	= (3,106 / 358,851) = 0.008655	= (888 / 358,851) = 0.00247	57,624
R ₁ , R ₂ , R ₃ & R ₄	= (56,921 / 478,468) = 0.1189	= (3,085 / 478,468) = 0.006447	= (708 / 478,468) = 0.00148	56,921

From Table 5.7, the present base system (feeding fresh feed in R_1 only) is the best for aromatics per naphtha feed and worst in terms of light gases and hydrogen produced per naphtha feed.

The scheme of introducing fresh feed in R_1 & R_3 improves aromatics production by 4% , improves hydrogen production by 110% and reduces light gases to 91% compared to the base case. However this involves handling 2 times of naphtha compared to the base value.

The scheme of introducing naphthenes only, improves aromatics production by 15% , improves hydrogen production by 139% and reduce light gases by to 98 % compared to the base case. However this involves pre-separation of naphthenes and handling 2.53 times of naphtha compared to the base value.

Feeding naphthenes alone can be the best option though naphtha pre-separation adds to the cost. Also this reduces the cost of handling aromatics and paraffins through the reactor (pumping and heating costs). However, the option of introducing fresh feed in R_1 & R_3 and withdrawn of the products from R_2 and R_4 is the easier to implement and to minimize hydro-cracking and consumption of hydrogen.

CHAPTER 6

CONCLUSIONS AND RECOMMENDATIONS

6.1. Conclusions

Aromatics and hydrogen required for the refinery and petrochemical applications are produced by catalytic naphtha reforming in a radial flow moving bed reactor with continuous recycling of regenerated catalyst. As the reactions are net endothermic in nature, the reactant stream is made to flow through four reactors, stacked on top of one another, in series with preheating of feed to each reactor unit to maximize the yield.

A compartment-in-series model is developed to explain the performance of catalytic naphtha reforming in a radial flow moving bed reactor. The naphtha feedstock is considered to consist of paraffins, naphthenes and aromatics. Dehydrogenation of paraffins and naphthenes produces aromatics and hydrogen while hydro-cracking consumes hydrogen to convert paraffins and naphthenes to light gases. Reaction kinetics depends on the characteristics of the catalyst; form of the reforming kinetics proposed by Smith [5] is adopted and tuned to match the information on the industrial data. Temperature and concentration profiles in industrial reactors could be explained better by assigning compartment size as equal to catalyst particle size. As the catalyst residence time in the radial flow moving bed reactor is less than 5 days compared to 180 days in SRR units, catalyst activity is assumed to decline linearly with time.

The reactor model is simulated to estimate the reformate composition and temperature profiles. The simulation results are in reasonable agreement with the plant data. Most of the endothermic reforming reactions took place in the first three reactors while exothermic hydro-cracking is predominant in the fourth reactor

(containing 45% of catalyst). Increasing the flow rate in the current configuration is not acceptable as it can increase pinning and disrupt production.

Introducing fresh feed into each unit and withdrawn the product from each unit is considered. From the simulations, feeding of fresh feed in first and third reactor and withdrawn product from second and fourth reactor can increase the productivity of aromatics and hydrogen while suppressing hydro-cracking reactions. Also the possibility of feeding naphthenes alone by removing paraffins and aromatics in naphtha can be advantageous.

A simple model for catalyst particle breakage is formulated; catalyst particle breakage can be reduced by decreasing the catalyst circulation rate.

6.2. Recommendations

The topic of Radial Flow Moving Bed Reactors received very little attention in academic circles though they are widely used in the industry. Present work explored modeling CP-Z configuration. Other configurations (such as CP- π , CF-Z and CF- π) need to be evaluated. Very little is known about gas and particle flow residence time distributions, particle breakage and pinning in radial flow moving bed reactors. These need to be explored in greater detail.

REFERENCES

- [1] A. M. Aitani and G. Antos. "Catalytic naphtha reforming," 2nd Ed., New York: Marcel Dekker, 2004.
- [2] A.M. Aitani (2006). Catalytic naphtha reforming. *Encyclopedia of Chemical Processing*, pp. 397-406.
- [3] C. Baird. "Catalytic naphtha reforming," HPI Consultants, Inc. 1983.
- [4] Z. Mu, J. Wang, T. Wang and Y. Jin (2003). Optimum design of radial flow moving-bed reactors based on a mathematical hydrodynamic model, *Elsevier*, pp. 409-417. Z.
- [5] R. B. Smith (1959). Kinetic analysis of naphtha reforming with platinum catalyst, *Chemical Engineering Processing*, pp. 76-80.
- [6] M. Mahdavian, S. Fatemi and A. Fazeli (2010). Modeling and simulation of industrial continuous naphtha catalytic reformer accompanied with delumping the naphtha feed, *Int. J. Chem. Reactor Eng*, pp. 1-17. Available: <http://www.bepress.com/ijcre/vol8/A8>.
- [7] Y. Hu, H. Su and J. Chu "Modeling, simulation and optimization of commercial naphtha catalytic reforming process, *Conference on Decision and Control*, Hawaii, USA, 2003.
- [8] J. Ancheyta-Juarez and E. Villafuerte-Macias (2000). Kinetic modeling of naphtha catalytic reforming reactions, *Energy and Fuels*, pp. 1032-1037.
- [9] J. Li and L. Liao "Modeling and optimization of a semi regenerative catalytic naphtha reformer," in *IEEE Conference on Control Applications*, Toronto, Canada, August 28-31, 2005.

- [10] J. Behin and H. R. Kavianpour (2009). A comparative study for the simulation of industrial naphtha reforming reactors with considering pressure drop on catalyst, *Petroleum & Coal* 51(3), pp. 208-215.
- [11] M. Z. Stijepovic, A. Vojvodic-Ostojic, I. Milenkovic and P. Linke (2009). Development of a kinetic model for catalytic reforming of naphtha and parameter estimation using industrial plant data, *Energy and Fuels*, pp. 979-983.
- [12] J. A. Moulijn, M. Makkee and A. E. Van-Diepen "Chemical process technology," John Wiley & Sons, 2001.
- [13] R. G. Tailleux and Y. Davila (2008). Optimal hydrogen production through revamping a naphtha-reforming unit: catalyst deactivation, *Energy and Fuels*, pp. 2892-2901.
- [14] M. R. Rahimpour (2009). Enhancement of hydrogen production in a novel fluidized-bed membrane reactor for naphtha reforming, *Int. Journal of Hydrogen Tech.* (34), pp. 2235-2251.
- [15] D. M. Little, "Catalytic Reforming," Oklahoma: Penwell Publishing, 1985.
- [16] J. Ancheyta-Juarez, E. Villafuerte-Macias, L. Diaz-Garcia and E. Gonzalez-Arredondo (2001). Modeling and simulation of four catalytic reactors in series for naphtha reforming, *Energy and Fuels*, pp. 887-893.
- [17] S. R. Mohaddecy, S. Zahedi, S. Sadighi and H. Bonyad (2006). Reactor modeling and simulation of catalytic reforming process, *Petroleum & Coal* 48(3), pp. 28-35.
- [18] A. Fazeli, S. Fatemi, M. Mahdavian and A. Ghaee (2009). Mathematical modeling of an industrial naphtha reformer with three adiabatic reactors in series, *Iran. J. Chem. Chem. Eng.* 28(3), pp. 97-102.
- [19] H. M. Arani, M. Shirvani, K. Safdarian and E. Dorostkhar (2009). Lumping procedure for a kinetic model of catalytic naphtha reforming, *Brazilian J. Chem. Eng.* 26(4), pp. 723-732.

- [20] K. Liang, H. Guo and S. Pan (2005). A study on naphtha catalytic reforming reactor simulation and analysis, *Journal of Zhejiang University SCIENCE*, pp. 590-596.2005.
- [21] A. K. Mostafazadeh and M.R. Rahimpour (2004). A membrane catalytic bed concept for naphtha reforming in the presence of catalyst deactivation, *Chemical Engineering and processing, Elsevier*, pp. 683-694.
- [22] J. W. Lee, Y. C. Ko, Y. K. Jung and K. S. Lee (1997). A modeling and simulation study on a naphtha reforming unit with a catalyst circulation and regeneration system, *Computers chem. Engineering, Pergamon*, pp. 1105-1110.
- [23] K. A. Pilcher and J. Bridgewater (1990). Pinning in a rectangular moving bed reactor with gas cross-flow, *Chem.Eng.Sci.* pp. 2535-2542.
- [24] J. C. Ginestra and R. Jackson (1985). Pinning of a bed particles in a vertical channel by a cross flow of gas, *Ind.Eng.Chem. Fund.* , pp. 121-124.
- [25] F. J. Doyle, R. Jackson and J. C. Ginestra (1986). The phenomenon of pinning in a annular moving bed reactor with cross flow of gas, *Chem. Eng. Sci.*, 41 (6), pp. 1485-1495.
- [26] Y. Chen, X. Zhu, Y. Wu and Z. Zhu (2007).Investigation of pinning in moving bed, *Journal of Chemical Engineering of Chinese Universities*, pp. 404-410.
- [27] A. A. Kareeri, H. D. Zughbi and H. H. Al-Ali (2006). Simulation of flow distribution in radial flow reactors, *Ind. Eng. Chem. Res.* pp. 2862-2874.
- [28] A. A. Kareeri. "Investigation of the flow and pinning phenomena in radial flow reactors," M.S. thesis, King Fahd Univ. of Petroleum and Minerals, Saudi Arabia, 2004.
- [29] S. Ergun, (1952). Fluid flow through packed columns, *Chemical Engineering Progress* 48.2. pp 89-94.
- [30] G. Young (2003). Size reduction of particulate material, *Educ. Reso. For Part. Techn.* Available: <http://www.erpt.org/032Q/youc-00.htm>.

APPENDIX A

Calculation of the Properties of Naphtha

1.1. Density of Naphtha Feed

Density of naphtha in liquid form at 25 °C = 750 kg/m³

Density of naphtha in gas form at 520 °C =

$$\rho_{520^{\circ}C} = \frac{M_f(\text{kg/kmol}) \times 273(\text{K}) \times P(\text{atm}) \times 1000(\text{L})}{22400(\text{L/kmol}) \times 793(\text{K}) \times 1(\text{atm}) \times 1(\text{m}^3)} \quad (\text{A.1})$$

$$\rho_{520^{\circ}C} = 13.9486 \text{ kg/m}^3 \quad (\text{A.2})$$

1.2. Velocity of Naphtha Feed

Velocity of naphtha gas entering the reactor,

$$u = \frac{F}{\rho A} \quad (\text{A.3})$$

$$u = \frac{113655 \text{ kg}}{h} \times \frac{\text{m}^3}{13.9486 \text{ kg}} \times \frac{1 \text{ hr}}{3600 \text{ s}} \times \frac{1}{\pi \times 2 \text{ m} \times 8.7 \text{ m}} \quad (\text{A.4})$$

$$u = 0.0414 \text{ m/s} \quad (\text{A.5})$$

1.3. Reynolds Number of Naphtha Gas Flow

Reynolds number of naphtha gas flow in the reactor,

$$N_{Re} = \frac{d_p u \rho}{\mu} \quad (\text{A.6})$$

$$N_{Re} = \frac{0.0016 \text{ m} \times 0.0414 \frac{\text{m}}{\text{s}} \times 13.9486 \frac{\text{kg}}{\text{m}^3}}{2.87 \cdot 10^{-5} \frac{\text{kg}}{\text{m} \cdot \text{s}}} \quad (\text{A.7})$$

$$N_{Re} = 32.2 \quad (\text{A.8})$$

1.4. Liquid Hourly Space Velocity (LHSV)

$$\text{LHSV} = \frac{\text{cubic feet of charge per hour}}{\text{cubic feet of catalyst (all reactors)}} \quad (\text{A.9})$$

$$\text{Charge} = \frac{113655 \text{ kg}}{h} \times \frac{m^3}{750 \text{ kg}} = \frac{151.54 m^3}{h} \quad (\text{A.10})$$

$$\text{Catalyst} = 63.08 m^3$$

$$\text{LHSV} = \frac{151.54 m^3}{h} \times \frac{1}{63.08 m^3} = 2.402 h^{-1} \quad (\text{A.11})$$

1.5. Weighted Average Inlet Temperature (WAIT)

$$\begin{aligned} \text{WAIT} = & (\text{Catalyst fraction in } R_1 * T_{in} R_1) + (\text{Catalyst fraction in } R_2 * T_{in} R_2) + \\ & (\text{Catalyst fraction in } R_3 * T_{in} R_3) + (\text{Catalyst fraction in } R_4 * T_{in} R_4) \end{aligned} \quad (\text{A.12})$$

$$\text{WAIT} = (0.14 * 520^\circ\text{C}) + (0.16 * 520^\circ\text{C}) + (0.25 * 520^\circ\text{C}) + (0.45 * 520^\circ\text{C}) \quad (\text{A.13})$$

$$\text{WAIT} = 520^\circ\text{C} \quad (\text{A.14})$$

1.6. Catalyst Residence Time

Circulation rate of catalyst: 433.22 kg/h

Total length of catalyst flow from top of first reactor to the bottom of fourth reactor,

$$L_t = 8.7 + 7.1 + 8.3 + 11.7 = 35.80 \text{ m} \quad (\text{A.15})$$

Area of catalyst flow in each reactor,

$$A_c = \frac{\pi}{4} (D_b^2 - D_{cp}^2) \quad (\text{A.16})$$

For reactor 1,

$$A_c = \frac{\pi}{4} (1.2^2 - 0.4^2) = 1.00571429 \text{ m}^2 \quad (\text{A.17})$$

For reactor 2,

$$A_c = \frac{\pi}{4} (1.4^2 - 0.4^2) = 1.41428572 \text{ m}^2 \quad (\text{A.18})$$

For reactor 3,

$$A_c = \frac{\pi}{4} (1.6^2 - 0.4^2) = 1.88571423 \text{ m}^2 \quad (\text{A.19})$$

For reactor 4,

$$A_c = \frac{\pi}{4} (1.8^2 - 0.4^2) = 2.42000001 \text{ m}^2 \quad (\text{A.20})$$

Time for catalyst to flow from top to the bottom of reactor,

$$t_R = \frac{L_R \cdot \rho_p \cdot A_c}{F_{cat}} \quad (\text{A.21})$$

For reactor 1,

$$t_{R1} = 8.7 \text{ m} \cdot \frac{\text{hr}}{433.22 \text{ kg}} \cdot \frac{670 \text{ kg}}{\text{m}^3} \cdot 1.00571429 \text{ m}^2 = 13.5323 \text{ hrs} \quad (\text{A.22})$$

For reactor 2,

$$t_{R2} = 7.1 \text{ m} \cdot \frac{\text{hr}}{433.22 \text{ kg}} \cdot \frac{670 \text{ kg}}{\text{m}^3} \cdot 1.41428572 \text{ m}^2 = 15.5296 \text{ hrs} \quad (\text{A.23})$$

For reactor 3,

$$t_{R3} = 8.3 \text{ m} \cdot \frac{\text{hr}}{433.22 \text{ kg}} \cdot \frac{670 \text{ kg}}{\text{m}^3} \cdot 1.88571423 \text{ m}^2 = 24.2058 \text{ hrs} \quad (\text{A.24})$$

For reactor 4,

$$t_{R4} = 11.7 \text{ m} \cdot \frac{\text{hr}}{433.22 \text{ kg}} \cdot \frac{670 \text{ kg}}{\text{m}^3} \cdot 2.4000001 \text{ m}^2 = 43.7893 \text{ hrs} \quad (\text{A.25})$$

Total time of catalyst to flow from top of reactor 1 to the bottom of reactor 4 is:

$$t_T = t_{R1} + t_{R2} + t_{R3} + t_{R4}$$

$$t_T = 13.5323 + 15.5296 + 24.2058 + 43.7893 = 97.0570 \text{ hrs}$$

$$t_T \approx 4 \text{ day} \quad (\text{A.26})$$

APPENDIX B

Temperature and Composition Calculation at *i-th* Compartment in 1D Compartment in Series of RFMBR

Basis = 113655 kg/h of naphtha.

= 50.26 mol% of paraffins.

= 39.75 mol% of naphthenes.

= 9.99 mol% of aromatics.

Molecular weight of naphtha = 114.3058 kg/ kmol.

Pressure inlet = 0.79433 MPa. (B.1)

Thus, naphtha fresh feed is

$$= \frac{113655 \text{ kg}}{h} \times \frac{\text{kmol}}{114.3058 \text{ kg}} = 994.3065 \text{ kmol/h.} \quad (\text{B.2})$$

Component	Flow rate in, F_{in} (kmol/h)	Mole fraction, y_{in}	Partial pressure, (MPa)
Paraffins	0.5026×994.3065 = 499.7384	$499.7385/3977.226$ = 0.1257	0.1257×0.79433 = 0.099808
Naphthenes	0.3975×994.3065 = 395.2368	$395.2368/3977.226$ = 0.09937	0.09937×0.79433 = 0.078937
Aromatics	0.099×994.3065 = 99.3312	$99.3312/3977.226$ = 0.02497	0.02497×0.79433 = 0.019838
Hydrogen	2982.9195	$32982.9195/3977.226$ = 0.75	0.75×0.79433 = 0.595748
TOTAL	3977.226	1.00	0.79433

$$\text{Temperature inlet} = 793 \text{ K.} \quad (\text{B.3})$$

Hydrogen to hydrocarbon mole ratio is 3.0.

$$\text{Thus, input hydrogen is} = 3.0 \times 994.3065 \text{ kmol/h} = 2982.9195 \text{ kmol/h} \quad (\text{B.4})$$

2.1. Paraffin dehydrogenation

$$\text{Reaction rate constant: } k_{f_1} = 9.87 \exp(35.98 - 58550/1.8/T)$$

$$k_{f_1} = 9.87 \exp(35.98 - 58550/1.8/793)$$

$$k_{f_1} = 0.06398 \text{ kmol/kg.cat.h.MPa}^2 \quad (\text{B.5})$$

$$\text{Equilibrium constant: } K_{e_1} = 9.87 \exp(-7.12 + 8000/1.8/T)$$

$$K_{e_1} = 9.87 \exp(-7.12 + 8000/1.8/793)$$

$$K_{e_1} = 2.16816 \text{ .MPa}^{-1} \quad (\text{B.6})$$

$$\text{Reaction rate: } r_1 = (k_{f_1}/K_{e_1})(K_{e_1}P_N P_H - P_P) \eta a$$

$$r_1 = (0.06398/2.16818) (2.16818 \times 0.07893 \times 0.5957 - 0.09985)(0.5)(1)$$

$$r_1 = 5.7753 \times 10^{-5} \text{ kmol/kg.cat.h} \quad (\text{B.7})$$

2.2. Naphthenes dehydrogenation

$$\text{Reaction rate constant: } k_{f_2} = 9.87 \exp(23.21 - 36350/1.8/T)$$

$$k_{f_2} = 9.87 \exp(23.21 - 36350/1.8/793)$$

$$k_{f_2} = 1.03419 \text{ kmol/kg.cat.h.MPa} \quad (\text{B.8})$$

Equilibrium constant: $K_{e2} = 1.04 \times 10^{-3} \exp(46.15 - 50784/1.8/T)$

$$K_{e2} = 1.04 \times 10^{-3} \exp(46.15 - 50784/1.8/793)$$

$$K_{e2} = 1122.72 \text{ MPa}^3 \quad (\text{B.9})$$

Reaction rate: $r_2 = (k_{f2}/K_{e2})(K_{e2}P_N - P_A P_H^3)\eta a$

$$r_2 = (1.03419/1122.72) (1122.72 \times 0.07893 - 0.01983 \times 0.5957^3)(1.25)(1)$$

$$r_2 = 0.06530517 \text{ kmol/kg.cat.h} \quad (\text{B.10})$$

2.3. Naphthenes Hydro-cracking

Reaction rate constant: $k_{f3} = \exp(42.97 - 63800/1.8/T)$

$$k_{f3} = \exp(42.97 - 63800/1.8/793)$$

$$k_{f3} = 0.17787 \text{ kmol/kg.cat.h.} \quad (\text{B.11})$$

Reaction rate: $r_3 = k_{f3}(P_N/P_I)\eta a$

$$r_3 = 0.17787 \times (0.07893/0.79433)(0.65)(1)$$

$$r_3 = 0.0088383 \text{ kmol/kg.cat.h} \quad (\text{B.12})$$

2.4. Paraffins Hydro-cracking

Reaction rate constant: $k_{f4} = \exp(42.97 - 63800/1.8/T)$

$$k_{f4} = \exp(42.97 - 63800/1.8/793)$$

$$k_{f4} = 0.17787 \text{ kmol/kg.cat.h.} \quad (\text{B.13})$$

Reaction rate: $r_4 = k_{f4}(P_P / P_t) \eta a$

$$r_4 = 0.17787 \times (0.09985 / 0.79433)(0.65)(1)$$

$$r_4 = 0.0111752 \text{ kmol} / \text{kg.cat.h} \quad (\text{B.14})$$

2.5. Catalyst activity

Catalyst deactivation constant: $k_d = 35 \exp(-83073.5/8.314/T)$

$$k_d = 35 \exp(-83073.5/8.314/793)$$

$$k_d = 0.000117991 \text{ hr}^{-1} \quad (\text{B.15})$$

Catalyst activity: $a = 1 - k_d t$

$$a = 1 - (0.000117991 \times 0)$$

$$a = 1$$

(B.16)

2.6. Mass of catalyst

Area of the catalyst bed: $A_c = 2 \pi R H$

$$A_c = 2\pi((0.6 - 0.0016) - 0.2) \times 7.9$$

$$A_c = 19.7834 \text{ m}^2 \quad (\text{B.17})$$

Mass of the catalyst: $M_c = A_c \rho$

$$M_c = 5792.58 \text{ kg} / \text{m} \quad (\text{B.18})$$

2.7. Changes of Components

Difference of paraffins flow rate:
$$\frac{\Delta F_P}{\Delta R} = (2\pi RH\rho) \sum_{j=1}^4 v_{ij} r_j$$

$$\frac{\Delta F_P}{\Delta R} = (2\pi RH\rho) \times (-\eta - r_4) \quad (\text{B.19})$$

$$\frac{\Delta F_P}{\Delta R} = (5792.58) \times (-5.7753 \times 10^{-5} - 0.0111752)$$

$$\frac{\Delta F_P}{\Delta R} = -66.4002178 \text{ kmol} / \text{m.h} \quad (\text{B.20})$$

$$\Delta F_P = -66.4002178 \text{ kmol} / \text{m.h} \times 0.0016 \text{ m}$$

$$\Delta F_P = -0.10624 \text{ kmol} / \text{h} \quad (\text{B.21})$$

Difference of naphthenes flow rate:
$$\frac{\Delta F_N}{\Delta R} = (2\pi RH\rho) \sum_{j=1}^4 v_{ij} r_j$$

$$\frac{\Delta F_N}{\Delta R} = (2\pi RH\rho) \times (\eta - r_2 - r_3) \quad (\text{B.22})$$

$$\frac{\Delta F_N}{\Delta R} = (5792.58) \times (5.7753 \times 10^{-5} - 0.06530517 - 0.0088383)$$

$$\frac{\Delta F_N}{\Delta R} = -433.17353 \text{ kmol} / \text{m.h} \quad (\text{B.23})$$

$$\Delta F_N = -433.17353 \text{ kmol} / \text{m.h} \times 0.0016 \text{ m}$$

$$\Delta F_N = -0.69307 \text{ kmol} / \text{h} \quad (\text{B.24})$$

Difference of aromatics flow rate:
$$\frac{\Delta F_A}{\Delta R} = (2\pi RH\rho) \sum_{j=1}^4 v_{ij} r_j$$

$$\frac{\Delta F_A}{\Delta R} = (2\pi RH\rho) \times (r_2) \quad (\text{B.25})$$

$$\frac{\Delta F_A}{\Delta R} = (5972.58) \times (0.06530517)$$

$$\frac{\Delta F_A}{\Delta R} = 390.041 \text{ kmol} / \text{m.h} \quad (\text{B.26})$$

$$\Delta F_A = 390.041 \text{ kmol} / \text{m.h} \times 0.0016 \text{ m}$$

$$\Delta F_A = 0.6241 \text{ kmol} / \text{h} \quad (\text{B.27})$$

Difference of hydrogen flow rate:
$$\frac{\Delta F_H}{\Delta R} = (2\pi RH\rho) \sum_{j=1}^4 v_{ij} r_j$$

$$\frac{\Delta F_H}{\Delta R} = (2\pi RH\rho) \times (r_1 + 3r_2 - 3r_3 - 2r_4) \quad (\text{B.28})$$

$$\frac{\Delta F_H}{\Delta R} = (5972.58) \times \left(\begin{array}{l} 5.7753 \times 10^{-5} + (3 \times 0.06530517) - \\ (3 \times 0.0088383) - (2 \times 0.0111752) \end{array} \right)$$

$$\frac{\Delta F_H}{\Delta R} = 877.923154 \text{ kmol} / \text{m.h} \quad (\text{B.29})$$

$$\Delta F_H = 877.923154 \text{ kmol} / \text{m.h} \times 0.0016 \text{ m}$$

$$\Delta F_H = 1.404677 \text{ kmol} / \text{h} \quad (\text{B.30})$$

Difference of light gases flow rate:
$$\frac{\Delta F_{LG}}{\Delta R} = (2\pi RH\rho) \sum_{j=1}^4 v_{ij} r_j$$

$$\frac{\Delta F_{LG}}{\Delta R} = (2\pi RH\rho) \times (r_3 + r_4) \quad (\text{B.31})$$

$$\frac{\Delta F_{LG}}{\Delta R} = (5972.59) \times (0.0088383 + 0.01111752)$$

$$\frac{\Delta F_{LG}}{\Delta R} = 119.533053 \text{ kmol} / \text{m.h} \quad (\text{B.32})$$

$$\Delta F_{LG} = 119.533053 \text{ kmol} / \text{m.h} \times 0.0016 \text{ m}$$

$$\Delta F_{LG} = 0.19125 \text{ kmol} / \text{h} \quad (\text{B.33})$$

2.8. Changes in Temperature

$$\text{Difference of temperature: } \frac{\Delta T}{\Delta R} = \frac{(2\pi RH\rho)}{F_l c_p} \sum_{j=1}^4 v_{ij} (-\Delta H_r) r_j \quad (\text{B.34})$$

$$\sum_{j=1}^4 v_{ij} (-\Delta H_r) r_j = \left[\begin{aligned} &(-36953 \times 5.7753 \times 10^{-5}) + (71038.1 \times 0.06530) + (-51939.3 \times 0.0088) \\ &+ (-56597.5 \times 0.01117) \end{aligned} \right]$$

$$\sum_{j=1}^4 v_{ij} (-\Delta H_r) r_j = 3548.742097 \text{ kJ} / \text{kg.ca.h} \quad (\text{B.35})$$

$$\frac{\Delta T}{\Delta R} = \frac{5972.58}{(3977.226 \times 88.1)} \times 3548.742097$$

$$\frac{\Delta T}{\Delta R} = 60.4337753 \text{ K} / \text{m} \quad (\text{B.36})$$

$$\Delta T = 60.4337753 \text{ K} / \text{m} \times (0.2 + 0.0016) \text{ m}$$

$$\Delta T = 12.1834 \text{ K} \quad (\text{B.37})$$

2.9. Results of Temperature and Flow Rate of Components

The temperature drop through the *i*-th compartment is 12.1834 K. Thus, the exit temperature at *i*-th compartment is:

$$T_i = T_{i-1} - \Delta T = 793 - (12.1834) \quad (\text{B.38})$$

$$T_i = 780.8166 \text{ K} = 507.8166 \text{ }^\circ\text{C}$$

Flow rate of paraffins and naphthenes decrease due to dehydrogenation and hydro-cracking.

$$F_{P_i} = F_{P_{i-1}} + \Delta F_P = 499.7384 + (-0.10624) \quad (\text{B.39})$$

$$F_{P_i} = 499.63216 \text{ kmol/h}$$

$$F_{N_i} = F_{N_{i-1}} + \Delta F_N = 395.2386 + (-0.69307) \quad (\text{B.40})$$

$$F_{N_i} = 394.54553 \text{ kmol/h}$$

Meanwhile, the production of aromatics and hydrogen increases from dehydrogenation process of naphthenes and light gases increase from hydro-cracking of naphthenes and paraffins.

$$F_{A_i} = F_{A_{i-1}} + \Delta F_A = 99.3312 + (0.6241) \quad (\text{B.41})$$

$$F_{A_i} = 99.9553 \text{ kmol/h}$$

$$F_{H_i} = F_{H_{i-1}} + \Delta F_H = 3579.5034 + (1.404677) \quad (\text{B.42})$$

$$F_{H_i} = 3580.9081 \text{ kmol/h}$$

$$F_{LG_i} = F_{LG_{i-1}} + \Delta F_{LG} = 0 + (0.19125) \quad (\text{B.43})$$

$$F_{LG_i} = 0.19125 \text{ kmol/h}$$

The exit flow rate of components from *i-th* compartment will be used as the input flow rate for calculation in *i+1-th* compartment. As the exit temperature from *i-th* compartment lower, the input flow rate entering *i+1-th* compartment need to reheat to 793 K.

Appendix C

C.1. Compartment in series model for naphtha reforming in R₁

	F _P	F _N	F _A	F _H	F _{LG}	TOTAL	T _{i-1}	P _P	P _N	P _A	P _H
comp.	kmol/hr	kmol/hr	kmol/hr	kmol/hr	kmol/hr	kmol/hr	K	Mpa	Mpa	Mpa	Mpa
1	499.7384	395.2368	99.3312	2982.9195	0	3977.2260	793.00	0.099808	0.078937	0.019838	0.595748
2	499.6322	394.5278	99.955284	2984.3242	0.191253	3978.4394	780.82	0.099756	0.078771	0.019957	0.595846
3	499.5291	393.6077	100.78899	2986.3601	0.380693	3980.2859	771.98	0.099689	0.078551	0.020114	0.595976
4	499.4391	392.6061	101.71263	2988.717	0.548719	3982.4748	765.13	0.099616	0.078308	0.020287	0.596119
5	499.3609	391.5692	102.68001	2991.2543	0.696372	3984.8644	759.57	0.099541	0.078054	0.020468	0.596267
6	499.2924	390.5176	103.66944	2993.899	0.827074	3987.3784	754.90	0.099465	0.077795	0.020652	0.596418
7	499.2317	389.4615	104.66940	2996.609	0.943929	3989.9716	750.89	0.099388	0.077535	0.020838	0.59657
8	499.1772	388.4066	105.67321	2999.3585	1.049404	3992.6156	747.39	0.099311	0.077273	0.021024	0.596722
9	499.128	387.3563	106.67680	3002.1305	1.145415	3995.2915	744.27	0.099235	0.077013	0.021209	0.596873
10	499.0831	386.3124	107.67754	3004.9135	1.233455	3997.9865	741.48	0.099159	0.076754	0.021394	0.597024
11	499.0418	385.2762	108.67371	3007.6995	1.3147	4000.6913	738.94	0.099084	0.076496	0.021577	0.597173
12	499.0037	384.2485	109.66416	3010.4828	1.390089	4003.3992	736.62	0.099009	0.07624	0.021759	0.597322
13	498.9684	383.2297	110.64808	3013.2591	1.46038	4006.1052	734.49	0.098935	0.075987	0.021939	0.597469
14	498.9353	382.22	111.62495	3016.0252	1.526196	4008.8055	732.51	0.098862	0.075735	0.022118	0.597614
15	498.9044	381.2197	112.59440	3018.779	1.588052	4011.4974	730.68	0.09879	0.075487	0.022295	0.597759
16	499.7384	395.2368	99.3312	2982.9195	0	3977.2260	793.00	0.099808	0.078937	0.019838	0.595748
17	499.6322	394.5278	99.955284	2984.3242	0.191253	3978.4394	780.82	0.099756	0.078771	0.019957	0.595846
⋮	⋮	⋮	⋮	⋮	⋮	⋮	⋮	⋮	⋮	⋮	⋮
250	497.8122	284.542	208.14676	3299.8759	3.8055	4290.3769	670.77	0.092166	0.052681	0.038537	0.610946

	k_{Γ}	K_{e1}	r_1	$k_{\Gamma 2}$	K_{e2}	r_2	$k_{\Gamma 3}=k_{\Gamma 4}$	r_3	r_4
comp	kmol/kg.cat.h.Mpa ²	Mpa ⁻¹	kmol/kg.cat.h	kmol/kg.cat.h.Mpa	Mpa ³	kmol/kg.cat.h	kmol/kg.cat.h.	kmol/kg.cat.h	kmol/kg.cat.h
1	0.063983155	2.168	5.77531E-05	1.034189295	1122.72	0.065305172	0.177879086	0.008838367	0.011175254
2	0.033736716	2.366	0.000145367	0.695073041	678.699	0.043797531	0.08856007	0.004391071	0.005560878
3	0.020938419	2.526	0.000138554	0.516914305	466.405	0.03247913	0.052662774	0.002603869	0.00330458
4	0.014358139	2.659	0.000119257	0.40897529	346.666	0.025616391	0.034911334	0.001720819	0.002189075
5	0.010517752	2.775	0.000101055	0.337112842	271.398	0.02104582	0.024869695	0.001221881	0.001558243
6	0.008072471	2.877	8.59703E-05	0.286042746	220.411	0.017797404	0.018640168	0.000912779	0.001167024
7	0.006414016	2.969	7.37994E-05	0.247984177	183.945	0.015376825	0.014508342	0.000708067	0.000907636
8	0.00523418	3.053	6.39826E-05	0.218582625	156.77	0.013507237	0.011625737	0.000565471	0.000726739
9	0.00436289	3.129	5.60011E-05	0.19521955	135.855	0.012022074	0.009533573	0.000462145	0.000595497
10	0.00369986	3.201	4.94436E-05	0.176229339	119.338	0.010815339	0.007966132	0.000384861	0.000497209
11	0.003182736	3.267	4.39975E-05	0.160503701	106.013	0.009816484	0.006760831	0.000325534	0.000421659
12	0.002771034	3.330	3.94272E-05	0.14727746	95.0708	0.008976787	0.005813626	0.00027899	0.00036231
13	0.002437501	3.389	3.55546E-05	0.136005814	85.95	0.008261553	0.005055403	0.000241797	0.000314821
14	0.002163223	3.444	3.22438E-05	0.126290625	78.2483	0.007645425	0.00443878	0.000211602	0.000276217
15	0.001934727	3.497	2.93904E-05	0.117834363	71.6717	0.007109449	0.003930383	0.00018675	0.000244401
16	0.063983155	2.168	5.77531E-05	1.034189295	1122.72	0.065305172	0.177879086	0.008838367	0.011175254
17	0.033736716	2.366	0.000145367	0.695073041	678.699	0.043797531	0.08856007	0.004391071	0.005560878
⋮	⋮	⋮	⋮	⋮	⋮	⋮	⋮	⋮	⋮
250	3.629E-05	6.022	5.51238E-07	0.009981378	3.14289	0.00039827	5.16134E-05	1.71125E-06	2.99387E-06

	k_d	L	t	$a=1-kdt$	η_{R1}	η_{R2}	η_c	$(-\Delta H_{r1})$	$(-\Delta H_{r2})$	$(-\Delta H_{r3})$	$(-\Delta H_{r4})$	ΔR	$2\pi RH\rho$
comp	h^{-1}	m	hr	-	-	-	-	kJ/kmol	kJ/kmol	kJ/kmol	kJ/kmol	(m)	(kg/m)
1	0.0001179	0	0	1	0.9	0.8	0.5	-36953	71038.06	-51939.3	-56597.5	0.0016	5972.58
2	9.698E-05	0.0349	0.0543	0.99999	0.9	0.8	0.5	-36953	71038.06	-51939.3	-56597.5	0.0016	5948.59
3	8.371E-05	0.0698	0.1086	0.99999	0.9	0.8	0.5	-36953	71038.06	-51939.3	-56597.5	0.0016	5924.61
4	7.455E-05	0.1048	0.1630	0.99998	0.9	0.8	0.5	-36953	71038.06	-51939.3	-56597.5	0.0016	5900.62
5	6.7759E-05	0.1397	0.2173	0.99998	0.9	0.8	0.5	-36953	71038.06	-51939.3	-56597.5	0.0016	5876.64
6	6.2469E-05	0.1747	0.2717	0.99998	0.9	0.8	0.5	-36953	71038.06	-51939.3	-56597.5	0.0016	5852.65
7	5.8209E-05	0.2096	0.3260	0.99998	0.9	0.8	0.5	-36953	71038.06	-51939.3	-56597.5	0.0016	5828.66
8	5.4685E-05	0.2445	0.3804	0.99997	0.9	0.8	0.5	-36953	71038.06	-51939.3	-56597.5	0.0016	5804.68
9	5.1710E-05	0.2795	0.4347	0.99997	0.9	0.8	0.5	-36953	71038.06	-51939.3	-56597.5	0.0016	5780.69
10	4.9157E-05	0.3144	0.4891	0.99997	0.9	0.8	0.5	-36953	71038.06	-51939.3	-56597.5	0.0016	5756.70
11	4.6935E-05	0.3494	0.5434	0.99997	0.9	0.8	0.5	-36953	71038.06	-51939.3	-56597.5	0.0016	5732.72
12	4.4980E-05	0.3843	0.5978	0.99997	0.9	0.8	0.5	-36953	71038.06	-51939.3	-56597.5	0.0016	5708.73
13	4.3243E-05	0.4192	0.6521	0.99997	0.9	0.8	0.5	-36953	71038.06	-51939.3	-56597.5	0.0016	5684.75
14	4.1686E-05	0.4542	0.7064	0.99997	0.9	0.8	0.5	-36953	71038.06	-51939.3	-56597.5	0.0016	5660.76
15	4.0280E-05	0.4891	0.7608	0.99996	0.9	0.8	0.5	-36953	71038.06	-51939.3	-56597.5	0.0016	5444.88
16	3.9004E-05	0.5241	0.8151	0.99996	0.9	0.8	0.5	-36953	71038.06	-51939.3	-56597.5	0.0016	5420.90
17	3.7838E-05	0.5590	0.8695	0.99996	0.9	0.8	0.5	-36953	71038.06	-51939.3	-56597.5	0.0016	5396.91
⋮	⋮	⋮	⋮	⋮	⋮	⋮	⋮	⋮	⋮	⋮	⋮	⋮	⋮
250	1.1875E-05	8.7000	13.532	0.99983	0.9	0.8	0.5	-36953	71038.06	-51939.3	-56597.5	0.0016	0.07945

	ΔF_P	ΔF_N	ΔF_A	ΔF_H	ΔF_{LG}	$c_{p,g}$	ΔT	T(K)	T(°C)
comp	kmol/m.h	kmol/m.h	kmol/m.h	kmol/m.h	kmol/m.h	kJ/kmol.K	K/m	793.00	520.0000
1	-66.400217	-443.17353	390.041	877.92315	119.53305	88.1	-60.433775	780.8166	507.8166
2	-32.214698	-287.51939	260.534	636.21606	59.200152	88.1	-43.500546	771.9772	498.9772
3	-18.757479	-208.67405	192.426	491.02044	35.005272	88.1	-33.450627	765.1266	492.1266
4	-12.213221	-162.01035	151.153	396.45901	23.070822	88.1	-26.943079	759.5655	486.5655
5	-8.5633662	-131.45312	123.679	330.58612	16.337787	88.1	-22.425149	754.9011	481.9011
6	-6.3270355	-110.00737	104.162	282.29605	12.172368	88.1	-19.120591	750.8934	477.8934
7	-4.8601580	-94.183635	89.6264	245.48715	9.4173966	88.1	-16.605801	747.3862	474.3862
8	-3.8470925	-82.058984	78.4052	216.56009	7.5008717	88.1	-14.631973	744.2726	471.2726
9	-3.1186598	-72.491182	69.4959	193.26476	6.1139029	88.1	-13.044033	741.4759	468.4759
10	-2.5776523	-64.760923	62.2608	174.12646	5.0778200	88.1	-11.740567	738.9400	465.9400
11	-2.1650258	-58.393596	56.2752	158.14021	4.2834469	88.1	-10.652583	736.6220	463.6220
12	-1.8432525	-53.063866	51.2461	144.59853	3.6610127	88.1	-9.7315748	734.4888	461.4888
13	-1.5875618	-48.541535	46.9649	132.98944	3.1642345	88.1	-8.9424773	732.5143	459.5143
14	-1.3810733	-44.659293	43.2789	122.93361	2.7614257	88.1	-8.2593349	730.6774	457.6774
15	-1.2119649	-41.292714	40.0744	114.14420	2.4302996	88.1	-3.7106823	713.3337	440.3337
16	-1.0717582	-38.347404	37.2644	106.40039	2.1548089	88.1	-3.5528840	712.4583	439.4583
17	-0.9542458	-35.750502	34.7816	99.529526	1.9231606	88.1	-3.4057899	711.6136	438.6136
⋮	⋮	⋮	⋮	⋮	⋮	⋮	⋮	⋮	⋮
▼	▼	▼	▼	▼	▼	▼	▼	▼	▼
250	-4.774E-05	-0.0092164	0.00918	0.0273536	8.111E-05	88.1	-0.0017153	663.261	390.261

C.2. Compartment in series model for naphtha reforming in R₂

comp.	F _P kmol/hr	F _N kmol/hr	F _A kmol/hr	F _H kmol/hr	F _{LG} kmol/hr	TOTAL kmol/hr	T _{i-1} K	P _P Mpa	P _N Mpa	P _A Mpa	P _H Mpa
1	497.8122	284.5420	208.1468	3299.8759	3.8055	4290.3769	793.00	0.088751	0.050729	0.037109	0.588311
2	497.7196	284.143	208.501353	3300.6211	3.942539	4290.9851	787.04	0.088722	0.050651	0.037167	0.58836
3	497.589	283.4968	209.083441	3301.914	4.137192	4292.0833	781.85	0.088676	0.050522	0.037261	0.58844
4	497.4452	282.693	209.81552	3303.6074	4.35273	4293.5612	777.29	0.08862	0.050362	0.037379	0.588539
5	497.2997	281.7859	210.648977	3305.5957	4.571952	4295.3302	773.25	0.088558	0.05018	0.037512	0.588651
6	497.1576	280.8098	211.552289	3307.8031	4.786811	4297.3228	769.64	0.088491	0.049983	0.037655	0.588771
7	497.0213	279.7872	212.504337	3310.175	4.993682	4299.4878	766.39	0.088423	0.049776	0.037806	0.588896
8	496.8915	278.7333	213.490558	3312.6711	5.191125	4301.7864	763.43	0.088352	0.049562	0.037961	0.589026
9	496.7685	277.6585	214.500647	3315.2613	5.378793	4304.1890	760.73	0.088281	0.049343	0.038119	0.589157
10	496.652	276.5705	215.527148	3317.9231	5.556881	4306.6727	758.25	0.088209	0.049121	0.038279	0.58929
11	496.5417	275.4744	216.564565	3320.6388	5.725842	4309.2194	755.96	0.088138	0.048898	0.038441	0.589424
12	496.4371	274.3744	217.608779	3323.3948	5.886238	4311.8151	753.83	0.088066	0.048673	0.038603	0.589558
13	496.3378	273.2734	218.656661	3326.1805	6.038659	4314.4483	751.84	0.087995	0.048448	0.038765	0.589692
14	496.2434	272.1736	219.705806	3328.9872	6.183689	4317.1100	749.98	0.087924	0.048223	0.038927	0.589826
15	496.1536	271.0767	220.754345	3331.8081	6.321879	4319.7927	748.23	0.087853	0.047999	0.039089	0.589959
16	496.0679	269.984	221.800817	3334.6376	6.453742	4322.4903	746.59	0.087783	0.047776	0.039249	0.590091
17	495.9861	268.8966	222.844072	3337.4711	6.579751	4325.1979	745.03	0.087714	0.047554	0.039409	0.590223
18	495.9079	267.8151	223.883197	3340.305	6.700336	4327.9112	743.56	0.087645	0.047333	0.039568	0.590354
⋮	⋮	⋮	⋮	⋮	⋮	⋮	⋮	⋮	⋮	⋮	⋮
312	491.9816	147.5923	342.283907	3682.1883	12.44871	4664.0461	683.69	0.080685	0.024205	0.056134	0.603876

	k_{Π}	K_{e1}	r_1	k_{Π}	K_{e2}	r_2	$k_{\Pi}=k_{\mu}$	r_3	r_4
comp	kmol/kg.cat.h.Mpa ²	Mpa ⁻¹	kmol/kg.cat.h	kmol/kg.cat.h.Mpa	Mpa ³	kmol/kg.cat.h	kmol/kg.cat.h.	kmol/kg.cat.h	kmol/kg.cat.h
1	0.063983155	2.168	-0.000637977	1.034189295	1122.72	0.041958334	0.177879086	0.00589761	0.010317993
2	0.046910869	2.262	-0.000397313	0.852935287	879.569	0.034549736	0.126837101	0.00419879	0.007354819
3	0.03565152	2.349	-0.000257309	0.719308455	708.813	0.029061882	0.094050908	0.003105553	0.005450817
4	0.027931057	2.428	-0.000172139	0.61817614	585.031	0.024895235	0.072088908	0.002372794	0.004175325
5	0.022445984	2.502	-0.000118194	0.539715098	492.616	0.0216556	0.056807537	0.001863037	0.003287913
6	0.018425929	2.570	-8.28092E-05	0.477477705	421.799	0.019082055	0.045815393	0.001496639	0.002649714
7	0.015399215	2.634	-5.88949E-05	0.427140536	366.285	0.01699859	0.037678431	0.001225728	0.002177416
8	0.013066824	2.694	-4.23168E-05	0.385733526	321.902	0.015283752	0.031504198	0.001020464	0.001819158
9	0.011232966	2.750	-3.0574E-05	0.351166884	285.809	0.013851793	0.026717998	0.000861612	0.00154154
10	0.00976564	2.803	-2.2103E-05	0.321936762	256.015	0.012640837	0.022938182	0.000736394	0.001322381
11	0.008573485	2.854	-1.58972E-05	0.29693841	231.1	0.011605329	0.01990424	0.000636084	0.00114654
12	0.007591764	2.901	-1.12915E-05	0.275344919	210.022	0.010711112	0.017433925	0.00055458	0.001003425
13	0.006773636	2.947	-7.83611E-06	0.256526769	192.008	0.009932142	0.015396922	0.000487518	0.000885464
14	0.006084563	2.990	-5.2207E-06	0.239997318	176.473	0.009248261	0.013698206	0.000431718	0.000787135
15	0.005498647	3.032	-3.2271E-06	0.225375119	162.966	0.008643653	0.012267247	0.000384822	0.000704342
16	0.004996166	3.072	-1.6994E-06	0.212357405	151.136	0.008105753	0.011050867	0.000345051	0.000633995
17	0.004561898	3.110	-5.24552E-07	0.200701095	140.705	0.007624465	0.010008385	0.000311046	0.000573733
18	0.00418394	3.147	3.80545E-07	0.190208984	131.454	0.007191594	0.009108271	0.000281757	0.000521723
⋮	⋮	⋮	⋮	⋮	⋮	⋮	⋮	⋮	⋮
312	9.07461E-05	5.313	-4.6443E-08	0.017632307	6.46185	0.00031432	0.000140118	2.2161E-06	7.38711E-06

	k_d	L	t	$a=1-kdt$	η_{R1}	η_{R2}	η_c	$(-\Delta H_{r1})$	$(-\Delta H_{r2})$	$(-\Delta H_{r3})$	$(-\Delta H_{r4})$	ΔR	$2\pi R H \rho$
comp	h^{-1}	m	hr	-	-	-	-	kJ/kmol	kJ/kmol	kJ/kmol	kJ/kmol	(m)	(kg/m)
1	0.0001179	0	0	0.999	0.9	0.8	0.5	-36953	71038.06	-51939.3	-56597.5	0.0016	5281.90
2	0.0001072	0.0228	0.0499	0.99983	0.9	0.8	0.5	-36953	71038.06	-51939.3	-56597.5	0.0016	5264.94
3	9.858E-05	0.0456	0.0998	0.99982	0.9	0.8	0.5	-36953	71038.06	-51939.3	-56597.5	0.0016	5247.98
4	9.1467E-05	0.0684	0.1498	0.99982	0.9	0.8	0.5	-36953	71038.06	-51939.3	-56597.5	0.0016	5231.03
5	8.5526E-05	0.0913	0.1997	0.99982	0.9	0.8	0.5	-36953	71038.06	-51939.3	-56597.5	0.0016	5214.07
6	8.0495E-05	0.1141	0.2496	0.99981	0.9	0.8	0.5	-36953	71038.06	-51939.3	-56597.5	0.0016	5197.11
7	7.6178E-05	0.1369	0.2996	0.99981	0.9	0.8	0.5	-36953	71038.06	-51939.3	-56597.5	0.0016	5180.16
8	7.2430E-05	0.1598	0.3495	0.99981	0.9	0.8	0.5	-36953	71038.06	-51939.3	-56597.5	0.0016	5163.20
9	6.9143E-05	0.1826	0.3994	0.99981	0.9	0.8	0.5	-36953	71038.06	-51939.3	-56597.5	0.0016	5146.25
10	6.6232E-05	0.2054	0.4494	0.99981	0.9	0.8	0.5	-36953	71038.06	-51939.3	-56597.5	0.0016	5129.29
11	6.3636E-05	0.2283	0.4993	0.99980	0.9	0.8	0.5	-36953	71038.06	-51939.3	-56597.5	0.0016	5112.33
12	6.1302E-05	0.2511	0.5492	0.99980	0.9	0.8	0.5	-36953	71038.06	-51939.3	-56597.5	0.0016	5095.38
13	5.9192E-05	0.2739	0.5992	0.99980	0.9	0.8	0.5	-36953	71038.06	-51939.3	-56597.5	0.0016	5078.42
14	5.7273E-05	0.2967	0.6491	0.99980	0.9	0.8	0.5	-36953	71038.06	-51939.3	-56597.5	0.0016	5061.46
15	5.5519E-05	0.3196	0.6990	0.9998	0.9	0.8	0.5	-36953	71038.06	-51939.3	-56597.5	0.0016	5044.51
16	5.3909E-05	0.3424	0.7490	0.99979	0.9	0.8	0.5	-36953	71038.06	-51939.3	-56597.5	0.0016	5027.55
17	5.2424E-05	0.3652	0.7989	0.99979	0.9	0.8	0.5	-36953	71038.06	-51939.3	-56597.5	0.0016	5010.59
18	5.1049E-05	0.3881	0.8489	0.99979	0.9	0.8	0.5	-36953	71038.06	-51939.3	-56597.5	0.0016	4993.64
⋮	⋮	⋮	⋮	⋮	⋮	⋮	⋮	⋮	⋮	⋮	⋮	⋮	⋮
▼	▼	▼	▼	▼	▼	▼	▼	▼	▼	▼	▼	▼	▼
312	1.5736E-05	7.1001	15.529	0.99959	0.9	0.8	0.5	-36953	71038.06	-51939.3	-56597.5	0.0016	8.47817

	ΔF_P	ΔF_N	ΔF_A	ΔF_H	ΔF_{LG}	$c_{p,g}$	ΔT	T(K)	T(°C)
comp	kmol/m.h	kmol/m.h	kmol/m.h	kmol/m.h	kmol/m.h	kJ/kmol.K	K/m	793.00	520.0000
1	-57.868344	-249.40061	221.62	465.78000	85.649205	88.1	-29.53983	787.0448	514.0448
2	-40.814543	-201.91700	181.902	404.03454	60.829104	88.1	-25.551801	781.8526	508.8526
3	-29.956178	-167.4639	152.516	352.79423	44.903729	88.1	-22.26428	777.2929	504.2929
4	-22.741724	-141.73946	130.228	310.66474	34.253422	88.1	-19.572538	773.2531	500.2531
5	-17.759700	-122.01167	112.914	275.92916	26.857442	88.1	-17.359466	769.6424	496.6424
6	-14.201248	-106.51955	99.1717	247.06910	21.549092	88.1	-15.524478	766.3884	493.3884
7	-11.584453	-94.099848	88.0555	222.86431	17.628840	88.1	-13.987863	763.4342	490.4342
8	-9.6111779	-83.963543	78.9132	202.36602	14.661553	88.1	-12.688147	760.7342	487.7342
9	-8.0904926	-75.561521	71.2848	184.84319	12.367222	88.1	-11.578214	758.2518	485.2518
10	-6.8962537	-68.502371	64.8386	169.73176	10.560061	88.1	-10.621842	755.9575	482.9575
11	-5.9427696	-62.500963	59.3304	156.59371	9.1133750	88.1	-9.7909816	753.8270	480.8270
12	-5.1703660	-57.345459	54.5772	145.08607	7.9386280	88.1	-9.0637122	751.8402	478.8402
13	-4.5365562	-52.875663	50.4396	134.93770	6.9725852	88.1	-8.4227352	749.9805	476.9805
14	-4.0104849	-48.968485	46.8098	125.93225	6.1691895	88.1	-7.8542641	748.2337	475.2337
15	-3.5693419	-45.527972	43.603	117.89547	5.4943011	88.1	-7.3472063	746.5879	473.5879
16	-3.1959914	-42.478343	40.7521	110.68573	4.9222097	88.1	-6.8925552	745.0329	472.0329
17	-2.8773726	-39.759041	38.2031	104.18697	4.4332734	88.1	-6.4829343	743.5600	470.5600
18	-2.6033981	-37.321145	35.9123	98.303286	4.0122901	88.1	-6.1122535	742.1615	469.1615
⋮	⋮	⋮	⋮	⋮	⋮	⋮	⋮	⋮	⋮
312	-6.302E-05	-0.0026832	0.00266	0.0078133	8.141E-05	88.1	-0.0004497	683.6875	410.6875

C.3. Compartment in series model for naphtha reforming in R₃

	F _P	F _N	F _A	F _H	F _{LG}	TOTAL	T _{i-1}	P _P	P _N	P _A	P _H
comp.	kmol/hr	kmol/hr	kmol/hr	kmol/hr	kmol/hr	kmol/hr	K	Mpa	Mpa	Mpa	Mpa
1	491.9816	147.5923	342.2839	3682.1883	12.44871	4664.0461	793.00	0.07655	0.022965	0.053257	0.572928
2	491.8528	147.344	342.513557	3682.5637	12.59618	4664.2740	790.33	0.076526	0.022925	0.053291	0.572959
3	491.6322	146.8921	342.933165	3683.2846	12.849	4664.7421	787.75	0.076484	0.022852	0.053351	0.573013
4	491.3482	146.2747	343.508532	3684.3165	13.17506	4665.4480	785.26	0.076428	0.022753	0.053432	0.573087
5	491.0215	145.5238	344.210769	3685.6239	13.55039	4666.3800	782.87	0.076362	0.022631	0.053531	0.573176
6	490.6675	144.6658	345.015797	3687.1721	13.95735	4667.5213	780.59	0.076288	0.022492	0.053643	0.573277
7	490.2973	143.7224	345.903716	3688.9288	14.3831	4668.8522	778.41	0.076209	0.022339	0.053765	0.573386
8	489.9188	142.7111	346.858162	3690.8647	14.81842	4670.3528	776.34	0.076126	0.022175	0.053896	0.573503
9	489.5376	141.6464	347.865712	3692.9536	15.25672	4672.0034	774.37	0.07604	0.022002	0.054034	0.573625
10	489.1578	140.54	348.91536	3695.1725	15.69337	4673.7856	772.50	0.075952	0.021822	0.054176	0.57375
11	488.782	139.4013	349.998075	3697.5011	16.12515	4675.6824	770.71	0.075863	0.021636	0.054322	0.573879
12	488.412	138.2381	351.106441	3699.9219	16.54988	4677.6786	769.02	0.075773	0.021446	0.054471	0.57401
13	488.0492	137.0568	352.23435	3702.4198	16.96612	4679.7602	767.40	0.075683	0.021254	0.054622	0.574142
14	487.6942	135.8626	353.376761	3704.9814	17.37297	4681.9150	765.85	0.075593	0.021059	0.054774	0.574275
15	487.3475	134.6596	354.529507	3707.5956	17.76991	4684.1322	764.38	0.075503	0.020862	0.054926	0.574408
16	487.0093	133.4513	355.689131	3710.2523	18.1567	4686.4021	762.98	0.075414	0.020665	0.055079	0.574541
17	486.6796	132.2408	356.852761	3712.943	18.53331	4688.7162	761.63	0.075326	0.020468	0.055232	0.574674
18	486.3583	131.0303	358.018007	3715.6605	18.89984	4691.0671	760.34	0.075239	0.02027	0.055385	0.574806
⋮	⋮	⋮	⋮	⋮	⋮	⋮	⋮	⋮	⋮	⋮	⋮
↓	↓	↓	↓	↓	↓	↓	↓	↓	↓	↓	↓
375	456.1463	14.11746	474.941167	4006.0368	49.10158	4951.2417	0.0668	0.002069	0.069612	0.587162	0.066857

	k_{Π}	K_{e1}	r_1	k_{Π}	K_{e2}	r_2	$k_{\Pi}=k_{r4}$	r_3	r_4
comp	kmol/kg.cat.h.Mpa ²	Mpa ⁻¹	kmol/kg.cat.h	kmol/kg.cat.h.Mpa	Mpa ³	kmol/kg.cat.h	kmol/kg.cat.h.	kmol/kg.cat.h	kmol/kg.cat.h
1	0.063983155	2.168	-0.001274503	1.034189295	1122.72	0.018984677	0.177879086	0.002813324	0.009377887
2	0.055714	2.210	-0.001077206	0.949045263	1006.95	0.017390604	0.152979936	0.002415315	0.008062624
3	0.048674173	2.251	-0.000914309	0.872700169	905.466	0.015940069	0.132040858	0.002078103	0.00695519
4	0.042699712	2.291	-0.000780124	0.804555125	816.856	0.014630496	0.114481421	0.001793892	0.006025821
5	0.037632583	2.331	-0.000669551	0.743868424	739.608	0.013453906	0.099759642	0.001554861	0.00524636
6	0.033329753	2.370	-0.000578224	0.689855608	672.252	0.012399525	0.087396622	0.001353801	0.004591728
7	0.029666675	2.408	-0.000502517	0.641751191	613.435	0.011455526	0.076983485	0.001184377	0.004040408
8	0.026537507	2.445	-0.000439469	0.598842677	561.951	0.010610109	0.068178611	0.001041196	0.003574365
9	0.023853669	2.481	-0.000386692	0.560486207	516.753	0.009852109	0.060700349	0.000919746	0.003178693
10	0.021541703	2.516	-0.000342269	0.526110886	476.941	0.009171302	0.054318283	0.0008163	0.002841181
11	0.019541	2.550	-0.000304668	0.495216651	441.746	0.008558515	0.048844636	0.000727796	0.002551867
12	0.017801651	2.582	-0.000272661	0.467368812	410.519	0.008005626	0.044126561	0.000651729	0.002302637
13	0.016282566	2.614	-0.000245263	0.44219121	382.709	0.007505505	0.04003955	0.000586049	0.002086878
14	0.014949868	2.645	-0.000221682	0.419359083	357.853	0.007051924	0.036481974	0.00052908	0.001899192
15	0.013775557	2.674	-0.000201281	0.39859225	335.555	0.00663946	0.033370634	0.000479444	0.001735158
16	0.012736426	2.703	-0.000183539	0.3796489	315.484	0.006263398	0.03063717	0.000436009	0.001591146
17	0.011813166	2.731	-0.000168036	0.362320093	297.356	0.005919635	0.028225196	0.000397842	0.00146416
18	0.010989656	2.758	-0.000154425	0.346424976	280.929	0.005604602	0.026088002	0.000364168	0.00135172
⋮	⋮	⋮	⋮	⋮	⋮	⋮	⋮	⋮	⋮
375	0.000562544	4.140	-7.55109E-06	0.054728802	27.1307	6.7782E-05	0.001022984	1.45685E-06	4.7072E-05

	k_d	L	t	$a=1-kdt$	η_{R1}	η_{R2}	η_c	$(-\Delta H_{r1})$	$(-\Delta H_{r2})$	$(-\Delta H_{r3})$	$(-\Delta H_{r4})$	ΔR	$2\pi RH\rho$
comp	h^{-1}	m	hr	-	-	-	-	kJ/kmol	kJ/kmol	kJ/kmol	kJ/kmol	(m)	(kg/m)
1	0.0001179	0	0	0.99959	0.9	0.8	0.5	-36953	71038.06	-51939.3	-56597.5	0.0016	7560.35
2	0.0001130	0.0221	0.0647	0.99958	0.9	0.8	0.5	-36953	71038.06	-51939.3	-56597.5	0.0016	7540.14
3	0.0001084	0.0443	0.1294	0.99958	0.9	0.8	0.5	-36953	71038.06	-51939.3	-56597.5	0.0016	7519.92
4	0.0001042	0.0665	0.1941	0.99957	0.9	0.8	0.5	-36953	71038.06	-51939.3	-56597.5	0.0016	7499.71
5	0.0001002	0.0887	0.2588	0.99956	0.9	0.8	0.5	-36953	71038.06	-51939.3	-56597.5	0.0016	7479.49
6	9.6570E-05	0.1109	0.3236	0.99956	0.9	0.8	0.5	-36953	71038.06	-51939.3	-56597.5	0.0016	7459.28
7	9.3177E-05	0.1331	0.3883	0.99955	0.9	0.8	0.5	-36953	71038.06	-51939.3	-56597.5	0.0016	7439.06
8	9.0040E-05	0.1553	0.4530	0.99955	0.9	0.8	0.5	-36953	71038.06	-51939.3	-56597.5	0.0016	7418.85
9	8.7139E-05	0.1775	0.5177	0.99955	0.9	0.8	0.5	-36953	71038.06	-51939.3	-56597.5	0.0016	7398.63
10	8.4453E-05	0.1997	0.5825	0.99954	0.9	0.8	0.5	-36953	71038.06	-51939.3	-56597.5	0.0016	7378.42
11	8.1961E-05	0.2219	0.6472	0.99954	0.9	0.8	0.5	-36953	71038.06	-51939.3	-56597.5	0.0016	7358.20
12	7.9647E-05	0.2441	0.7119	0.99953	0.9	0.8	0.5	-36953	71038.06	-51939.3	-56597.5	0.0016	7337.99
13	7.7495E-05	0.2663	0.7766	0.99953	0.9	0.8	0.5	-36953	71038.06	-51939.3	-56597.5	0.0016	7317.77
14	7.5488E-05	0.2885	0.8413	0.99953	0.9	0.8	0.5	-36953	71038.06	-51939.3	-56597.5	0.0016	7297.56
15	7.3615E-05	0.3107	0.9061	0.99952	0.9	0.8	0.5	-36953	71038.06	-51939.3	-56597.5	0.0016	7277.34
16	7.1863E-05	0.3328	0.9708	0.99952	0.9	0.8	0.5	-36953	71038.06	-51939.3	-56597.5	0.0016	7257.13
17	7.0221E-05	0.3550	1.0355	0.99952	0.9	0.8	0.5	-36953	71038.06	-51939.3	-56597.5	0.0016	7236.91
18	6.8679E-05	0.3772	1.1002	0.99951	0.9	0.8	0.5	-36953	71038.06	-51939.3	-56597.5	0.0016	7216.70
⋮	⋮	⋮	⋮	⋮	⋮	⋮	⋮	⋮	⋮	⋮	⋮	⋮	⋮
375	2.7561E-05	8.3001	24.206	0.99892	0.9	0.8	0.5	-36953	71038.06	-51939.3	-56597.5	0.0016	7.0E-13

	ΔF_P	ΔF_N	ΔF_A	ΔF_H	ΔF_{LG}	$c_{p,g}$	ΔT	T(K)	T(°C)
comp	kmol/m.h	kmol/m.h	kmol/m.h	kmol/m.h	kmol/m.h	kJ/kmol.K	K/m	793.00	520.0000
1	-80.535862	-155.16495	143.531	234.61895	92.169896	88.1	-13.226299	790.3336	517.3336
2	-68.915610	-141.21715	131.128	225.28304	79.005141	88.1	-12.723894	787.7481	514.7481
3	-59.178054	-128.61980	119.868	214.99340	67.929702	88.1	-12.160233	785.2577	512.2577
4	-51.042632	-117.32747	109.725	204.27936	58.645596	88.1	-11.566891	782.8703	509.8703
5	-44.248037	-107.25012	100.628	193.52426	50.869712	88.1	-10.966900	780.5891	507.5891
6	-38.564131	-98.276801	92.4916	182.99068	44.349374	88.1	-10.376194	778.4143	505.4143
7	-33.795127	-90.29083	85.2184	172.84781	38.867534	88.1	-9.8051891	776.3434	503.3434
8	-29.778039	-83.178959	78.7148	163.19603	34.242167	88.1	-9.2602133	774.3729	501.3729
9	-26.378988	-76.836062	72.8922	154.08693	30.322867	88.1	-8.7446807	772.4980	499.4980
10	-23.488841	-71.167343	67.6697	145.53875	26.986440	88.1	-8.2599951	770.7138	497.7138
11	-21.018981	-66.088795	62.9753	137.54765	24.132443	88.1	-7.8062183	769.0152	496.0152
12	-18.897518	-61.52682	58.7452	130.09585	21.679116	88.1	-7.3825517	767.3970	494.3970
13	-17.066090	-57.417417	54.9236	123.15727	19.559890	88.1	-6.9876727	765.8541	492.8541
14	-15.477215	-53.705110	51.4619	116.70139	17.720465	88.1	-6.6199669	764.3818	491.3818
15	-14.092142	-50.341955	48.3177	110.69584	16.116431	88.1	-6.2776837	762.9756	489.9756
16	-12.879128	-47.286525	45.4543	105.10805	14.711339	88.1	-5.9590397	761.6312	488.6312
17	-11.812071	-44.503005	42.8399	99.906332	13.475161	88.1	-5.6622831	760.3448	487.3448
18	-10.869405	-41.960404	40.4468	95.060485	12.383058	88.1	-5.3857347	759.1125	486.1125
⋮	⋮	⋮	⋮	⋮	⋮	⋮	⋮	⋮	⋮
▼	▼	▼	▼	▼	▼	▼	▼	▼	▼
375	437.9502	437.9502	437.9502	437.9502	437.9502	437.9502	437.9502	437.9502	437.9502

C.4. Compartment in series model for naphtha reforming in R₄

	F _P	F _N	F _A	F _H	F _{LG}	TOTAL	T _{i-1}	P _P	P _N	P _A	P _H
comp.	kmol/hr	kmol/hr	kmol/hr	kmol/hr	kmol/hr	kmol/hr	K	Mpa	Mpa	Mpa	Mpa
1	456.7012	14.7656	474.2315	4004.8333	48.60814	4950.5316	793.00	0.064411	0.002082	0.066883	0.564823
2	456.5538	14.74796	474.260214	4004.6576	48.74452	4950.2195	791.53	0.064394	0.00208	0.066892	0.564834
3	456.2834	14.71354	474.314724	4004.3405	48.99487	4949.6521	790.18	0.064364	0.002075	0.066907	0.564854
4	455.9086	14.66335	474.392639	4003.908	49.34187	4948.8726	788.95	0.064321	0.002069	0.066929	0.564882
5	455.4444	14.59836	474.491862	4003.3799	49.77183	4947.9146	787.80	0.064268	0.00206	0.066956	0.564917
6	454.9027	14.51954	474.610544	4002.7721	50.27371	4946.8049	786.74	0.064206	0.002049	0.066987	0.564958
7	454.2932	14.4278	474.747031	4002.0968	50.83845	4945.5649	785.74	0.064136	0.002037	0.067023	0.565004
8	453.6241	14.32407	474.899824	4001.3641	51.45851	4944.2121	784.81	0.064059	0.002023	0.067063	0.565055
9	452.9022	14.20924	475.06755	4000.5821	52.12754	4942.7611	783.92	0.063976	0.002007	0.067107	0.565111
10	452.1333	14.08416	475.248944	3999.7575	52.84011	4941.2239	783.09	0.063887	0.00199	0.067153	0.56517
11	451.3224	13.94966	475.442834	3998.8957	53.59156	4939.6106	782.29	0.063793	0.001972	0.067203	0.565233
12	450.474	13.80656	475.648125	3998.0012	54.37782	4937.9299	781.54	0.063695	0.001952	0.067254	0.565299
13	449.5918	13.65561	475.863792	3997.0779	55.19535	4936.1890	780.81	0.063593	0.001932	0.067309	0.565367
14	448.6791	13.49756	476.088875	3996.1289	56.04099	4934.3944	780.12	0.063487	0.00191	0.067365	0.565439
15	447.7389	13.33313	476.322469	3995.1569	56.91196	4932.5514	779.46	0.063377	0.001887	0.067423	0.565512
16	446.774	13.163	476.563724	3994.1641	57.80577	4930.6649	778.82	0.063265	0.001864	0.067483	0.565588
17	445.7867	12.98782	476.811835	3993.1526	58.72017	4928.7389	778.20	0.06315	0.00184	0.067545	0.565666
18	444.7791	12.80821	477.066046	3992.1239	59.65314	4926.7773	777.61	0.063032	0.001815	0.067608	0.565745
⋮	⋮	⋮	⋮	⋮	⋮	⋮	⋮	⋮	⋮	⋮	⋮
437	241.2886	1.928678	505.383488	3722.409	245.7057	4471.0097	732.54	0.03768	0.000301	0.078921	0.581297

	k_{Π}	K_{e1}	r_1	k_{Ω}	K_{e2}	r_2	$k_{\Omega}=k_{\mu}$	r_3	r_4
comp	kmol/kg.cat.h.Mpa ²	Mpa ⁻¹	kmol/kg.cat.h	kmol/kg.cat.h.Mpa	Mpa ³	kmol/kg.cat.h	kmol/kg.cat.h.	kmol/kg.cat.h	kmol/kg.cat.h
1	0.063983155	2.168	-0.000911649	1.034189295	1122.72	0.001712349	0.177879086	0.000254967	0.007886134
2	0.059282538	2.191	-0.000835355	0.98633901	1057.33	0.001630715	0.163687142	0.000234356	0.007254977
3	0.055281237	2.212	-0.00077094	0.944461826	1000.79	0.001557488	0.151685555	0.000216689	0.006719754
4	0.051829545	2.231	-0.000715792	0.907404132	951.316	0.001491005	0.141394709	0.000201328	0.006259639
5	0.048818015	2.250	-0.000668014	0.874300408	907.57	0.001430036	0.132466109	0.000187814	0.005859468
6	0.046164694	2.267	-0.000626198	0.844486817	868.547	0.001373651	0.124640274	0.000175801	0.005507925
7	0.043806949	2.283	-0.00058927	0.817444561	833.468	0.001321137	0.11771993	0.000165031	0.005196394
8	0.041696057	2.299	-0.000556404	0.792761573	801.719	0.001271933	0.111552371	0.000155302	0.004918192
9	0.039793532	2.314	-0.000526948	0.770105917	772.808	0.001225599	0.106017516	0.000146454	0.004668056
10	0.038068551	2.328	-0.000500384	0.749206872	746.338	0.001181778	0.101019625	0.000138364	0.004441784
11	0.03649614	2.341	-0.000476294	0.729841208	721.986	0.001140182	0.09648142	0.000130927	0.00423598
12	0.035055835	2.354	-0.000454337	0.711823052	699.483	0.001100577	0.092339837	0.000124063	0.004047866
13	0.033730714	2.366	-0.000434232	0.69499627	678.604	0.001062768	0.088542903	0.000117701	0.003875154
14	0.032506654	2.378	-0.000415746	0.679228675	659.162	0.001026592	0.0850474	0.000111786	0.003715934
15	0.031371778	2.390	-0.000398684	0.664407547	640.995	0.000991914	0.081817098	0.000106269	0.003568608
16	0.030316027	2.401	-0.00038288	0.650436145	623.969	0.000958619	0.078821402	0.000101109	0.003431821
17	0.029330821	2.412	-0.000368195	0.63723094	607.967	0.000926608	0.076034297	9.6273E-05	0.003304422
18	0.028408798	2.423	-0.000354508	0.624719423	592.886	0.000895798	0.073433526	9.17299E-05	0.003185423
⋮	⋮	⋮	⋮	⋮	⋮	⋮	⋮	⋮	⋮
437	0.002166059	3.444	-1.1626E-05	0.126393372	78.3289	1.04133E-05	0.004445121	9.19833E-07	0.000115076

comp	k_d h ⁻¹	L m	t hr	a=1-kdt -	η_{R1} -	η_{R2} -	η_c -	$(-\Delta H_{r1})$ kJ/kmol	$(-\Delta H_{r2})$ kJ/kmol	$(-\Delta H_{r3})$ kJ/kmol	$(-\Delta H_{r4})$ kJ/kmol	ΔR (m)	$2\pi R H \rho$ (kg/m)
1	0.0001179	0	0	0.99900	0.9	0.8	0.5	-36953	71038.06	-51939.3	-56597.5	0.0016	10470.0
2	0.0001152	0.0268	0.0995	0.99899	0.9	0.8	0.5	-36953	71038.06	-51939.3	-56597.5	0.0016	10446.0
3	0.0001128	0.0536	0.1991	0.99897	0.9	0.8	0.5	-36953	71038.06	-51939.3	-56597.5	0.0016	10422.0
4	0.0001105	0.0804	0.2987	0.99896	0.9	0.8	0.5	-36953	71038.06	-51939.3	-56597.5	0.0016	10398.0
5	0.0001085	0.1073	0.3983	0.99895	0.9	0.8	0.5	-36953	71038.06	-51939.3	-56597.5	0.0016	10374.0
6	0.0001067	0.1341	0.4979	0.99894	0.9	0.8	0.5	-36953	71038.06	-51939.3	-56597.5	0.0016	10350.0
7	0.0001050	0.1609	0.5975	0.99893	0.9	0.8	0.5	-36953	71038.06	-51939.3	-56597.5	0.0016	10326.1
8	0.0001034	0.1878	0.6971	0.99893	0.9	0.8	0.5	-36953	71038.06	-51939.3	-56597.5	0.0016	10302.1
9	0.0001019	0.2146	0.7966	0.99892	0.9	0.8	0.5	-36953	71038.06	-51939.3	-56597.5	0.0016	10278.1
10	0.0001005	0.2414	0.8962	0.99891	0.9	0.8	0.5	-36953	71038.06	-51939.3	-56597.5	0.0016	10254.1
11	9.9300E-05	0.2683	0.9958	0.99890	0.9	0.8	0.5	-36953	71038.06	-51939.3	-56597.5	0.0016	10230.1
12	9.8079E-05	0.2951	1.0954	0.99889	0.9	0.8	0.5	-36953	71038.06	-51939.3	-56597.5	0.0016	10206.1
13	9.6925E-05	0.3219	1.1950	0.99888	0.9	0.8	0.5	-36953	71038.06	-51939.3	-56597.5	0.0016	10182.1
14	9.5831E-05	0.3487	1.2946	0.99887	0.9	0.8	0.5	-36953	71038.06	-51939.3	-56597.5	0.0016	10158.1
15	9.4790E-05	0.3756	1.3942	0.99887	0.9	0.8	0.5	-36953	71038.06	-51939.3	-56597.5	0.0016	10134.2
16	9.3799E-05	0.4024	1.4937	0.99886	0.9	0.8	0.5	-36953	71038.06	-51939.3	-56597.5	0.0016	10110.2
17	9.2852E-05	0.4292	1.5933	0.99885	0.9	0.8	0.5	-36953	71038.06	-51939.3	-56597.5	0.0016	10086.2
18	9.1945E-05	0.4561	1.6929	0.99884	0.9	0.8	0.5	-36953	71038.06	-51939.3	-56597.5	0.0016	10062.2
⋮	⋮	⋮	⋮	⋮	⋮	⋮	⋮	⋮	⋮	⋮	⋮	⋮	⋮
437	4.1702E-05	11.697	43.419	0.99719	0.9	0.8	0.5	-36953	71038.06	-51939.3	-56597.5	0.0016	11.9931

	ΔF_P	ΔF_N	ΔF_A	ΔF_H	ΔF_{LG}	$c_{p,g}$	ΔT	T(K)	T(°C)
comp	kmol/m.h	kmol/m.h	kmol/m.h	kmol/m.h	kmol/m.h	kJ/kmol.K	K/m	793.00	520.0000
1	-92.112912	-11.052845	17.9283	-109.81446	85.237442	88.1	7.3037784	791.5276	518.5276
2	-84.511829	-10.75644	17.0345	-99.086035	78.23377	88.1	6.6126673	790.1839	517.1839
3	-78.068321	-10.455773	16.2322	-90.110741	72.291891	88.1	6.0335318	788.9482	515.9482
4	-72.530915	-10.154130	15.5036	-82.502919	67.181495	88.1	5.5417435	787.8044	514.8044
5	-67.716545	-9.8536512	14.8353	-75.982318	62.734909	88.1	5.1194092	786.7395	513.7395
6	-63.488670	-9.5557649	14.2174	-70.340221	58.827033	88.1	4.7532058	785.7433	512.7433
7	-59.743317	-9.2614519	13.6422	-65.417887	55.362585	88.1	4.4330026	784.8070	511.8070
8	-56.399881	-8.9713989	13.1036	-61.092373	52.267682	88.1	4.1509551	783.9237	510.9237
9	-53.394890	-8.6860972	12.5969	-57.266939	49.484132	88.1	3.9008922	783.0873	510.0873
10	-50.677671	-8.4059049	12.1181	-53.864394	46.965465	88.1	3.6778910	782.2929	509.2929
11	-48.207270	-8.131087	11.6642	-50.822375	44.674119	88.1	3.4779752	781.5361	508.5361
12	-45.950227	-7.8618422	11.2327	-48.089943	42.57939	88.1	3.2978978	780.8132	507.8132
13	-43.878933	-7.5983203	10.8213	-45.625074	40.655961	88.1	3.1349804	780.1210	507.1210
14	-41.970404	-7.3406341	10.4283	-43.392787	38.882718	88.1	2.9869944	779.4567	506.4567
15	-40.205351	-7.0888676	10.0523	-41.363730	37.241956	88.1	2.8520699	778.8178	505.8178
16	-38.567466	-6.8430817	9.69185	-39.513095	35.718701	88.1	2.7286268	778.2023	505.2023
17	-37.042866	-6.6033179	9.34599	-37.819770	34.300198	88.1	2.6153205	777.6081	504.6081
18	-35.619662	-6.3696012	9.01374	-36.265684	32.975523	88.1	2.5110004	777.0335	504.0335
⋮	⋮	⋮	⋮	⋮	⋮	⋮	⋮	⋮	⋮
437	-0.0015195	3.512E-06	0.00012	-0.0022792	0.0013911	88.1	0.0001641	732.5358	459.5358